University of Miami
Scholarly Repository

Open Access Dissertations | Electronic Theses and Dissertations

2014-03-17

Multi-objective Design Optimization of Engineering Systems: Uncertainty Approach and Practical Applications.

Aparna Aravelli
University of Miami, aparna.aravelli@gmail.com

Follow this and additional works at: https://scholarlyrepository.miami.edu/oa_dissertations

Recommended Citation
Aravelli, Aparna, "Multi-objective Design Optimization of Engineering Systems: Uncertainty Approach and Practical Applications." (2014). *Open Access Dissertations*. 1156.
https://scholarlyrepository.miami.edu/oa_dissertations/1156

This Open access is brought to you for free and open access by the Electronic Theses and Dissertations at Scholarly Repository. It has been accepted for inclusion in Open Access Dissertations by an authorized administrator of Scholarly Repository. For more information, please contact repository.library@miami.edu.

UNIVERSITY OF MIAMI

MULTI-OBJECTIVE DESIGN OPTIMIZATION OF ENGINEERING SYSTEMS: UNCERTAINTY APPROACH AND PRACTICAL APPLICATIONS

By

Aparna Aravelli

A DISSERTATION

Submitted to the Faculty
of the University of Miami
in partial fulfillment of the requirements for
the degree of Doctor of Philosophy

Coral Gables, Florida

May 2014

©2014
Aparna Aravelli
All Rights Reserved

UNIVERSITY OF MIAMI

A dissertation submitted in partial fulfillment of
the requirements for the degree of
Doctor of Philosophy

MULTI-OBJECTIVE DESIGN OPTIMIZATION OF ENGINEERING SYSTEMS: UNCERTAINTY APPROACH AND PRACTICAL APPLICATIONS

Aparna Aravelli

Approved:

_____ Singiresu S. Rao, Ph.D. Professor of Mechanical and Aerospace Engineering	_____ Qingda Yang, Ph.D. Associate Professor of Mechanical and Aerospace Engineering
_____ Xiangyang Zhou, Ph.D. Associate Professor of Mechanical and Aerospace Engineering	_____ M. Brian Blake, Ph.D. Dean of the Graduate School
_____ James W. Giancaspro, Ph.D. Associate Professor of Civil, Architectural and Environmental Engineering	

ARAVELLI, APARNA (Ph.D., Mechanical and Aerospace Engineering)

Multi-objective Design Optimization of Engineering Systems: Uncertainty Approach and Practical Applications. (May 2014)

Abstract of a dissertation at the University of Miami.

Dissertation supervised by Professor Singiresu S. Rao.
No. of pages in text. (214)

The increase in complexity of optimization problems results in an emerging need for simpler, faster and non-classical solutions. One of the options is conversion of a traditional non-hierarchical optimization system to a hierarchical system using an approach called multi-level (ML) decomposition (for optimization). Most of the work in the literature deals with the application of multi-level approach to deterministic optimization problems. But, in nature, many applications are uncertain, and hence, it is realistic to introduce uncertainty in the analysis and optimization. The first part of the present research deals with the development of a multi-level optimization procedure for uncertain engineering systems. The uncertainty in the problem is assumed to be stochastic and interval in nature. The methodology developed is illustrated by considering the optimization of structural and mechanical engineering problems. The second part of the present study deals in modifying a relatively new swarm intelligence technique based on the foraging behavior of ants called Ant Colony Optimization (ACO). A new multi-objective ant colony optimization algorithm is developed and applied to structural and mechanical engineering problems. The illustrative examples in the present research include the design optimization of an electric transmission tower (space truss), plane truss, gear box and the combustion chamber of an internal combustion engine. The third part of the research attempts to apply optimization techniques to practical engineering

systems in the field of Heating Ventilation and Air Conditioning (HVAC) and Micro-Electronics. Novel design optimization models are created and hybrid optimization algorithms are developed for chiller plants and micro-channel heat exchangers used in electronic cooling. Illustrative case studies are performed.

Acknowledgements

I would like to express my gratitude to my dissertation supervisor and the chairman of the committee, Dr. Singiresu S. Rao, for all his support, guidance and patience throughout the years of my Ph.D.

I would like to thank Dr. Xiangyang Zhou, Dr. Qingda Yang, from Mechanical and Aerospace Engineering, and Dr. James Giancaspro from Civil, Architectural and Environmental Engineering, University of Miami, for accepting to be the committee members and for their support and feedback.

My sincere gratitude goes to the Department of Mechanical and Aerospace Engineering for providing financial assistance and to the graduate school for extending my period of study.

My special thanks go to Mr. Igor Gonzalez from ESI Consulting Engineers Inc., Miami, for his valuable guidance in the HVAC systems optimization.

I must thank my former classmate and long term friend Mr. Hari Adluru, from Florida International University for his support in all possible ways. My thanks also go to Dr. Ravi Krishna Gudavalli from Florida International University for his help in editing the document.

Lastly, my deepest sense of gratitude goes to my family, including my parents, brother, husband and kids for their unconditional love, support, encouragement and sacrifice in making this a possibility.

Aparna Aravelli

May 2014

TABLE OF CONTENTS

LIST OF FIGURES

LIST OF TABLES

NOMENCLATURE

$a_1, a_2, \ldots a_n$	Coefficients
A	Cross sectional area
b	Cylinder bore
b_1, b_2	Base dimensions of the truss
c_l	Weight assigned to each objective function l
C_p	Specific heat
c_r	Compression ratio
Ch_{max}	Maximum chiller capacity
d	Mean/nominal diameter
d_e	Exhaust valve diameter
d_i	Intake valve diameter
d_i	Mean/nominal diameter of element i
d_{kj}	Displacement of node k in direction j
d_1, d_2, d_3	Coefficients
$d_{inner}^{(i)}$	Inner diameter of element i
$d_{outer}^{(i)}$	Outer diameter of element i
D	Diameter
E	Young's modulus
f	Objective function
f^*	Optimum value of the objective function
$f^{(0)}$	Initial value of the objective function
$f(X)$	Objective function
$f_{nl}(X)$	Normalized objective function
F_x, F_y, F_z	Load along x, y and z directions respectively

$F(Y)$	Stochastic objective function
FC	Pareto-optimal objective
g	Constraint function
g_j	Constraint j
$g(X)$	Constraint function
G_w	Mass flow rate of water
h	Convective heat transfer coefficient
h_1	Height of the truss from the base to the mid-span
h_2	Height of the truss from the mid-span to the top
H	Function of flowrate
I	Area moment of inertia
IL	Input load
k	Thermal conductivity
k, k_1, k_2	Constants
l	Length
L	Length
m	Number of constraints
$\dot{m}$	Coolant mass flow rate
n	Number
nch	Number of chillers
N	Number of Ag columns in a row
Nu	Nusselt number
$\vec{p}$	Load vector
p_{ai}	Load in member i
p_b	Buckling load
P_p	Pump power

P_{ch}	Power consumed by chiller
P_{ctf}	Cooling tower fan power
$p_i(X)$	Buckling stress in member i
P	Probability
P	Power
PL_{ch}	Chiller load (%)
PS_f	Speed of fan (%)
$\dot{Q}$	Rate of heat transfer
R	Thermal resistance
R_{Agpad}	Thermal resistance of Ag pad
$R_{conduction}$	Conductive thermal resistance
$R_{convection}$	Convective thermal resistance
s	Allowable stress
s	Mid-span dimension of the truss
s	Stroke length
S	Supercriterion
S, S1, S2, S3	Sets of discrete design variables
S_v	Surface to volume ratio
t	Thickness
$T_{bulkmean}$	Bulk mean temperature
T_{ce}	Condenser entering water temperature
T_{in}	Inlet temperature
T_{out}	Outlet temperature
T_1	Constant wall source temperature
V	Coolant velocity
w	Engine rpm/min

w_1, w_2, w_3	Constants (weights) for the objective function
x_i	Design variable i
X	Vector of design variables
Y	Vector of random variables
δ	Allowable nodal displacement
$\delta_x, \delta_y, \delta_z$	Displacement along x, y and z directions respectively
ΔT	Entering and leaving condenser water temperature difference
ΔT	Source and coolant temperature difference
ΔP	Pressure drop
σ	Axial stress
$\sigma_{ij}(X)$	Axial stress in member i for load condition j
ω_n	Natural frequency
ρ	Density
$\bar{\Psi}$	Mean value
σ_{Ψ}	Standard deviation
η	Efficiency

Subscript

i	Member
u	Upper bound
l	Lower bound
Ag	Silver
eq	Equivalent
t	Thermal
v	Volumetric

CHAPTER 1 - INTRODUCTION AND LITERATURE REVIEW

Optimization is the act of obtaining the best solution under given circumstances. This technique provides a powerful tool in improving the engineering design in a rational manner and has been proved to be much more efficient than the traditional trial-and-error design process. Today, the optimization tool has become a part of every engineering industry for design improvement. Higher customer expectations and tighter industry standards require more efficient designs. Developments in faster digital computers, sophisticated computing techniques and more frequent use of finite element methods facilitate this to a certain extent, but there arises a need to explore approaches which could use these aids in a better way and solve complex engineering problems. The present research investigates two of the recently developed alternative approaches, namely the Multi-level optimization (MLO) and the Ant Colony Optimization (ACO).

There are many classical optimization techniques developed and extensively used in the literature. These methods are based on mathematical programming techniques and cover a wide range, including linear, non-linear, geometric and quadratic programming. The more recent methods, like neural networks, simulated annealing and genetic algorithms are called non-classical optimization methods. One of the most recent methods is the use of swarm intelligence techniques in the design optimization of mechanical and structural engineering systems. Present research explores one such technique called Ant Colony Optimization. This algorithm is based on the foraging behavior of ants.

In traditional optimization procedure, the designs are often considered at a stretch or all-in-one approach which is non-hierarchical. This method suits well for problems of average size which include a few design variables and constraints. But this is not often

the case. Large scale engineering problems like design of an airplane or a power plant require the satisfaction of a large number of constraints and deal with many design variables. Most of them also have subparts or disciplines which might have no direct effect on other disciplines, but indirectly contribute to the overall convergence of the system. Such problems, called multidisciplinary optimization problems, can be easily solved using a different approach. This is done by a non-traditional hierarchical decomposition based optimization strategy also known as multilevel decomposition. Present research aims at developing a modified Multi-level (ML) technique for use in structural and mechanical engineering problems involving uncertainties.

As an inherent characteristic of nature, uncertainty appears everywhere and cannot be avoided. Uncertainties in engineering systems arise due to imprecise or vagueness of information. For example, in structural engineering, many types of loads such as wind, earthquake and snow loads acting on the structures are never known exactly. Only their past data is available in imprecise terms. The experimental results obtained for material properties like Young's modulus of elasticity and yield strength are often scattered and inexact. Also, mechanical components are subjected to errors in manufacturing or machining and hence, tolerance and nominal values are specified instead of the exact dimensions. Hence, it becomes essential to include uncertainties in the design and optimization. This aspect of uncertainty analysis is also considered in present research. In the literature, uncertainties are mainly grouped and modeled as stochastic and fuzzy/interval quantities. Present research aims at developing algorithms and solutions accounting for these types of uncertainties using the multilevel strategy.

Dealing with multiple and sometimes conflicting objectives in an optimization problem has always been a challenge for engineers. The widely accepted and used solution is the game theory approach. Game theory approach has been used for solving single level or general optimization problems. The present research develops a procedure to extend the game theory for solving multi-objective, multilevel and ant colony optimization problems.

One of the important contributions of the present research is a novel application of optimization in the Heating Ventilation and Air Conditioning (HVAC) systems and thermal management in micro-electronic systems. A novel chiller plant optimization formulation is made and a hybrid solution strategy is developed. The hybrid technique uses the classical method of sequential quadratic programing combined with a modified branch and bound method of integer programing. Also, a micro-channel heat exchanger embedded in Low Temperature Co-fired Ceramic (LTCC), used for cooling in electronic components, is optimized for maximum heat transfer.

A brief literature review of the important topics of the present work is given next.

1.1 Multi-objective Optimization (MOO)

Many practical applications in engineering (with optimization) often involve models with many goals to be satisfied simultaneously. Hence, the optimization of multiple objectives is necessary to solve such problems. In most cases, the objectives are conflicting, and so the minimization of one objective results in an increase in the value of the other. For example, in structural optimization of a truss, three objectives can be considered, namely, minimization of the total weight of the truss, minimization of the maximum nodal

displacement and maximization of the fundamental natural frequency of vibration. It is evident that the first two objectives are non-conflicting (both are to be minimized) whereas the third objective conflicts with the first two because it is to be maximized. Similarly, the design optimization of an automobile could be seen as a multi-objective problem with two conflicting objectives, namely, the minimization of weight and the maximization of the crash resistance. However, a decrease in the weight of the automobile would result in an increase in the crash resistance, and vice-versa.

The multi-objective optimization methods are broadly divided into three major categories: methods with priori articulation of preferences, methods with postpriori articulation of preferences and methods requiring no articulation of preferences. There are several techniques developed for multi-objective optimization, like the weighted sum method, lexicographic method, min-max method, global criterion method, goal programming method, bounded objective method and normal constraint method.

The concept of optimizing multiple objectives (in decision making) in mathematical programing was first introduced by Kuhn and Tucker (1951). The procedure is referred as Vector Maximization. One of the earliest and simplest methods used to deal with multiple objectives is the formation of a single overall objective function combining individual objectives. This is usually done by a linear combination of the objectives by allocating weights to the individual objectives (Walley (1991), Salama et al., (1988)). This type of formulation assumes that the objectives are independent which might be unreal in some cases. Also, this procedure might not span the entire region of optimization.

Kioski and Silvennoinen (1987) present a partial weighing method in which the original objective functions are grouped as sets involving common features. Each set is then used to form an independent weighted sum function with a unique set of weights and thus reduced the total number of objective functions. Steuer (1989) mathematically related the weights to the designer's preference function. Das and Dennis (1997) provided a graphical representation of the weighted sum method using bi-objective problems. In addition, they explained some of the deficiencies of the weighing method. Eschenauer et al., (1990) gave a brief overview of the weighed sum method. Koski and Silvennoinen (1987) illustrated the weighted sum method as a special case of another method called the p-norm method.

The selection of weights is an important aspect of the weighing method. Misinterpretation of the theoretical and practical meaning of the weights can mislead the efficient selection based on intuition. Many authors have focused on this aspect. A survey of works based on the systematic selection of weights, was provided by Eckenrode (1965), Hobbs (1980) and Hwong (1981).

Rao and Roy (1989) provided a method for determining the weights based on fuzzy set theory. For cases in which the relative importance of objective functions is unclear, Wierzbicki (1986) provided an algorithm that calculated weights based on feasible and infeasible points.

The limitations and difficulties involved in the weighted sum approach were detailed by many authors (Koski (1985), Stadler (1995), Athan and Papalambros (1996). Messac (1996) concluded that, in order for a weighted sum method to mimic a preference

function accurately, the weights must be functions of original objective, not constraints. Other important limitation concluded by Messac (1996) was that, despite the many methods for determining weights, a satisfactory pre-selection of weights did not necessarily guarantee the final solution to be acceptable.

A final difficulty with the weighted sum approach is that varying the weights consistently and continuously may not necessarily result in an even distribution of Pareto optimal (compromise) points, and an accurate, complete representation of the Pareto optimal set. Das and Dennis (1997) discussed this topic in detail. They suggested the necessary conditions for a series of weighted sum iterations to yield an even spread of Pareto optimal points.

Although, several approaches have been suggested for solving multi-objective optimization problems, the best approach would be to use the techniques of operations research originally designed for solving such problems, and modifying them based on the applications. In case of engineering applications, the game theory approach has been proven to be more efficient than many other techniques (Rao (1987)). This is due to its capability to not only find the best compromise (Pareto-optimal) solution but also the relative contribution of the individual objectives for the best solution. Hence, the present research uses modified game theory approach for solving multi-objective optimization problems.

1.2 Multilevel Optimization (MLO)

The design of complex engineering problems involves a large number of design variables and constraints. Optimization of such systems requires a greater computational effort and

often the problem is less tractable. One of the viable solutions is to split the complex problem into smaller fragments and solve the smaller problems either separately or in parallel. This strategy is the basis for decomposition based multilevel optimization (ML). The ML approach decomposes a primary problem into a system level design problem and a set of uncoupled component level sub problems. The solution is obtained by repeated iterations between the two levels.

The basics of multilevel optimization come from Calculus of Variations and Theoretical Mechanics. Initially, it was developed in the period after 1960 and was used to simplify the optimization of large scale industrial systems. It's applications in engineering were developed and reported almost four decades ago. Some of the earliest works were by Kirsh (1975, 1978). Kirsch proposed a multilevel approach to optimum structural design (1978). Two methods were used for the solution procedure. These were the goal coordination and the modal coordination methods. Illustrative examples included trusses, beams and columns. Schmidt and Ramanathan (1978) proposed a ML approach for the optimization of truss structures and wing structures using local buckling constraints. Sobiesczanski et al., (1985) redefined and applied the multi-level decomposition to a portal frame problem. Initially, a two level decomposition technique was used (Sobiesczanski et al., (1985)). Later on, it was generalized to a three level technique (Sobiesczanski et al., (1995)). In the numerical example, a portal frame was decomposed into beams. Each beam was considered to be a box, which was further decomposed into stiffened plates. The solution obtained using the three-level technique was compared to that obtained using a single (one) level optimization. Multilevel optimization required more time in dealing with the coupling of the sub problems. This limitation was dealt by

Barthelemy and Riley (1988). They tried to reduce the computational effort by using constraint approximation and temporary constraint deletion techniques used in single level optimization. The new procedure was tested on three, ten and fifty-two bar plane trusses. It was concluded that multilevel approach was economical for large scale problems if parallel processing was used for the analysis. Rohl and Schrage (1992) applied multilevel optimization to a large scale problem. A preliminary design of a high speed civil transport aircraft wing structure was described. Three levels were used for decomposition. Optimization results were verified with the experimental data obtained earlier. They reported minimization of weight and an increase in the productivity index of the aircraft wing structure. Another large scale example problem using a multi-level approach was considered by Walsh et al., (1994). Integrated aerodynamic, dynamic and structural optimization was done for helicopter rotor blades. Two levels were considered using decomposition in which the upper level performed aerodynamic and dynamic design and the lower level performed a detailed structural design with some coupling between levels. This approach was suggested to be compatible with industrial design practices. Recently, Zeljkovic and Maksimovic (2005) solved a large scale multidisciplinary structural optimization problem using a multi-level approach. They applied the multilevel approach to optimization of an aircraft nose landing gear. Li et al., (1999) used multilevel optimization for multi-objective problems. Steel frames under gravity and earthquake loads were designed for minimum weight and maximum strain energy. A numerical comparison of the various multilevel optimization techniques based on a small truss example was done by Wit and Keulen (2007).

In most multilevel decomposition based optimization procedures, the system level problem acts only as a coordinator between the various sub problems (disciplines) and helps in the overall convergence of the system. It rarely does any optimization by itself. On the other hand, the multilevel based collaborative optimization (CO) procedure does optimization in both the system and the disciplinary levels and thus provides more flexibility and effectiveness in the convergence. Also, CO (Kroo et al., (1994)) was developed to capture the multidisciplinary characteristics of engineering design. Braun at al., (1995) employed the CO framework for the launch vehicle design. Sobieski and Kroo (1995) used it for the aircraft configuration. CO has been widely used in decision making (Gu at al., (2002)) and conceptual design Rawling and Balling (1998)). CO with multiple objectives was considered by Tappeta and Renaund (1997). Three different types of multi objective collaborative optimization formulations were developed and tested for the sizing optimization of an aircraft. The analytical and computational aspects of CO were studied by Alexandrov and Lewis (2002). Goal programming based multi-disciplinary optimization with collaborative optimization was developed by Allister and Simpson (2003).

Design optimization of multilevel systems with uncertainty has been studied by various researches (Antonsson and Otto (1995), Su and Renauld (1997), Du and Chen (2000), Kokkolaras et al., (2006). Uncertainty in the multidisciplinary mechanical systems was studied by Oakley et al., (1998). Sues et al, (2001) studied reliability based optimization considering manufacturing and operational uncertainties in the design process. Recently, Sakalkar and Hajela (2008) introduced stochasticity (probability) in the multilevel optimization. A portal frame example problem was solved. The stochastic methods

require mean and standard deviation of the input data which in some situations might not be readily available. In such cases, the uncertain variables are stated as intervals and interval arithmetic is used for design analysis and optimization. This concept of interval based uncertainty analysis and optimization is introduced in present work. To the best of the author's knowledge, no research work addressing the multilevel multidisciplinary optimization with interval based uncertainty is reported in the literature. The scope of present work is to develop a multi-level collaborative optimization based optimization method to account for interval based uncertainties. Also, a stochastic multi-level collaborative optimization method has been proposed for suitable comparison with the deterministic and interval based formulations. The stochastic method uses a modified form of the approach suggested by Schmidt and Ramanathan (1978). It is to be noted that the words multi-level and bi-level are assumed to have the same meaning in the context of the present work as two levels have been considered in the ML approach.

1.3 Ant Colony Optimization (ACO)

The basic behavior of a group of birds, ants, insects or fish, is used to develop algorithms to solve optimization problems. These algorithms are known as evolutionary algorithms in general, or swarm intelligence techniques in particular. Swarm intelligence is an artificial intelligence based on the collective behavior of decentralized, self-organized systems. The agents in the system interact locally and develop simple rules in their struggle for survival. This leads to a global set of rules for the colony, even if there is no central agent commanding them. The expression for swarm intelligence was first quoted by Gerardo Beni and Jing Wang in 1989. Some of the swarm intelligence algorithms are

Ant Colony Optimization (ACO), Particle Swarm Optimization (PSO) and stochastic diffusion search. Present work uses ACO.

ACO is an optimization technique which uses the basic behavior of ants in searching for food. ACO was first developed by Marco Dorigo (Dorigo et al., (1991)). Since then it has been applied to a variety of problems. Initially, it was used to solve combinatorial optimization problems. One of the earliest examples included the traveling salesman problem (TSP). The other applications of ACO included various assignment, scheduling, network routing and machine learning problems (Dorigo and Stutzle (2004)).

Engineering applications of ACO are very recent. Aditya et al., (2004) used it to solve an engineering mechanics problem. Two types of algorithms, based on the foraging behavior of two different types of ants, were developed. The first type used the pheromone trail and solved TSP. This was mostly based on the basic ant colony algorithm called the Ant System (AS) algorithm. They solved two-dimensional and three-dimensional TSP problems with a size of almost 50 cities. The second type of ants, called the Pachycondyla Apicalis (API) ants, made use of visual landmarks for feedback as opposed to a pheromone trail. Aditya et al., (2004) used two strategies, one for local search and another for global search. The second type of ants was used to solve function minimization related to a spring mass system with no constraints.

Serra and Venini (2005) used ACO metaheuristic to solve structural optimization problems. An ACO algorithm was proposed and implemented for discrete optimization of plane trusses. Two examples were solved. One was a seven bar statically determinate truss and the other was a ten bar statically indeterminate planar truss. A simple algorithm

was suggested for ACO. Camp et al., (2004) used a modified version of the TSP ACO to design space trusses. It was based on the rank based Ant Colony Optimization. The design of space trusses using discrete variables was transformed into a modified TSP where the network of the TSP reflected the structural topology and the length of the tour represented the weight of the structure. The resulting truss, mapped into a TSP, was minimized using an ACO algorithm. The results obtained from ACO were compared with those given by Genetic Algorithms (GA) and classical continuous optimization methods.

Fonseca et al., (2007) used a variant of ACO called Rank Based Ant System (RBAS) for structural optimization using discrete variables. Penalty function method was used in handling the constraints in the optimization problem. In a subsequent work, Fonseca et al., (2007) used the same Rank Based ACO for the minimum weight design with discrete variables. The stochastic ranking approach was used to balance the objective and penalty functions stochastically. This was to overcome the difficulty of calculating penalty parameters in constrained optimization problems. The balancing technique resulted in an improved search performance thereby leading to better solutions when compared to the standard penalty technique.

Kaveh et al., (2007) designed skeletal structures using ACO. Sizing of space trusses was considered. Examples included 10 bar, 25 bar and 244 bar trusses. Also, a single bay eight storey frame, a braced frame of a 26-storey building and an industrial building were designed using ACO. This reference mainly applied ACO to large scale problems to demonstrate its ability. Sandesh et al., (2007) did structural identification using ant colony optimization in the time domain. This was a new area for solving inverse problems using ACO. A parametric structural identification using ACO-SI technique was

developed for multi-degree of freedom dynamic system in time domain. Sameer et al., (2007) applied ACO to structural and mechanical engineering applications. An I-beam was designed for minimum weight under bending, shear and deflection constraints. Also, an air storage tank (pressure vessel) was designed for minimum cost.

ACO has also been applied to solve several types of multi-objective (MO) optimization problems. Based on the modifications of the initial AS and ACS algorithms different kinds of algorithms have been proposed by many researchers in literature. Due to the nature of ACO in constructing feasible solutions, it was employed as an alternative tool instead of an exact method for solving MO problems. ACO is suitable for solving MO problems where a larger number of non-dominated solutions are needed. Iredi et al., (2001) developed a MO ACO algorithm on the basis of AS for bi-criteria vehicle routing problem. Each objective had its own pheromone trail and information on pheromone trails was combined for calculating the probability distribution of the transition rule. In order to force the ants to search in different regions of solution space, they defined a parameter that differs with the index of ants in the colony. This parameter was used as a weighing factor in transition rule. Doerner et al., (2004), designed a MO ACO algorithm on the basis of ACS. Several pheromone matrices were considered for each objective. The ants used maximum selection method for selecting next node and they combined the pheromone trails information of different objectives to calculate the probability distribution of transition rule. At the end of each iteration, best ant and the second best ant generated in the current iteration updated the pheromone trails. Multiple ant colony system proposed in Baran and Schaerer (2003) was devised for vehicle routing problem with time windows based on ACS. It used only one pheromone matrix but multiple

heuristic parameters based on the number of objectives. The transition rule used both the pheromone and heuristic information. Also, a parameter based on the index of ants, forced the ants to search in a different region of solution space. Doerner et al., (2003), proposed the COMPETants algorithm for bi-objective transportation problem. The algorithm worked on the basis of rank-based AS and used two colonies of ants, two pheromone trail matrices and two heuristic parameters, one for each objective. This method differed from the others in selecting non-fixed number of ants in each colony based on the solutions that the ants constructed. The colony that built better solution got more ants in the next iteration. Also, some of the ants in each colony were designated as spy ants which mixed the pheromone trails and the heuristic information of all colonies to search in the central areas of Pareto-frontier. Garcia et al., (2007), recently proposed a taxonomy and analysis of the performance of various existing multi-objective ant colony optimization algorithms in comparison with multi-objective genetic algorithms.

Recently, some researchers have developed hybrid optimization algorithms combining ACO and other methods like PSO and GA. Panahi et al., (2011) solved a multi-objective open shop scheduling problem by a novel hybrid optimization algorithm. An efficient method based on multi-objective ACO and simulated annealing has been proposed. Initially, the ant colony optimization algorithm was applied to the problem and due to the sensitivity of the ultimate solution's quality to the quality of the initial solutions; another algorithm (multi-objective) simulated annealing has been used. A decoding operator has been used and the results obtained were compared with those obtained from the standard algorithms.

An improved ACO combined with PSO for multi-objective flexible job shop scheduling problems has been presented by Li et al., (2010). The developed algorithm involved two parts. The first part used the fast convergence property of PSO to search the particle's optimum and took that as an initial design for ACO. The second part used the merit of positive feedback and the structure of the solution set provided by ACO, to search for the global optimum.

An efficient ACO algorithm for multi-objective resource allocation problem was addressed by Chaharsooghi et al., (2008). In order to obtain a set of Pareto solutions effectively, a modified ACO was proposed. It was based on a concept in which the ants were considered smart and had increased learning.

Bi-objective ACO approach was applied to optimize production and maintenance scheduling by Berrichi et al., (2010). Two objectives were considered and tradeoff solutions were found between the two objectives of production and maintenance. To improve the quality of solutions, a multi-objective ACO was considered and the experimental results were compared to those obtained by multi-objective genetic algorithms.

An application of multi-objective ACO in emergency evacuation process was proposed by Zong et al., (2010). The two objectives considered were the total evacuation time of all the people and the path crowding degree in the building. The aim was to develop an optimization method based on ACO for efficient, rapid and reasonable plans for complex evacuation routing problems.

A disassembly line balancing problem was solved using multi-objective ACO by Ding et al., (2010). A multi-objective mathematical model was created based on three objectives and an improved ACO based on Pareto-set was developed. A practical case was considered for illustration. Another application of multi-objective ACO for flow shop scheduling problem was studied by Yagmahan et al. (2010). Two objectives were considered, namely, the make span and the total flow-time. The developed ACO combined the ant algorithms with a local search strategy in order to solve the problem.

ACO for assembly line balancing was studied by Chica et al., (2010). Two new multi-objective proposals were presented based on ACO and random greedy search algorithms. Some variants of these algorithms were compared to find out the impact of different design choices based on heuristic information. Benchmark example problems and real world automobile case studies were provided.

Dispatch problems in environmental and economic dispatch (EED) were solved using ACO by Cai et al., (2010). A multi-objective chaotic ant swarm optimization algorithm was developed for solving the dispatch problems of thermal generators in power systems. Chaotic ant colony optimization was based on a combination or balance between the chaotic (unorganized) and organized nature of ants.

Multi-colony ant algorithms were used for multi-objective optimization by Reddy and Kumar (2007) for application in multi-purpose reservoir operation. The paper presented a non-dominated archiving ant colony optimization method, which benefited from the concept of multiple colonies and a new information exchange policy. After a certain number of iterations, the ant colonies exchanged information on the assigned objective

which resulted in a set of non-dominated solutions. These solutions were then sent to an offline achieve for further pheromone updating. Performance of the new method was tested and applied to the reservoir operation.

Recently, the optimization of laminate stacking sequence using ACO was performed by Hemmatiana et al., (2013). Elitist ant algorithms were used to optimize the stacking sequence with weight and cost objectives. Multi-objective ACO was applied to injection molding process by Huang et al., (2011). The developed hybrid method used ACO with crossover and mutation feature (generally used in GA) to generate the Pareto solutions. The parameters (results) obtained from the ACO were used to manufacture actual samples in injection molding process.

Aerodynamic shape optimization of an airfoil was performed by Kumar et al., (2011) using multi-objective ant colony optimization. In this method, the multi-objective optimization problem was converted into a single objective optimization problem using goal vector optimization by scalarization strategy. The ACO algorithm was integrated with a mesh less computational fluid dynamics solver to perform the shape optimization.

Optimal mechanism design of shearing machine using multi objective ant colony optimization was done by Zhou et al., (2011). The paper presented the basic ACO method with modifications. It dispersed a search space of the design variables by setting several design search steps and the ACO algorithm was adopted to search the best searching step of each design variable dynamically throughout the optimization process.

A new multi-objective resolution method was suggested by Hicham et al., (2010) and applied to buffer sizing in assembly lines. The method was based on a multi-objective ant

colony optimization but using a Lorenz dominance criterion instead of Pareto dominance. This provided a better dominance area by rejecting the solutions found on the extreme sides of the Pareto front. The results obtained were compared with those of the classical multi-objective methods and showed the advantages of the method.

A review of the literature indicates that each of the works used its own version of ACO modified to the needs. The present research develops a new multi-objective ACO technique for solving multi-objective optimization problems in engineering design optimization.

In this chapter, an introduction to the present research work is given. A brief literature review of the multi-objective, multi-level and ant colony optimization is provided.

CHAPTER 2 - OPTIMIZATION METHODS

Optimization methods are used to formulate and solve different types of optimization problems. In this chapter, single and multi-objective optimization problem formulations are explained and various approaches used to solve multi-objective optimization problems are indicated briefly. Game theory method for solving multi-objective optimization problems is described in detail. Also, the concepts of multi-level optimization and ant colony optimization are detailed. The developed procedures for multi-level and ACO in the present work are explained.

2.1 Single objective optimization

A general optimization problem can be stated as

Find $X = \{x_1\ x_2\ \dots\ x_n\}^T$ which minimizes $f(X)$ (2.1)

subject to

$$g_j(X) \leq 0, \qquad j = 1,2,\dots,m \tag{2.2}$$

$$h_k(X) = 0, \qquad k = 1,2,\dots,p \tag{2.3}$$

$$x_i^{(l)} \leq x_i \leq x_i^{(u)} \qquad i = 1,2,\dots,n \tag{2.4}$$

Where x_i is the design variable, $f(X)$ is the objective function, $g_j(X)$ and $h_k(X)$ are the constraints. $x_i^{(l)}$ and $x_i^{(u)}$ denote the lower and upper bounds on x_i. The above problem is called a single objective optimization problem, since there is only one objective to be minimized.

2.2 Multi-objective optimization

When the number of objective functions is more than one, then the single objective optimization problem converts into a multi-objective optimization problem. Usually, the objective functions are conflicting. Some are to be minimized while the others are to be maximized. Hence, it is not possible to find a single solution that is optimal for all the objective functions simultaneously. The main aim is to provide a rational approach to find optimal design solutions in the presence of conflicting objective functions.

Multi-objective optimization problems are solved using several approaches. Most of the methods used in literature are broadly classified into three categories as:

- Pareto-optimal set generation methods – In these methods, the decision maker or the designer chooses one of the alternative optimal solutions within the Pareto-optimal set (section 2.2.2) after the set is generated.
- Preference-based methods – In these methods, the preference of the decision maker or the designer is taken into consideration before the optimization process.
- Interactive methods – In these methods, the preference of the decision maker or the designer is considered during the course of the optimization process.

Generally, each of these methods is problem specific and can be combined, if necessary, to develop hybrid methods of solutions for the multi-objective optimization problems. Irrespective of the method, there exists a generic procedure for solving various multi-objective optimization problems. Various steps involved in the generic procedure are given as:

- Step 1: Problem formulation
- Step 2: Computing the feasible design variables domain
- Step 3: Performing global sensitivity analysis (loop between 1 and 3)
- Step 4: Computation of Pareto-optimal set
- Step 5: Performing design synthesis

2.2.1 Multi-objective formulation

A general multi-objective optimization problem can be stated as

$$\text{Minimize } f_1(\vec{X}), f_2(\vec{X}), \ \ldots, f_k(\vec{X}) \tag{2.5}$$

$$\text{subject to } g_j(\vec{X}) \ \leq 0 \ ; \quad j = 1,2, \ldots, m \tag{2.6}$$

$$\text{and } h_l(\vec{X}) = 0 \ ; \quad l = 1,2, \ldots, p \tag{2.7}$$

where $\vec{X} = \{x_1 \ x_2 \ \ldots \ x_n\}^T$ is an *n*-component design vector. $f_1(\vec{X}), f_2(\vec{X}), \ \ldots, f_k(\vec{X})$ are the multiple objective functions. Many procedures are available in literature for solving multi-objective optimization problems. Some of them are the weighted sum, global criterion, bounded objective, lexicographic, goal programming, goal attainment and trade–off curve methods. In this work, a modified cooperative game theory approach, is used for the solution of the multi-objective optimization problem. The basic concept of game theory approach is presented below.

2.2.2 Game theory approach for solving a multi-objective optimization problem

The basics of game theory are based on the behavior of a group of players interacting with each other in a game. Two main theories have been developed for interacting

systems. These are the non-cooperative game theory and the cooperative game theory. A multi-objective optimization problem can be seen as a game in which the players represent the objective functions and the resources available represent the constraints. Each player competes to optimize his/her own standing in the system.

The non-cooperative game theory is based on the concept of Nash Equilibrium and the cooperative game theory is based on the concept of Pareto minimum solution. In the non-cooperative game theory, the players do not cooperative/agree with each other initially. This means that each player is interested in reaching his own goal (minimizing or maximizing his objective) irrespective of the others. With this interest he selects his own share of resources. Once this is done, the players bargain/exchange resources among themselves until they reach an equilibrium state. This is called the Nash Equilibrium solution. It is a solution where there is a stable equilibrium condition in such a way that no player deviates unilaterally (by exchanging resources) from this point for further improvement of his own objective without effecting the objectives of any/all other players (Rao and Hati (1979), Rao (1987)). This is a possible solution, but there can be solutions where the players have better objective function values than the Nash equilibrium solution. This situation is addressed using the cooperative game theory approach.

In the cooperative game theory approach, all the players are willing to agree/cooperate with each other. Each player is ready to compromise on his own objective in improving the team's (multi-objective) solution. The willingness to cooperate and compromise among themselves results in a set of solutions but not a single solution. Hence, a set of feasible solutions called Pareto optimal (non-inferior) solutions are found to eliminate

many of these solutions. A feasible solution is called Pareto optimal if there is no other feasible solution that would reduce some objective function without causing a simultaneous increase in at least one other objective function. Thus, in a Pareto optimal solution, the team allocates the resources such that the players are as optimal as possible. Then, the resources are distributed in a way that no single player's gain results in an unacceptable loss to the other player(s). Hence, after determining the Pareto optimal set, a particular element (unique solution) is to be selected from it. One method to do that is to take the players far from their worst cases. To do this, a supercriterion or a bargaining model is to be specified as a measure of compromise. This supercriterion is generally a function of the objectives, penalizing solutions with objectives that are very near to their previously defined worst cases.

Thus, solving a multi-objective optimization problem using cooperative game theory involves two steps. The first step generates the set of Pareto optimal solutions and the second step selects an element from the Pareto optimal set. A procedure for implementing these steps, termed as modified or extended game theory approach, is presented next.

2.2.2.1 Modified game theory

The modified game theory approach is used for solving multi-objective optimization problem. In the present study the modified game theory approach is coupled with the SQP method to handle multiple objectives. This approach converts the multiple objective optimization problem to an equivalent single objective optimization problem. The resulting problem is then solved using the SQP algorithm to find the compromise solution. The step-by-step procedure of the modified game theory is given below:

1. Each of the k objectives is minimized separately using a common initial design vector:

$$\left.\begin{array}{l}\text{Minimize } \mathrm{f_i}(\mathbf{X}) \\ \text{subject to } \mathbf{X} \epsilon \mathrm{S_f}\end{array}\right\} \quad ; \qquad i = 1, 2, \ldots, k \tag{2.8}$$

where S_f denotes the feasible design space. If $\vec{X}_i^*$ denotes the minimum of $f_i(\vec{X})$, the values of the other (remaining) objectives at the i^{th} optimal design vector are recorded as $f_j(\vec{X}_i^*)$; $j = 1, 2, ..., i-1, i+1, ..., k$ for $i = 1, 2, ..., n$.

2. All the objectives are normalized so that no objective, due to its magnitude, is favored. The following normalization procedure is used:

$$f_{ni}(X) = \frac{f_i(X) - f_i(X_i^*)}{F_{iu} - f_i(X_i^*)} \tag{2.9}$$

where F_{iu} is the worst value, and $f_i(X_i^*)$ is the optimum (best) value of the i^{th} objective.

3. A super criterion S is formulated as

$$S = \prod_{i=1}^{n} [1 - f_{ni}(X)] \tag{2.10}$$

where $0 \leq S \leq 1$ due to the normalization of objective functions.

4. A Pareto optimal objective, FC is defined using normalized objectives. The weighted sum method is used so that :

$$FC = \sum_{i=1}^{n} c_i \, f_{ni}(X) \tag{2.11}$$

subject to the normalization of the weights c_i as $\sum_{i=1}^{n} c_i = 1$.

5. The Pareto optimal objective FC is to be minimized and the supercriterion S is to be maximized. Hence, they are combined to generate a new objective for

$$\text{minimization as :} \quad \left.\begin{array}{c} \text{OBJ} = \text{FC} - \text{S} \\ \text{subject to} \\ \text{X} \in \text{S and} \\ 0 \le f_{ni}(X) \le 1 \; ; \; i = 1,2, \ldots, k \end{array}\right\} \tag{2.12}$$

The solution of the problem stated in Eq. (2.12) gives the desired compromise (Pareto optimal) solution of the multi-objective optimization problem.

2.3 Multi-level approach

Multilevel optimization is a process in which a bigger problem is fractioned into smaller and simpler problems. The smaller problems (also called sub problems) are solved separately. Finally, all of them are integrated or coordinated by a system level problem which optimizes the required objective(s). For a clear understanding of the procedure, it is explained in the form of equations.

In this, the design vector X is partitioned into two subvecters Y and Z:

$$X = \begin{Bmatrix} Y \\ Z \end{Bmatrix} \tag{2.13}$$

where Y denotes the vector of system level design variables and Z denotes the vector of component level design variables (specific to the subsystems). The vector Z is further partitioned as

$$Z = \begin{Bmatrix} Z_1 \\ \vdots \\ Z_k \\ \vdots \\ Z_K \end{Bmatrix} \tag{2.14}$$

where Z_k represents the variables associated with the k^{th} subsystem only and *K* denotes the number of subsystems. Now, the constraints are also partitioned as

$$G_q(Y, Z) \leq 0; \quad q \in Q \text{ and } g_{l,k}(Y, Z_k) \leq 0; \; l \in L; \; k \in K \tag{2.15}$$

where Q denotes the set of system level constraints and L denotes a set of local constraints of the k^{th} subsystem problem, and

$$Y^{(l)} \leq Y \leq Y^{(u)}; z_k^{(l)} \leq Z_k \leq Z_k^{(u)}; \; k = 1,2, \ldots, K \tag{2.16}$$

After redefining the problem, the two levels can be stated as:

System level: The system level problem is given as

Find Y which minimizes $f(Y) = \sum_{k=1}^{K} f^{(k)}(Y, \; Z_k^*)$ (2.17)

subject to

$$G_q(Y, Z*) \leq 0; \quad q \in Q \qquad \text{and} \qquad Y^{(l)} \leq Y \leq Y^{(u)} \tag{2.18}$$

Subproblem/component level: In this level the values of the components of the vector Y are fixed and the main problem is decomposed into *K* independent subproblems, each of which is stated as

Find Z_k which minimizes ${f_1}^{(k)}(Y^*, Z_k) = [\, S^{(k)}(Y^*) - S^{(k)}(\, Z_k)]$ (2.19)

where S denotes a function of the problem parameters (like stiffness) in terms of the design variables in each level, subject to

$$g^{(k)}(Y^*,\ Z_k)\ \leq 0 \tag{2.20}$$

$$h^{(k)}(Y^*,\ Z_k) = 0 \tag{2.21}$$

$$z_k^{(l)}\ \leq\ Z_k\ \leq\ Z_k^{(u)} \qquad k = 1,2,\dots,K \tag{2.22}$$

Each of these sub-problems is solved and summed to get the minimum of the overall objective function given by

$$fC(Y,Z) = \sum_{k=1}^{K} f1^{(k)}(Y,\ Z_k) \tag{2.23}$$

Thus, the system level specifies an overall design, while the component level gives a detailed design.

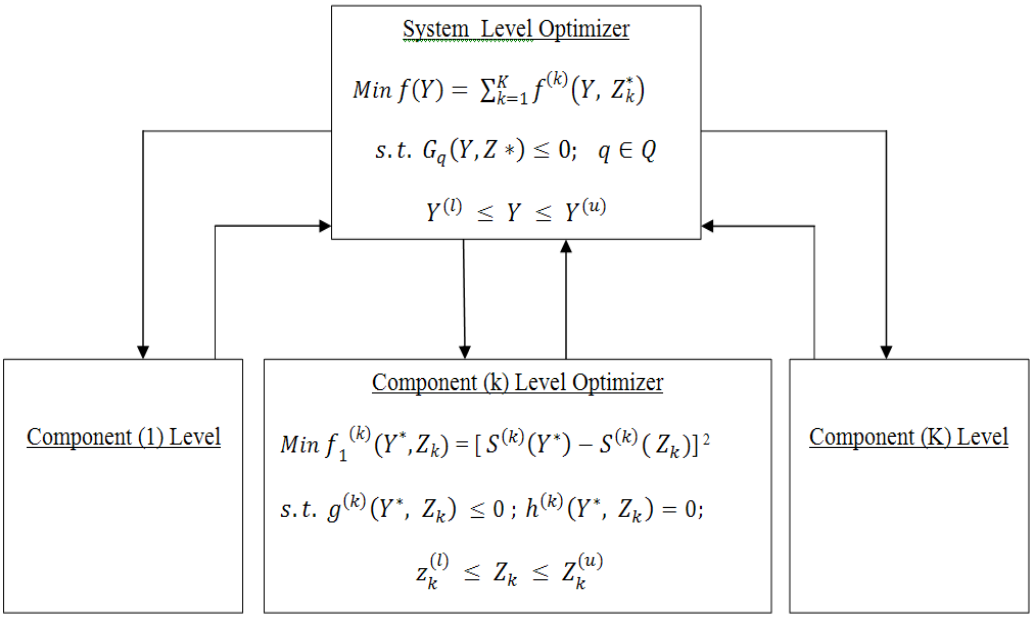

Figure 2.1 Block diagram for multilevel optimization

An extension of the multilevel optimization methodology shown in Figure 2.1 is used in present work. A multi-level collaborative optimization frame work is developed to consider discipline specific sub-problems or constraints. Instead of the inequality constraints in the system level, a set of equality constraints matching the system and component (discipline) levels are taken into account. That is done to assign target values for the design variables. The system level optimization maintains the compatibility among the sub-problems and minimizes the overall objective function. Each disciplinary sub problem design satisfies local constraints while satisfying the discipline specific objective discrepancy function.

2.4 Ant colony approach

The basic ideas of ACO are taken from how ants move and behave to search for food. In nature, ants wander randomly to locate food. Once they find food, they return to their nest or colony. During their journey, they secrete a chemical (called pheromone) on their paths. Other ants behind them tend to follow the same path instead of searching here and there. This is because they smell the pheromone. In this way, they reinforce the path for the next set of ants. However, after a certain amount of time the pheromone starts to evaporate. So, if the path is longer, the pheromone on it evaporates because it takes more time to travel by that path. The shorter paths in turn are left with higher concentration of pheromone because they retain larger amount of pheromone than the amount that is evaporated. So, the chances of following the shorter paths increase with time. In the language of ACO algorithm, evaporation process helps in avoiding convergence to a local minimum. In the absence of evaporation, the path taken by the initial ants is

obviously followed by other ants and so the search is not effective. Hence, when ants find shorter paths from nest to food, other ants follow them. This leads to a positive feedback and finally all ants follow the same shortest path. The ACO algorithm simulates this behavior assuming "artificial ants" to be walking in the search space.

2.4.1 Basic Procedure of ant colony optimization

ACO is basically a discrete optimization technique. Its basic procedure can easily be explained using a relevant example from literature, the Traveling Salesman Problem (TSP). Suppose that a salesman has to travel through *n* cities making sure that he doesn't stop in any city more than once. The problem is to find the shortest path through all the *n* cities. ACO algorithm assumes that there are *m* ants. Each of the *m* ants constructs a solution through all the *n* cities. This process is repeated for all iterations. These solutions are called ant tables. At each city an ant randomly chooses the next city based on a probabilistic rule. The probabilities are calculated based on heuristic and pheromone values. The heuristic information is denoted by η_{ij} (from city *i* to city *j*) and the pheromone values are denoted by τ_{ij} . η shows the desirability of the travel and τ gives the effectiveness of the past choice. The probability to move from city *i* to city *j* is computed as

$$p_{ij} = \frac{\tau_{ij}^{\alpha}\eta_{ij}^{\beta}}{\sum_{l=1}^{c}\tau_{il}^{\alpha}\eta_{il}^{\beta}} \tag{2.24}$$

where α and β are the control parameters that determine the relative influences of the heuristic and the pheromone values on the ant's decision and the summation extends over the neighborhood of city *j* (over all permissible discrete values of the j^{th} design variable).

Once the ants construct solutions, the pheromone values are updated for the best ant's path. This is done as

$$\tau_{ij} = \tau_{ij} + \Delta\tau_{ij} \ ; \text{ where } \Delta\tau = \frac{q}{L} \tag{2.25}$$

and q is a constant and L is the length or the distance between the two cities. After a certain number of iterations, the pheromone is evaporated. This is to avoid convergence to local minimum and to favor the exploration of new regions. The evaporation equation is given by

$$\tau_{ij} = \tau_{ij}(1 - \rho) \tag{2.26}$$

where ρ is the evaporation constant with $0 < \rho < 1$.

This cycle of solution construction (tour), updating the paths and evaporation of the pheromone, is continued until all the ants converge to a single path or a few best paths which represent the final solution (shortest path).

Many forms of ACO are available in literature. Some of the important ones are the Ant System, Elitist Ant System, Ant Colony System, Max-Min Ant System and the Rank-Based Ant System (Dorigo, (2004)). These versions differ from the basic ACO in the pheromone updating process, pheromone evaporation process or the probabilistic node selection process.

2.4.2 ACO for engineering design optimization

Most of the problems in the engineering design optimization deal with minimizing an objective function such as cost, weight or volume of a system subjected to constraints such as deflections, stresses and/or torques.

The ACO procedure explained previously for the case of TSP problem is modified with assumptions and applied to engineering problems. The major assumptions are summarized as: The cities/nodes in the TSP represent the design variables in the case of an engineering design problem. In TSP, only one path exists between two cities, but in the case of the engineering design problem, many paths exist between any two design variables (because of the discrete values of the design variables). In TSP, the order of visiting the cities is important, but in the engineering design problems, it is not. In TSP, the tour (objective) is always feasible whereas in an engineering design problem, the solution obtained by a set of design variables need not always be feasible. With these assumptions, a new multi-objective ACO algorithm is developed in this study and is applied to multi-objective engineering optimization examples.

Developed Multi-objective ACO algorithm for engineering design optimization

The step-by-step Multi-objective ACO procedure used to solve the objective function $f(\vec{X})$, containing all the multiple objectives, and subject to the constraints $g_j(\vec{X}) \leq 0$, $j = 1,2,\dots,m$, where $\vec{X}$ is an n component design vector, is given as below.

1. Start with a random initial design which need not satisfy the behavior constraints. For simplicity, the lower bounds on the design variables are chosen as the starting

values *i.e.* $\vec{X}^{(0)} = \vec{L}$ and $f^{(0)} = f(\vec{L})$ where $\vec{X}^{(0)}$ indicates the initial/starting design vector and $\vec{L}$ denotes the design vector containing lower bound values of the design variables. $f^{(0)}$ Indicates the initial value of the objective functions calculated using lower bound values of the design variables.

2. Initialize the number of ants *N* and the maximum number of iterations permitted for termination *I*.

3. For each of the *N* ants carry out steps 4 through 6.

4. Initialize the pheromone matrix $[\tau_{ij}]$ where i and j extend over the number of discrete values of the design variables and the number of design variables, respectively. For simplicity, choose all the elements of the initial pheromone matrix equal to 1.

5. Compute the probabilities with the current pheromone matrix using

$$[p_{ij}] = \frac{[\tau_{ij}]}{\sum[\tau_{ij}]} \tag{2.27}$$

where the summation extends over the neighborhood of each design variable. The constraints are handled using the penalty approach (Rao, (2009)) as

$$f_p = C\, f_a \tag{2.28}$$

where f_p is the penalized value of the objective function, f_a is the actual (current) value of the objective function and $C = (1 + \sum C_i)$ where $\sum C_i$ is the cumulative constraint violation (with constraints normalized) with C_i denoting the magnitude of violation of constraint.

6. Build a design (path) randomly based on the calculated probabilities. For this, cumulative probabilities are calculated and random numbers are generated. Then the values of the design variables are chosen based on the roulette wheel selection process. Finally, the value of the objective functions (length of tour) is evaluated which represents an initial solution set.

7. Now, a new solution set is created using the following equation

$$f_{new} = w_1 f_1 + w_2 f_2 + \cdots + w_k f_k \tag{2.29}$$

Where the values of the weights are randomly assigned based on $\sum_{i=1}^{k} w_i = 1$.

8. Check the designs corresponding to all ants for feasibility/optimality. Satisfaction of the constraints is checked and then among the selected designs, the best *h* designs are chosen in the vector $f^{(iterbest)}$ based on the values of the objective functions in f_{new} and those *h* paths are updated using step 12.

9. Test the current best design vector for convergence.

    - If $f^{(iterbest)} \leq f^{(best)}$ where $f^{(best)}$ denotes the value of the best design vector obtained so far for all the iterations, then go to step 10.
    - Else if iteration = *I* then print the best solution so far and terminate the program.
    - Else go to step 1.

10. Check for termination condition.

- If for a certain number of iterations the design does not change (stagnation) or
- If the number of iterations reaches the maximum allowable number of iterations.

11. If step 10 is satisfied then stop the iterative process and terminate the program by printing the best solution; or else go to step 12.

12. Update the pheromone matrix of all the ants using the best ant's path as:

$$[\tau_{ij}] = [\tau_{ij}] + [\Delta\tau_{ij}] \tag{2.30}$$

where $[\Delta\tau_{ij}] = {}^{b}/_{f(best)}$ and b is a constant whose value is to be suitably chosen according to the problem, and go to step 3.

The above-mentioned algorithm is used for solving the engineering design optimization problems.

Different optimization methods are considered in this chapter. Formulations for single and multi-objective optimization are given. Game theory approach and modified game theory approach for solving multi-objective optimization problems are discussed. Basic concepts of multi-level and ant colony optimization techniques are explained. Developed multi-objective ant colony optimization approach for engineering design is discussed. Uncertainty based models for multi-level optimization, are discussed in the next chapter.

CHAPTER 3 - UNCERTAINTY MODELS

In engineering design optimization, the design data are often assumed to be precisely known and the constraints are assumed to delimit a well-defined set of feasible solutions. However, incompleteness and uncertainty of input information are often encountered in practical situations. For example, the geometric parameters of components obtained through construction/manufacturability/machining process, are usually specified in terms of nominal values with tolerances. Many types of loads, such as wind, earthquake and snow loads are not know in precise but information from the past is available. Similarly, when material properties such as yield strength and young's modulus are experimentally determined, their values are found to exhibit scatter. Thus, all or most parameters involved in engineering design optimization problems are uncertain. Hence, it is important to consider uncertainty in the design and optimization of engineering systems.

There exist various mathematical models of uncertainty in engineering design optimization. These models can be broadly classified into probabilistic or stochastic models and non-probabilistic models which include fuzzy and interval models. A brief description of each of these models is given in this chapter. The uncertainty models are developed for the multi-level optimization and are detailed in this chapter.

3.1 Probabilistic/stochastic model

In the probabilistic model, the uncertain parameters are treated as random variables, which are described by suitable probability distributions. The prevailing model for uncertainties in engineering, especially structural engineering is stochastic model. The Probability Distribution Function (PDF) and Cumulative Distribution Function (CDF) are

used to define the occurrence properties of uncertain quantities which are random in nature.

3.1.1 Stochastic optimization

In some situations, the behavior or the distribution of the design data is known based on experiments. In such cases, it is easy to define the problem as a stochastic optimization problem. There are different methods available in literature to solve stochastic optimization problems. One of the methods is the conversion of a stochastic optimization problem to a deterministic optimization problem using chance constrained programming technique. In this method, objective function and constraints are expanded about their mean values and are redefined in terms of the mean and standard deviation of random variables. The resulting problem is an equivalent deterministic problem of the original stochastic problem. Present work uses this technique. A brief mathematical formulation of the stochastic approach is given next.

A stochastic nonlinear optimization problem can be stated as

Find X which minimizes $f(Y)$, subject to

$$P\left[g_j(Y) \leq 0\right] \geq p_j, \qquad j = 1,2,\dots,m \tag{3.1}$$

Where Y is the vector of n random variables $y_1, y_2, \dots, y_n$ and includes the decision variables $x_1, x_2, \dots, x_n$.The constraint equation indicates that the probability of the constraint being satisfied is greater than a certain specified probability.

The objective function $f(Y)$ is expanded about the mean values of $y_i, \bar{y}_i$, as

$$f(Y) = f(\overline{Y}) + \sum_{i=1}^{N} \left(\frac{\partial f}{\partial y_i}\Big|_{\bar{Y}} \right) (y_i - \bar{y}_i) + \text{higher order derivative terms} \quad (3.2)$$

Assuming that the standard deviations of $y_i, \bar{y}_i$, are small, $f(Y)$ is approximated using the first two terms as

$$f(Y) \cong (\overline{Y}) - \sum_{i=1}^{N} \left(\frac{\partial f}{\partial y_i}\Big|_{\bar{Y}} \right) \bar{y}_i + \sum_{i=1}^{N} \left(\frac{\partial f}{\partial y_i}\Big|_{\bar{Y}} \right) y_i \equiv \Psi(Y) \quad (3.3)$$

y_i is assumed to follow normal distribution and hence, $\Psi(Y)$ also follows normal distribution and its mean and variance are

$$\bar{\Psi} = \Psi(\bar{Y}) \quad (3.4)$$

$$Var(\Psi) = \sigma_{\Psi}{}^2 = \sum_{i=1}^{N} \left(\frac{\partial f}{\partial y_i}\Big|_{\bar{Y}} \right)^2 \sigma_{y_i}^2 \quad (3.5)$$

Using these values, a new objective function for the equivalent deterministic problem is given

$$F(Y) = k_1 \bar{\Psi} + k_2 \sigma_{\Psi} \quad (3.6)$$

Where k_1 and k_2 are positive constants and give the relative importance of the mean and standard deviation.

Similar to the objective function f, the constraint functions g_j can also be expanded around their mean values and approximated as:

$$g_j(Y) = g_j(\overline{Y}) + \sum_{i=1}^{N} \left(\frac{\partial g_j}{\partial y_i}\Big|_{\bar{Y}} \right) (y_i - \bar{y}_i) \quad (3.7)$$

From the above equation, the mean value, $\bar{g}_j$, and the standard deviation, σ_{g_j}, of $\bar{g}_j$ can be obtained as

$$\bar{g}_j = g_j(\overline{Y}) \tag{3.8}$$

$$\sigma_{g_j} = \left\{ \sum_{i=1}^{N} \left(\frac{\partial g_j}{\partial y_i}\Big|_{\bar{Y}} \right)^2 \sigma_{y_i}^2 \right\}^{1/2} \tag{3.9}$$

The constraints are to be satisfied with a minimum probability. This condition is stated as

$$P\left[g_j(Y) \leq 0\right] \geq p_j, \qquad j = 1,2,\dots,m \tag{3.10}$$

or

$$P\left[\frac{g_j(Y)-g_j(\overline{Y})}{\sigma_{g_j}} \leq \frac{0-g_j(\overline{Y})}{\sigma_{g_j}}\right] \geq p_j, \qquad j = 1,2,\dots,m \tag{3.11}$$

Considering

$$Z = \frac{g_j(Y)-g_j(\overline{Y})}{\sigma_{g_j}}; Z_1 = \frac{-g_j(\overline{Y})}{\sigma_{g_j}} \tag{3.12}$$

Eq. (3.11) becomes

$$P[Z \leq Z_1] \geq p_j, \qquad j = 1,2,\dots,m \tag{3.13}$$

or

$$\int_{-\infty}^{Z_1} f_Z(Z)dz \geq \int_{Z_0}^{\infty} f_Z(Z)dz \tag{3.14}$$

Where

$$Z_0 = -\emptyset_j(p_j) \tag{3.15}$$

$\emptyset_j(p_j)$ is the value of the standard normal variate corresponding to the probability p_j. The normal density functions are shown in Figure 3.1.

Thus,

$$-Z_1 \leq Z_0 \tag{3.16}$$

Substituting Eq. (3.12) and Eq. (3.15) in Eq. (3.16), the constraint is obtained as

$$\bar{g}_j + \emptyset_j(p_j)\,\sigma_{g_j} \leq 0, \quad j = 1,2,\ldots,m \tag{3.17}$$

Hence, the stochastic optimization problem is converted into an equivalent deterministic optimization problem given by Eq. (3.6) and Eq. (3.17).

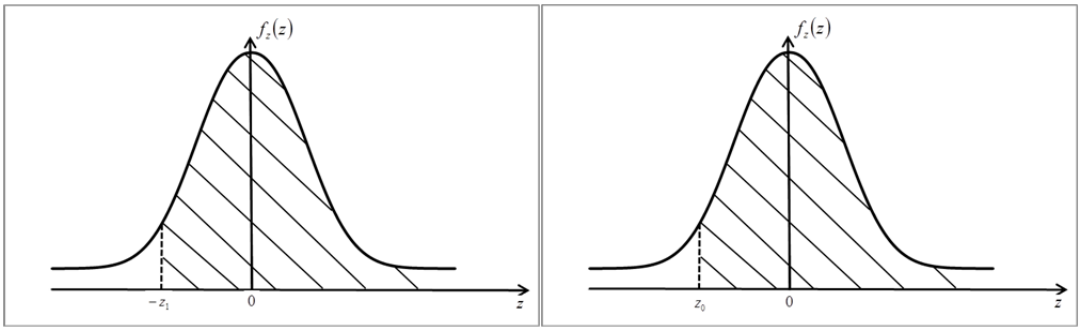

Figure 3.1 Normal density functions

3.2 Interval model

In some situations, the probability variation of the design data is unavailable and hence, the mean and standard deviation of the design variables cannot be determined. In such cases, the imprecision in the system can be defined by assuming a set of interval parameters for the design data. Hence, all the parameters are treated as interval numbers as A= [A-ΔA, A+ΔA] with A denoting the mean value and ΔA the deviation from the mean on either side. For example, the mean diameter of a shell, P can vary between $\underline{P}$

and $\overline{P}$ and hence, can be taken as an interval $[\underline{P}, \overline{P}]$. Also, it is to be noted that the interval parameters result in interval arithmetic being used in all the steps for calculation.

When the parameters of a system contain information and features that are vague, qualitative and linguistic, a fuzzy approach is used to predict the response. In the fuzzy model of engineering design problems, the uncertainty is modeled as fuzzy numbers rather than random values with certain distribution. In other words, the fuzzy model presents a possibility rather than a probability description of uncertainty. In order to develop a suitable method for processing convex fuzzy input parameters, the concept of α-level discretization is adopted (Rao and Sawyer (1995), Rao and Berke (1997)). This method ensures ease of numerical processing of fuzzy information. The core procedure is called α-level optimization (Mullen and Muhanna (1995, 1996, and 1999)). This procedure results in different levels and at each level there is a range of interval. This means that the fuzzy uncertainties are converted to interval uncertainties and hence, these uncertainties are bounded within a specified interval.

3.2.1 Interval optimization

In this procedure all the parameters are defined as interval numbers. Thus, the objective function and constraints are rewritten in terms of intervals. This requires solving the problem using interval arithmetic. A brief description of the interval arithmetic operations is given below.

Consider an interval number as $\tilde{x} = (\underline{x}, \overline{x}) \equiv (x_1, x_2)$ where the lower bound is given by $\underline{x} = x_1 = x_o - \Delta x$ and the upper bound is given by $\overline{x} = x_2 = x_o + \Delta x$. The value x_o represents the crisp or nominal value and Δx the tolerance on x. The set

$\{x_o \mid x_1 \le x_o \le x_2\}$ is a set of all real numbers between and including the endpoints x_1 and x_2.

Let '$\bullet$' denote any one of the arithmetic operations $(+,-,\times,\div)$ on real numbers x and y, then the corresponding interval arithmetic operation is given by $X \bullet Y = \{x \bullet y \mid x \in X, y \in Y\}$ where the interval $X \bullet Y$ contains every possible number that can be formed as $x \bullet y$ from the two intervals $X = [X_1, X_2]$ and $Y = [Y_1, Y_2]$. The basic interval arithmetic operations are given by

$$X + Y = [X_1 + Y_1, X_2 + Y_2] \tag{3.18}$$

$$X - Y = [X_1 - Y_2, X_2 - Y_1] \tag{3.19}$$

$$X.Y = \min[(X_1 \cdot Y_1, X_1 \cdot Y_2, X_2 \cdot Y_1, X_2 \cdot Y_2)], \max(X_1 \cdot Y_1, X_1 \cdot Y_2, X_2 \cdot Y_1, X_2 \cdot Y_2) \tag{3.20}$$

$$X \div Y = [X_1, X_2] \cdot [1/Y_2, 1/Y_1] \tag{3.21}$$

Note that the division operation $X \div Y$ is not defined if $0 \in [Y_1, Y_2]$. We can see that interval addition and interval multiplication are both associative and commutative. Interval computation can also be extended to matrices. This is given by:

$$[A][B] = [C] = c_{ij} \quad (p \times r) \tag{3.22}$$

With $[A] = a_{ij} = [\underline{a}_{ij}, \bar{a}_{ij}]$ $(p \times q), [B] = b_{ij} = [\underline{b}_{ij}, \bar{b}_{ij}] (q \times r)$, and the elements of the matrix $[C]$ are given by:

$$c_{ij} = \sum_{k=1}^{q} a_{ik} b_{kj}; \qquad i = 1,2,\cdots, p, \quad i = 1,2,\cdots, r, \tag{3.23}$$

where the multiplication rule is to be used for each product $a_{ik} b_{kj}$.

It is to be noted that after a certain number of interval operations, the width of the interval increases which makes it difficult to compare the numerical results. This is particularly a problem in complex engineering problems with several variables and parameters. To avoid this, a combinatorial approach or an interval-truncation approach (Rao and Berke (1997)) can be used. The truncation method is based on a comparison of the ranges of the input and output ranges of the parameters and computed responses.

There are several steps associated with solving problems with interval computations and in some of the steps using interval arithmetic may not only seem to be redundant, but also could result in an erroneous result, according to physics of the problem. In such cases, a combinatorial approach is used instead of the interval operation in order to comply with the physical logic of the problem. Hence, it is essential to develop the computational procedure based on the complexity of the equations in terms of the interval parameters.

In the interval optimization problems, since the objective functions and the design variables are all defined as interval functions, the solution of such problems requires interval computations at each and every step. Hence, during actual programming, order of the different interval parameters is adjusted in any specific equation. This is required during the execution of the program with the interval equations since the new order minimizes the computational time and leads to reduced and realistic interval ranges and hence, reasonably accurate solutions.

3.3 Multi-level stochastic optimization model

In present work, the multi-level optimization formulation under stochastic uncertainty is done using the chance constrained technique as described in section 3.1.1. The stochastic optimization problem at the system and component (disciple) level is converted to an equivalent deterministic optimization problem and then solved using the classical optimization algorithm (sequential quadratic programming (SQP)). The basic block diagram of the multi-level formulation is as shown in Figure 3.2. The system level stochastic objective function is a combination of the mean and standard deviation of the deterministic objective function. The stochastic constraints are to be satisfied with a certain level of probability. The system level equality constraints are approximated to deal with the uncertainty propagation between two levels.

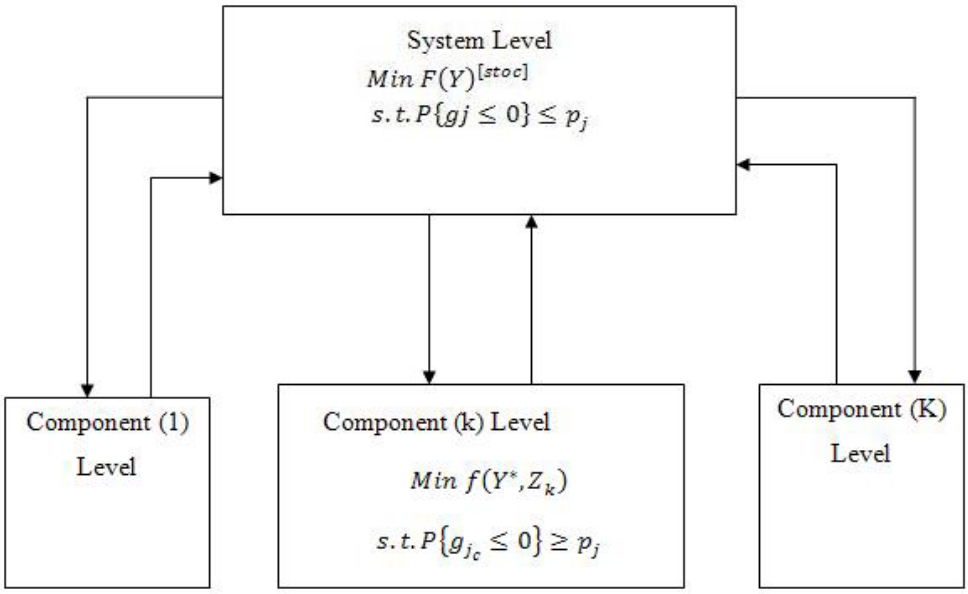

Figure 3.2 Block diagram for multilevel stochastic optimization

3.4 Multilevel interval optimization model

The concept of interval optimization (section 3.2.1) is used in the multi-level approach. The block diagram for ML Interval optimization developed in this work is shown in Figure 3.3. The system level and the component levels consist of interval functions. This is different from the deterministic multi-level approach. It can be seen from the figure that the deterministic variables as mentioned in the ML optimization, are changed to interval variables in the ML interval optimization with minimum and maximum values. In the multilevel interval optimization it is evident that the objective function and constraint values are all interval numbers. Hence, an overall objective function is constructed, which is minimized (or maximized) based on the mean values of the intervals. The interval values at the constraints are considered as extra sets of constraints to be satisfied.

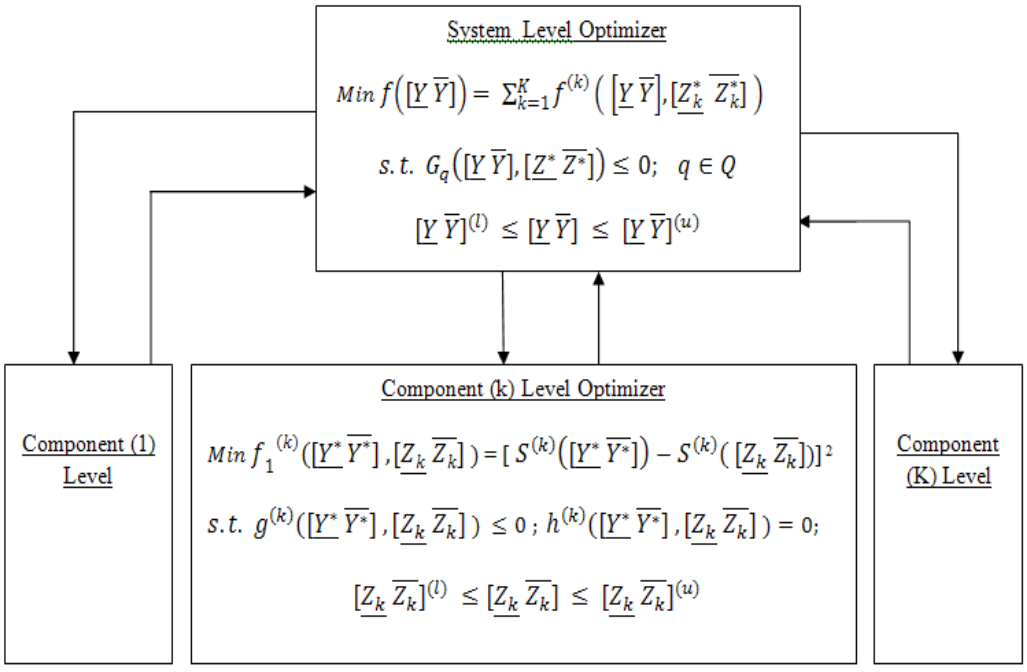

Figure 3.3 Block diagram for multilevel interval optimization

In this chapter, uncertainty models (stochastic and interval) are explained. The developed multi-level optimization models with stochastic and interval uncertainties are discussed. These models are applied to structural engineering problems in the next chapter.

CHAPTER 4 - STRUCTURAL DESIGN PROBLEMS

In this chapter, benchmark examples in structural design are considered. These problems are solved using the ant colony and multi-level approaches and the results are compared to those obtained using classical methods. The classical method used to solve these problems is Sequential Quadratic Programming (SQP) (Rao, (2009)). The structural examples considered are a ten bar plane truss and a twenty-five bar space truss.

4.1 Example 1: Ten bar plane truss

A ten bar plane truss example, taken from literature (Rajeev and Krishnamoorty (1992)), is solved using the classical method SQP for deterministic and stochastic formulations. Multi-level approach is then used to solve the problem and the sensitivity analysis is performed.

4.1.1 Deterministic formulation

Consider the ten bar plane truss, shown in Figure 4.1. This truss is required to support the given load condition shown in Table 4.1. It is to be designed with constraints on the member stresses as well as nodal displacements. The cross sectional areas of the members (A_i) are taken as the design variables with lower and upper bounds. The minimum allowable stresses for all members are specified by *s* in both tension and compression. The nodal coordinates and the design data for the truss are given in Table 4.2 and Table 4.3 respectively.

The vector of design variables is given as

$$X = \{A_i\} \ ; i=1,2,\ldots 10. \tag{4.1}$$

The objective function is total weight of the truss and is given by

$$f = \sum_{i=1}^{10} \rho A_i l_i \tag{4.2}$$

Stress and displacement constraints are

$$\sigma_i(X) \leq s \quad ; i = 1,2,\dots,10 \tag{4.3}$$

$$d_{kj} \leq \delta \quad ; k = 1,2,\dots,4 \; ; j = 1,2 \tag{4.4}$$

Where σ_i is the stress in member *i,* given by

$$\sigma_i(X) = {}^{P_{ai}}\!/_{A_i} \; ; i = 1, 2, \dots, 10 \tag{4.5}$$

where P_{ai} is the load , d_{kj} is the nodal displacement of node *k* along direction *j* (*j* = 1 for *x*, 2 for *y)*, *s* is the allowable stress, δ is the allowable nodal displacement of each node in both *x* and *y* directions, ρ is the density of the material and l_i represents the length of the i^{th} member.

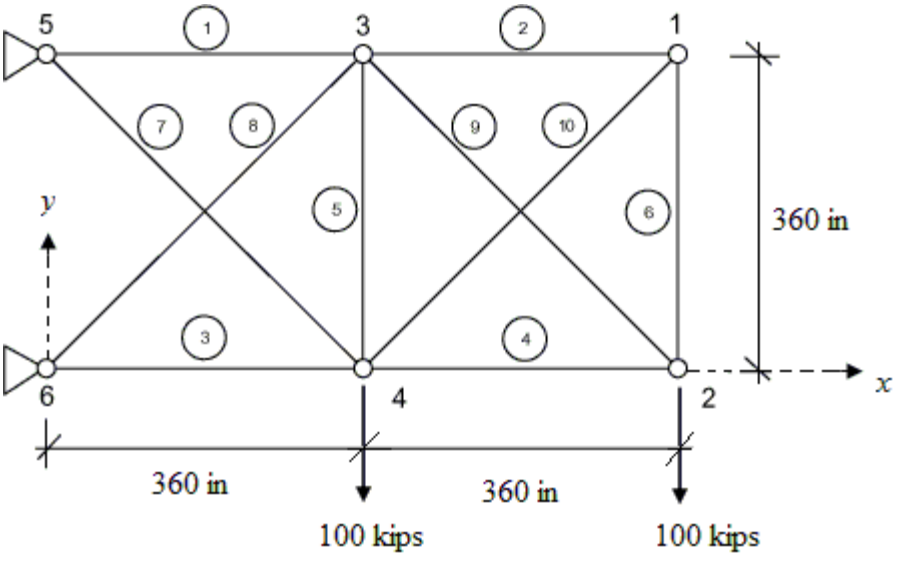

Figure 4.1 Ten bar plane truss

4.1.2 Stochastic formulation

The deterministic optimization problem for the ten bar truss is converted into a stochastic problem assuming the cross sectional areas of the truss members (A_i) density of the material (ρ), modulus of elasticity (E), allowable stress (s) and loads ($\vec{p}$) (as shown in Figure 4.1) on the members to be probabilistic, following normal distribution. The coefficient of variation of E, $\vec{p}$ and s is assumed to be 0.1(i.e. the standard deviation is 10% of the mean value). The coefficient of variation of A_i, and ρ is assumed to be 0.01. The objective is to minimize the sum of mean and standard deviation of the weight of the truss subjected to stress and displacement constraints. Constraints are assumed to be satisfied with a probability of at least 0.95. The vector of random variables (Y) is given by

$$Y = \begin{Bmatrix} A_i \\ \rho \\ E \\ s \\ \vec{p} \end{Bmatrix} \quad ; i = 1 \text{ to } 10 \tag{4.6}$$

As indicated earlier, ((Eq. (3.6)), the stochastic objective function is taken as

$$F(Y) = k_1 \bar{\Psi} + k_2 \sigma_{\Psi} \tag{4.7}$$

where k_1 and k_2 are constants equal to 1. Similar to the objective function f, the constraint functions g_j are also expanded about their mean values and approximated as outlined in section 3.1.1 (Eq. (3.7)). The new constraints are constructed as

$$\bar{g}_j + 1.645\, \sigma_{g_j} \leq 0, \qquad j = 1,2,\dots,m \tag{4.8}$$

4.1.3 Multilevel deterministic formulation

In the multi-level deterministic formulation of the 10 bar truss, two levels are considered. These two levels are specified as

a) System level: Design variables are taken as areas and the objective function is to minimize the weight. Constraints are that the nodal displacement of each node is less than or equal to 2.0 in in *x* and *y* directions.

b) Component level: Design variables are thickness (t_i) and mean diameter (d_i) (average of inner diameter ($d_{inner}^{(i)}$) and outer diameter ($d_{outer}^{(i)}$)) of the tubular cross section of the bars. Constraint is that stress in each member is less than the allowable stress. Objective function is obtained by taking the summation of the squares of the difference between the areas calculated using the areas (fixed) obtained from system level and the areas calculated using the thickness and mean diameter (design variables in component level). Formulation used in the multi-level process is given below:

<u>System level problem:</u>

Minimize $f(X) = \sum_{i=1}^{10} \rho A_i l_i$ (4.9)

Subject to

$d_{kj} \leq \ 2 \ ; k = 1,2, \dots, 4 \ ; j = 1,2$ (4.10)

and $X = \{A_i\} \ ; \ i = 1,2, \dots ,10$ (4.11)

<u>Component level problem:</u>

Minimize $f(X) = \sum_{i=1}^{10} (A_i - \pi d_i t_i)^2$ (4.12)

Subject to

$$\sigma_i(X) \leq 25000 \quad ; i = 1,2,\dots,10 \; ; \tag{4.13}$$

and $X = \{d_i, t_i\} \; ; \; i = 1,2,\dots,10$ (4.14)

where $d_i = \frac{d_{inner}^{(i)} + d_{outer}^{(i)}}{2}$ (4.15)

Algorithm/Procedure

1. Find the areas to minimize the weight with displacement constraint.
2. Find the mean diameter of each member with constraint as the stress constraint and objective function as the square of the difference in areas obtained from the design variables in the two levels.
3. Calculate the areas from the mean diameters (and the corresponding thicknesses) obtained in step 2 and check for convergence with areas in step 1. Stop if converged. Else take the calculated areas as the initial values and
4. Repeat steps 1 to 3 until convergence. The convergence criterion used in this example is based on the change in the system level objective function value during consecutive cycles (iterations between the two levels).

It is to be noted that in the above algorithm, only the mean diameter (d_i) is considered as a design variable in the system level since, the ratio d_i/t_i is fixed as 20.

4.1.4 Multilevel stochastic formulation

In this approach, both the levels in the multilevel process are considered as stochastic. At each level, the probabilistic problem is converted into an equivalent deterministic

problem and then solved. At the system level, the objective is to minimize the sum of mean and standard deviation of the weight of the truss. Constraints at the system level are the displacement constraints which are to be satisfied with a probability of at least 0.95. Design variables are taken as cross section areas of each member. At the component level, the objective is to minimize the discrepancy between the areas obtained from the system level and the areas calculated at the component level. At the component level, the stress constraints are probabilistic and are to be satisfied with a probability of at least 0.95. Component level design variables are the mean diameter and thickness of each member.

System level problem:

Minimize $f(X) = k_1 \bar{\Psi} + k_2 \sigma_{\Psi}$ (4.16)

Subject to

$P[d_{kj} \leq 2] \geq 0.95 \; ; k = 1,2,\dots,4 \; ; j = 1,2$ (4.17)

and $X = \{A_i\} \; ; \; i = 1,2,\dots,10$ (4.18)

Component level problem:

Minimize $f(X) = \sum_{i=1}^{10} (A_i - \pi d_i t_i)^2$ (4.19)

Subject to

$P[\sigma_i(X) \leq 25000] \geq 0.95 \quad ; i = 1,2,\dots,10 \; ;$ (4.20)

and $X = \{d_i, t_i\} \; ; \; i = 1,2,\dots,10$ (4.21)

The results obtained by the deterministic approach, for the 10-bar truss, are tabulated in Table 4.4. Both discrete and continuous variables are considered. For continuous optimization, SQP is used and for discrete optimization ACO is used in the present work. The results are compared with those in literature (Rajeev and Krishnamoorthy (1992)). Although buckling is an important consideration in the design of truss structures, it is not considered in the present work because the original reference (Rajeev and Krishnamoorthy (1992)) did not consider buckling. The purpose of this example is to compare the results obtained by the present methods (continuous and discrete optimization) with those given by Rajeev and Krishnamoorthy (1992) and to demonstrate the developed ML deterministic and stochastic approaches.

It can be seen from the table , that the minimum weight obtained using the discrete variable values is 5536.6276 lb. whereas the minimum weight obtained using the continuous variables is 5482.6314 lb. Also, the minimum weights obtained in both the cases (discrete and continuous) are lower than that reported by Rajeev and Krishnamoorthy (1992) (5613.8413 lb). In SQP, the initial design value is randomly chosen as 2 in^2 for each of the design variables and the initial weight is obtained as 839.2319 lb. At the initial point, there are no active constraints. In SQP, the number of iterations and the number of function evaluations for convergence is 22 and 246 respectively. The discrete set used for ACO is given in Table 4.5. In ACO, a set of 25 ants is used and it took 550 iterations to converge.

Multi-level approach (ML) is used to solve the 10-bar truss problem and the results obtained are compared with those of the deterministic approach or the All-in-one (AIO) approach as shown in Table 4.6. Both AIO and ML methods use SQP for their solution. It

can be seen from the table that the minimum weight obtained by AIO approach is 5482.6314 lb. while the minimum weight obtained using the present ML approach is 5482.8334 lb. The number of iterations taken to reach the optimum design in AIO approach is 23 while in ML approach it is 24. Also, the number of objective function evaluations is 255 in AIO and 807 in ML. The initial design for the AIO and ML approaches is randomly chosen with area as 2 in^2 for each of the design variable. Initial value of the objective function (weight) is 839.2319 lb. There are no active constraints at the initial design point. At the optimum solution (both AIO and ML approaches), the displacement along y direction is active for node 2. Details of convergence of the ML deterministic optimization are given in Table 4.7 and Table 4.8. Table 4.7 shows the convergence of the design variables for every iteration between the system and the component levels. From the table it is evident that the convergence in the ML process is achieved in 9 cycles (iterations between the levels). Variation of the weight at the end of every iteration between the two levels is given in Table 4.8. The convergence is evident with equal values of weight in both the levels at the final design.

Table 4.1 Load conditions for 10 bar truss

Node	F_x (lb)	F_y (lb)
2	0	-100000
4	0	-100000

Table 4.2 Nodal coordinates for 10 bar truss

Node	x (in)	y (in)
1	720	360
2	720	0
3	360	360
4	360	0
5	0	360
6	0	0

Table 4.3 Design data for 10 bar truss

Young's modulus $(E) = 10^7$ psi Material density (ρ) = 0.1 lb/in^3 Lower bounds on the area of cross section $(A_i^{(l)})$ = 1.62 in^2 Upper bounds on the area of cross section $(A_i^{(u)})$ = 33.5 in^2 Lower bounds on the mean diameter $(d_i^{(l)})$ = 3.21 in Upper bounds on the mean diameter $(d_i^{(u)})$ = 14.6 in $d_i/t_i = 20$ Maximum allowable stress (s) = ±25000 psi Maximum allowable nodal displacement (δ) = 2 in

Table 4.4 Results obtained for 10-bar bar truss (deterministic optimization)

Quantity	Rajeev and Krishnamoorty (1992)	Present work (discrete)	Present work (continuous)
Design variables: (in^2)			
A_1	33.5000	33.5000	32.2357
A_2	1.6200	1.6200	1.6200
A_3	22.0000	22.9000	23.2959
A_4	15.5000	14.2000	15.2624
A_5	1.6200	1.6200	1.6200
A_6	1.6200	1.6200	1.6200
A_7	14.2000	11.5000	8.3064
A_8	19.9000	22.0000	22.6870
A_9	19.9000	19.9000	21.5843
A_{10}	2.6200	1.9900	1.6200
Objective function:			
weight (lb)	5613.8413	5536.6276	5482.6314

Table 4.5 Discrete variable set for 10-bar truss

SI	{ 1.62, 1.80, 1.99, 2.13, 2.38, 2.62, 2.63, 2.88, 2.93, 3.09, 3.13, 3.38, 3.47, 3.55, 3.63, 3.84, 3.87, 3.88, 4.18, 4.22, 4.49, 4.59, 4.80, 4.97, 5.12, 5.74, 7.22, 7.97, 11.5, 13.5, 13.9, 14.2, 15.5, 16.0, 16.9, 18.8, 19.9, 22.0, 22.9, 26.5, 30.0, 33.5}

Table 4.6 Results of AIO and multilevel deterministic optimization of 10-bar truss

AIO approach			ML approach	
Quantity	Initial design	Optimum design	Initial design	Optimum design
Design variables: (areas in in^2)				
A_1	2	32.2357	2	32.2354
A_2	2	1.6200	2	1.6200
A_3	2	23.2959	2	23.2958
A_4	2	15.2624	2	15.2624
A_5	2	1.6200	2	1.6200
A_6	2	1.6200	2	1.6200
A_7	2	8.3064	2	8.3063
A_8	2	22.6870	2	22.6872
A_9	2	21.5843	2	21.5844
A_{10}	2	1.6200	2	1.6200
Objective function:				
Weight (lb)	839.2319	5482.6314	839. 2319	5482.8334

Table 4.7 Optimum design vectors at each cycle in the multi-level deterministic optimization of 10 bar truss

cycle	optimum design vectors at system level and component level	
1	x^*	{4.3021, 1.6200, 6.1951, 1.6200, 1.6200, 1.6200, 1.6200, 2.9502, 1.6200, 1.6200}
	d^*	{6.5910, 3.3915, 7.6432, 4.2244, 3.3914, 3.2504, 6.8267, 5.0576, 5.0237, 3.5999}
2	x^*	{14.4896, 1.6200, 13.0617, 4.6637, 1.6200, 1.6200, 5.3582, 16.3488, 6.5780, 2.2339}
	d^*	{9.6044, 3.2116, 9.1188, 3.2116, 9.6044, 3.2114, 5.8405, 10.2019, 6.4712, 3.7714}
3	x^*	{16.8721, 1.6200, 19.4950, 5.0304, 1.7748, 1.6200, 7.2727, 13.0755, 6.7651, 2.3326}
	d^*	{10.3639, 3.2114, 11.1405, 5.6590, 3.3614, 3.2114, 6.8044, 9.1237, 6.5626, 3.8535}
4	x^*	{22.4291, 1.6200, 19.6018, 11.7403, 1.6200, 1.6200, 7.3040, 14.9384, 20.5186, 1.6200}
	d^*	{11.9494, 3.2115, 11.1709, 8.6453, 11.9494, 3.2113, 6.8190, 9.7520, 11.4292, 3.2115}
5	x^*	{33.2304, 1.6200, 23.5700, 10.2469, 1.6200, 1.6200, 9.5976, 20.9939, 16.7425, 1.6200}
	d^*	{14.5448, 3.2114, 12.2496, 8.0768, 3.2114, 3.2114, 7.8167, 11.5608, 10.3240, 3.2114}
6	x^*	{27.4168, 1.6200, 22.3436, 15.6417, 1.6200, 1.6200, 6.9561, 25.5262, 22.1660, 1.6200}
	d^*	{13.2114, 3.2115, 11.9266, 9.9789, 3.2115, 3.2115, 6.6546, 12.7478, 11.8791, 3.2113}
7	x^*	{32.1050, 1.6200, 23.2814, 15.0664, 1.6200, 1.6200, 8.6258, 22.5563, 21.6120, 1.6200}
	d^*	{14.2964, 3.2114, 12.1743, 9.7936, 3.2114, 3.2114, 7.4104, 11.9832, 11.7297, 3.2114}
8	x^*	{32.2521, 1.6200, 23.2732, 15.2828, 1.6200, 1.6200, 8.3099, 22.6672, 21.5905, 1.6200}
	d^*	{14.3291, 3.2115, 12.1722, 9.8637, 3.2115, 3.2115, 7.2735, 12.0126, 11.7239, 3.2115}
9	x^*	{32.2354, 1.6200, 23.2958, 15.2624, 1.6200, 1.6200, 8.3063, 22.6872, 21.5844, 1.6200}
	d^*	{14.3254, 3.2115, 12.1781, 9.8572, 3.2115, 3.2115, 7.2720, 12.0180, 11.7222, 3.2115}

x^* - system level areas in in^2; d^* - component level mean diameters in in

Table 4.8 Convergence results of multi-level deterministic optimization of 10 bar truss

cycle	f^* (system level)	$f^{(0)}$ (component level)	f^* (component level)	Weight (component level)
1	1008.8090	294.8124	47.2356	1749.4751
2	2888.4713	306.3289	1.7133e-07	2888.5031
3	3169.9863	398.1729	8.94888e-09	3169.9855
4	4370.2372	739.8193	3.5017e-08	4370.2412
5	5080.9941	1320.3768	6.3799e-10	5080.9930

6	5394.1405	1342.0169	3.1148e-08	5394.1400
7	5481.5733	1455.9496	7.9532e-09	5481.5668
8	5482.8306	1468.3549	1.1976e-07	5482.8602
9	5482.8334	1468.3545	8.1974e-08	5482.8602

f^* - optimum value ; $f^{(0)}$ - initial value

The results obtained by the stochastic optimization using both the AIO and ML approaches are given in Table 4.9. Two cases are considered. Case 1 denotes the minimization of the mean value of the weight of the truss and Case 2 denotes the minimization of the linear sum of mean and standard deviation of the weight. It can be seen that the minimum value of the objective function obtained using the AIO approach in both the cases, is greater than the deterministic value of 5482.6314 lb. This is as expected because of the randomness of the variables in stochastic optimization. When comparing the optimized weights in the AIO and ML stochastic optimizations, it is evident that the ML approach converged to greater values (6482.4012 lb and 6552.5127 lb) than the AIO approach (5692.1382 lb and 5753.6054 lb). Also, the number of iterations and number of function evaluations for ML approach with combined objective function are 34 and 189 respectively. In the case of AIO approach, the corresponding numbers are found to be 26 and 290. For the AIO and ML stochastic approaches, the initial design is chosen randomly with area as 2 in^2 for each of the design variables. The mean value of the objective function at the initial design point is 839.2319 lb and the standard deviation is 8.8763 lb. There are no active constraints at the initial design point. At the optimum designs, the displacement along y direction for node 2 is active. The mean value and standard deviation of the weight at the final design are found to be 5692.1 lb and 61.5 lb for the AIO approach and 6482.4 lb and 70.1 lb for the ML approach.

Details of convergence of the ML stochastic optimization are given in Table 4.10 and Table 4.11. Variation of the weight at the end of each iteration between the two levels is given in Table 4.10. Table 4.11 shows the convergence of the design variables for every iteration between the system and the component levels. From the table it is evident that the convergence in the ML process is achieved in 7 cycles (iterations between the levels).

Table 4.9 Results of AIO and multilevel stochastic optimization of 10-bar truss

AIO approach				ML approach		
Quantity	Initial design	Optimum design		Initial design	Optimum design	
		Case 1[@]	Case 2 [&]		Case 1	Case 2
Design Variables: (area in in^2)						
A_1	2	33.5033	33.5033	2	33.4898	33.5033
A_2	2	1.6184	1.6184	2	1.6184	1.6184
A_3	2	24.3474	24.3516	2	28.6743	28.6792
A_4	2	16.0015	16.0057	2	19.1785	19.1838
A_5	2	1.6184	1.6184	2	1.6184	1.6184
A_6	2	1.6184	1.6184	2	1.6184	1.6184
A_7	2	8.5298	8.5372	2	9.8335	9.8420
A_8	2	23.6446	23.6355	2	27.8539	27.8438
A_9	2	22.3545	22.3503	2	27.0597	27.0541
A_{10}	2	1.6184	1.6184	2	1.6184	1.6184
Objective function: ($f(X)$)	848.108	5692.1382	5753.6056	848.108	6482.4012	6552.5127

[@] mean of weight, [&] linear sum of mean and standard deviation of weight (Eq. 3.6)

Table 4.10 Convergence results of multi-level stochastic optimization of 10 bar truss

cycle	f^* (system level)	$f^{(0)}$ (component level)	f^* (component level)	weight (component level)
1	1028.8023	292.6415	0.0976	2095.6345
2	3520.7134	468.9023	1.2346e-04	3483.0845
3	4482.7845	841.2034	4.2159e-05	4434.5671
4	5310.4675	1170.2936	3.5601e-06	5253.7812
5	6436.7982	2094.8734	4.7675e-03	6367.4563
6	6552.2017	2168.6532	6.2502e-09	6481.5643
7	6552.5127	2171.1098	1.7309e-06	6481.9029

f^* - optimum value ; $f^{(0)}$ - initial value

Table 4.11 Optimum design vectors at each cycle in the multi-level stochastic optimization of 10 bar truss

cycle	optimum design vectors at system level and component level	
1	x^*	{4.5260, 1.6184, 1.6184, 1.6184, 1.6184, 1.6184, 3.1071, 1.6184, 1.6184, 1.6184}
	d^*	{7.3234, 3.5769, 8.3976, 4.7569, 3.2127, 3.5771, 7.3919, 5.6079, 5.6140, 3.9052}
2	x^*	{18.7818, 1.6184, 15.5933, 1.6184, 1.6184, 1.6184, 5.9682, 19.5846, 8.0035, 2.4928}
	d^*	{10.9347, 3.2099, 9.9634, 6.4516, 3.2101, 3.2099, 6.1640, 11.1660, 7.1380, 3.9838}
3	x^*	{22.2766, 1.6184, 19.9571, 1.6184, 1.6184, 1.6184, 7.7246, 25.0699, 10.9228, 1.6184}
	d^*	{11.9087, 3.2098, 11.2717, 8.7327, 3.2098, 3.2098, 7.0126, 12.6333, 8.3389, 3.2098}
4	x^*	{27.7009, 1.6184, 20.2112, 1.6184, 1.6184, 10.3562, 22.6258, 22.1200, 1.6184}
		{13.2797, 3.2096, 11.3432, 3.2096, 3.2100, 3.2096, 8.1197, 12.0017, 11.8668,

cycle	optimum design vectors at system level and component level	
	d^*	3.2101}
5	x^*	{33.5033, 17.4770, 29.9912, 17.4770, 1.6184, 1.6184, 10.6137, 27.4819, 24.6745, 1.6184}
	d^*	{14.6015, 3.2098, 13.8177, 10.5480, 3.2099, 3.2099, 8.2200, 13.2271, 12.5333, 3.2097}
6	x^*	{33.5033, 1.6184, 28.8024, 19.1390, 1.6184, 1.6184, 9.9636, 27.7448, 26.9690, 1.6184}
	d^*	{14.6015, 3.2098, 13.5411, 11.0382, 3.2097, 3.2097, 7.9644, 13.2902, 13.1030, 3.2098}
7	x^*	{33.5033, 1.6184, 28.6792, 19.1838, 1.6184, 1.6184, 9.8420, 27.8438, 27.0541, 1.6184}
	d^*	{14.6015, 3.2098, 13.5121, 11.0511, 3.2098, 3.2098, 7.9156, 13.3139, 13.1237, 3.2098}

x^* - system level areas in in^2; d^* - component level mean diameters in in

4.1.5 Sensitivity analysis

In order to study the effect of randomness of the uncertain parameters in the ML approach, different numerical experiments were conducted for the 10 bar truss example. The standard deviation (SD) of all the random variables was changed from 1% to 10% of the corresponding mean values. The results obtained from the multilevel optimization with new values of standard deviation of random variables are shown in the Figure 4.2 and the corresponding values are given in Table 4.12. Two cases are considered. Case 1 denotes the minimization of the mean value of the weight of the truss and Case 2 denotes the minimization of the linear sum of mean and standard deviation of the weight.

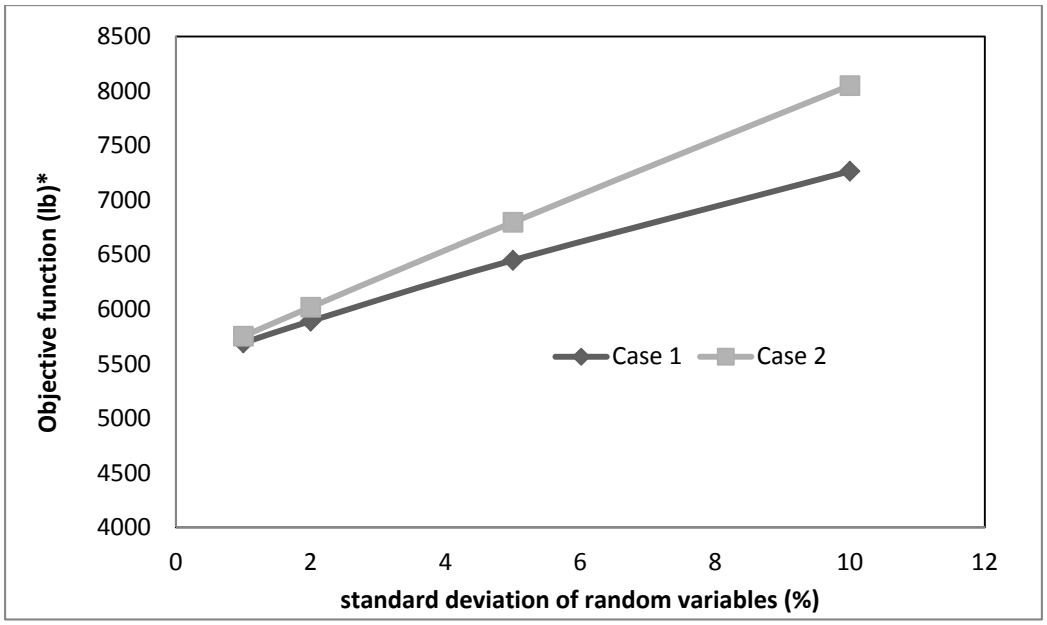

*Case 1- mean of weight, Case 2 - linear sum of mean and standard deviation of weight (Eq. 3.6).

Figure 4.2 Sensitivity of objective function to changes in standard deviation of random variables in ML stochastic approach

Table 4.12 Variation of objective function to changes in standard deviation of random variables in ML stochastic approach

SD* (%)	Case 1@	Case 2&	Mean of weight	SD of weight
1.0	5692.0	5753.6	5692.0	61.6
2.0	5891.9	6019.3	5891.9	127.4
5.0	6450.0	6798.7	6450.0	348.7
10.0	7265.6	8051.6	7265.6	785.9

* standard deviation, @ mean of weight, & linear sum of mean and standard deviation of weight (Eq. 3.6).

It can be seen from Figure 4.2 that, the optimized objective function value increases with an increase in the standard deviation (%) of the random variables from 1% to 10%, in both cases. Also, at 1% standard deviation of random variables, the difference between the optimum values of the objective functions (5692.0 lb and 5753.6 lb), in both cases, is less and increases with an increase in the standard deviation (%) of the random variables.

The values of the optimized objective functions, in both cases, for the ML and AIO approaches are given in Table 4.12 .

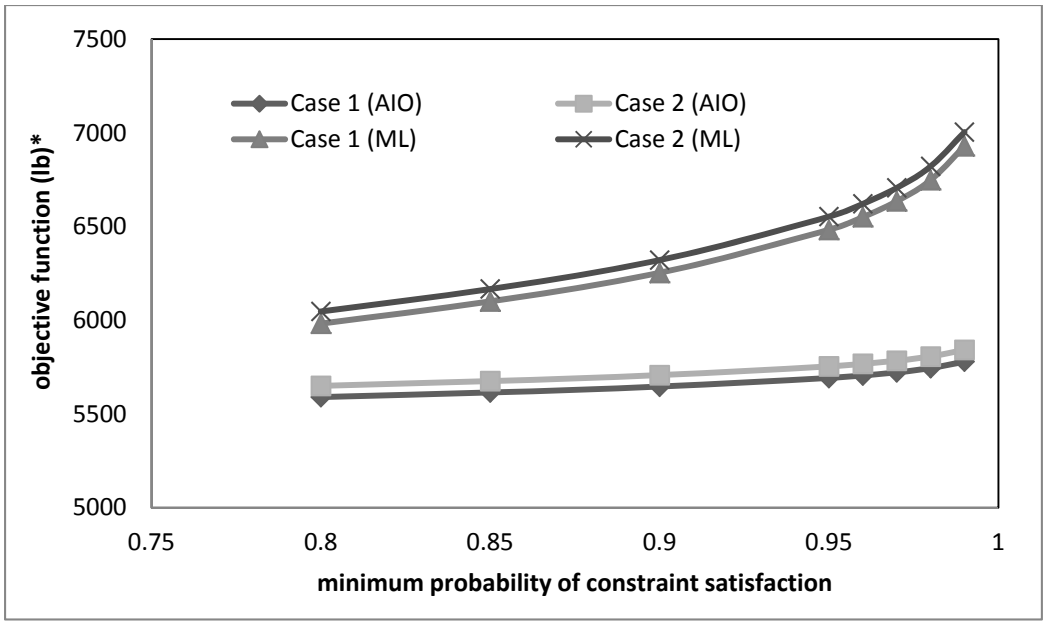

*Case 1- mean of weight, Case 2 - linear sum of mean and standard deviation of weight (Eq. 3.6).

Figure 4.3 Sensitivity of objective function with respect to the probability of constraint satisfaction

Further, the variation of the optimal objective function value with respect to the minimum probability level at which the constraints are satisfied is shown in Figure 4.3. The corresponding values (of the optimum objective function) along with the mean and standard deviation are given in Table 4.13. Similar to the previous analysis (sensitivity with variation in standard deviation), two cases are considered with mean value of weight and a linear sum of mean and standard deviation of weight as objective functions. From Figure 4.3, it is evident that the AIO approach gives an optimum value lower than the ML approach in both the cases. It can be noticed that in both the approaches, the optimum objective function value increases with increase in the probability level of constraint satisfaction.

Table 4.13 Variation of objective function with probability of constraint satisfaction

Probability	Case 1 (AIO)	Case 2 (AIO)	Mean	SD	Case 1 (ML)	Case 2 (ML)	Mean	SD
0.80	5589.7	5650.2	5589.8	60.4	5981.8	6046.5	5981.8	64.7
0.85	5614.6	5675.3	5614.6	60.7	6100.7	6166.7	6100.7	66.0
0.90	5645.8	5706.8	5645.8	61.0	6252.7	6320.3	6252.7	67.6
0.95	5692.0	5753.5	5692.0	61.5	6482.4	6552.5	6482.4	70.1
0.96	5705.5	5767.2	5705.5	61.7	6550.3	6621.1	6550.3	70.9
0.97	5722.1	5784.0	5722.2	61.8	6634.5	6706.2	6634.5	71.8
0.98	5744.2	5806.4	5744.3	62.1	6747.5	6820.5	6747.5	73.0
0.99	5779.2	5841.7	5779.2	62.5	6928.5	7003.5	6928.5	75.0

Case 1- mean of weight, Case 2 - linear sum of mean and standard deviation of weight (Eq. 3.6),
SD – standard deviation

4.2 Example 2: Twenty-five bar space truss

The 25-bar space truss shown in Figure 4.4 is to be optimized for three objectives with constraints on the member stresses as well as Euler buckling (Rao (2009)). The member areas are linked to define the design variables as shown in Table 4.14. Thus, there are eight independent areas considered as design variables with lower and upper bounds on each of the variables. The nodal coordinates and the design data for the truss are given in Table 4.15 and Table 4.16. Two load conditions are considered at nodes 1, 2, 3 and 6 in the x, y and z directions Table 4.17. Members are assumed to be tubular with nominal diameter (d_i) and thickness (t_i). Three objective functions considered are: minimization of weight, minimization of deflection of node 1 under both load conditions and maximization of fundamental natural frequency of vibration (ω_n) of the truss.

The objective functions can be expressed as:

$$f_1 = \sum_{i=1}^{25} \rho A_i l_i \tag{4.22}$$

$$f_2 = \sum_{i=1}^{2} \left(\delta_{xi}^2 + \delta_{yi}^2 + \delta_{zi}^2\right)^{1/2} \tag{4.23}$$

$$f_3 = \omega_n \tag{4.24}$$

where A_i and l_i are the area of cross section and length of the i^{th} member respectively. δ_{xi}, δ_{yi} and δ_{zi} are the x, y and z components of displacement of node 1 for load condition i (i =1,2). Stress and buckling constraints on members are stated as:

$$\sigma_{ij}(X) \leq 40000\ psi \text{ (tension and compression)}\ ;\ \ i = 1,2,\dots,25;\ \ j = 1,2 \tag{4.25}$$

$$\sigma_{ij}\,(X) \leq p_i(X)\ ;\ \ i = 1,2,\dots,25;\ \ j = 1,2 \tag{4.26}$$

where $\sigma_{ij}(X)$ is the stress in member i for load condition j and $p_i(X)$ is the buckling stress in member i ($i=1,2,\dots,25$) given by

$$p_i(X) = {}^{100.01\pi E A_i}\Big/_{8l_i^2} \tag{4.27}$$

The buckling stress in Eq. 4.27 is derived as below:

$$p_i(X) = p_b/A_i \tag{4.28}$$

where p_b is the buckling load and is given by

$$p_b = {}^{\pi^2 E I_i}\Big/_{l_i^2} \tag{4.29}$$

where I_i is the area moment of inertia of each member i and is given by

$$I_i = \frac{\pi}{8} d_i t_i (d_i^2 + t_i^2) \tag{4.30}$$

Substituting Eq. 4.29, Eq. 4.30 and ${}^{d_i}/_{t_i} = 100$ in Eq. 4.28 gives Eq. 4.31.

Also, the mean diameter (d_i) and thickness (t_i) are derived in terms of the member areas (A_i) as below:

$$A_i = \pi d_i t_i \tag{4.31}$$

$$\text{since } {}^{d_i}/_{t_i} = 100 \tag{4.32}$$

$$A_i = \pi * 100 * t_i^2 \tag{4.33}$$

$$t_i = \sqrt{\frac{A_i}{100\pi}} \tag{4.34}$$

$$\text{Similarly, } d_i = \sqrt{\frac{100A_i}{\pi}} \tag{4.35}$$

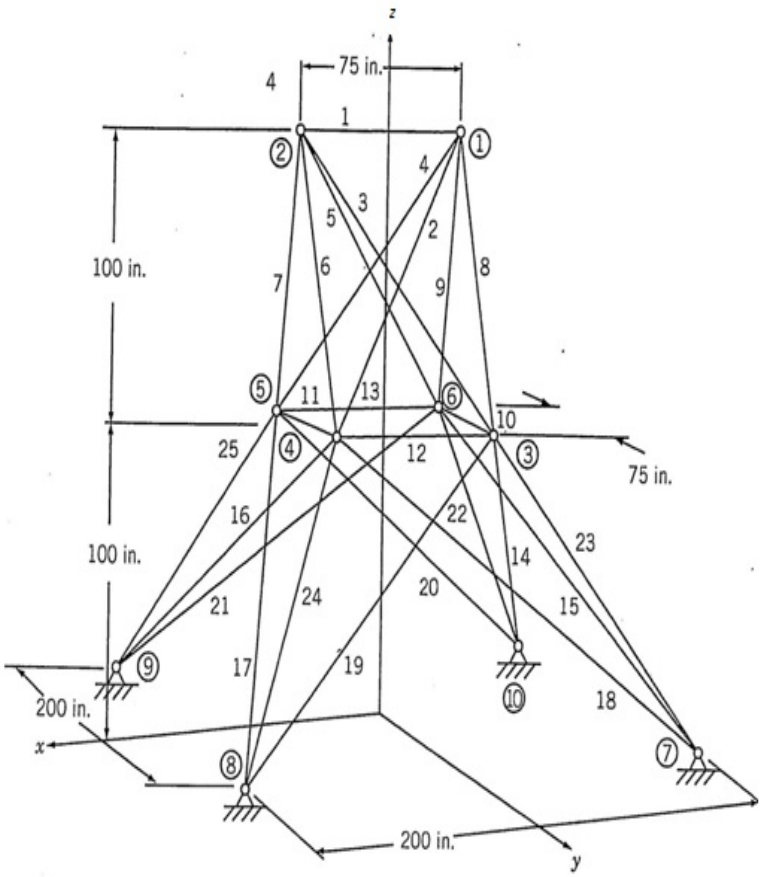

Figure 4.4 Twenty-five bar space truss (Rao (2009))

Table 4.14 Design variables corresponding to areas of truss members

Design Variable	Member Area
x_1	A_1
x_2	A_2, A_3, A_4, A_5
x_3	A_6, A_7, A_8, A_9
x_4	A_{10}, A_{11}
x_5	A_{12}, A_{13}
x_6	$A_{14}, A_{15}, A_{16}, A_{17}$
x_7	$A_{18}, A_{19}, A_{20}, A_{21}$
x_8	$A_{22}, A_{23}, A_{24}, A_{25}$

Table 4.15 Coordinates for 25 bar truss

Node	x (in)	y (in)	z (in)
1	-37.5	0.0	200.0
2	37.5	0.0	200.0
3	-37.5	37.5	100.0
4	37.5	37.5	100.0
5	37.5	-37.5	100.0
6	-37.5	-37.5	100.0

Node	x (in)	y (in)	z (in)
7	-100.0	100.0	0.0
8	100.0	100.0	0.0
9	100.0	-100.0	0.0
10	-100.0	-100.0	0.0

Table 4.16 Design data for 25 bar truss

Young's modulus $(E) = 10^7$ psi Material density (ρ) = 0.1 lb/in^3 Lower bounds on the area of cross section $(A_i^{(l)})$ = 0.1 in^2 Upper bounds on the area of cross section $(A_i^{(u)})$ = 5 in^2 Maximum allowable stress (s) = ±40,000 psi

Table 4.17 Load conditions for 25-bar truss

	Joint			
	1	2	3	6
	Load Condition 1, Loads in Pounds			
F_x	0	0	0	0
F_y	20,000	-20,000	0	0
F_z	-5,000	-5,000	0	0
	Load Condition 2, Loads in Pounds			
F_x	1,000	0	500	500
F_y	10,000	10,000	0	0
F_z	-5,000	-5,000	0	0

The 25-bar truss optimization problem is solved using the SQP procedure considering each of the objectives separately. The results obtained are given in Table 4.18. These results are compared to those given by Rao (2009) Table 4.19. It can be seen that the minimum weight obtained in the present method is 232.3612 lb and the minimum weight obtained by Rao (2009) is 233.07265 lb. Minimum deflection obtained in the present method is 0.30931 in and that obtained by Rao (2009) is 0.30834 in and the maximum frequency obtained by the present work is 113.8905 Hz whereas the maximum frequency obtained in Rao (2009) is 108.6224 Hz. Hence, the minimum weight and deflection obtained by both methods is almost the same whereas the frequency is slightly higher in the present work. This is due to more number of active constraints at the optimum point.

The number of iterations for convergence, in the minimization of weight is 10, in the minimization of deflection is 4 and in maximization of frequency is 16. The corresponding values for the number of objective function evaluations are 90, 36 and 145 respectively.

Table 4.18 Results of single objective optimization of 25-bar truss (SQP)

Quantity	Minimization of weight	Minimization of deflection	Maximization of frequency
Design variables: (in^2)			
x_1	0.1	0.4550	0.1021
x_2	0.8008	5.0	0.7789
x_3	0.7438	5.0	0.7564
x_4	0.1	0.1115	1.2030
x_5	0.1288	0.8194	0.1
x_6	0.5690	5.0	5.0
x_7	0.9737	5.0	3.1062
x_8	0.8023	5.0	5.0
Objective functions:			
weight $f_1(\vec{X})$ (lb)	232.3612	1483.5389	947.5341
deflection $f_2(\vec{X})$ (in)	1.9311	0.30931	1.2772
frequency $f_3(\vec{X})$ (Hz)	73.4926	73.1503	113.8905

Constraints: number of active behavior constraints	9[§]	0	5[$]

[§] buckling stress in members 2, 5, 7, 8, 19 and 20 in load condition1 and in members 12, 16 and 24 in load condition 2. [$] buckling stress in members 1, 2, 5, 7 and 8 in load condition1.

Table 4.19 Results of single objective optimization of 25-bar truss (Rao (2009))

Quantity	Minimization of weight	Minimization of deflection	Maximization of frequency
Design variables: (in^2)			
x_1	0.1	3.7931	0.1
x_2	0.80228	5.0	0.79769
x_3	0.74789	5.0	0.74605
x_4	0.1	3.3183	0.72817
x_5	0.12452	5.0	0.84836
x_6	0.57117	5.0	1.9944
x_7	0.97851	5.0	1.9176
x_8	0.80247	5.0	4.1119
Objective functions:			
weight $f_1(\vec{X})$ (lb)	233.07265	1619.3258	600.87891
deflection $f_2(\vec{X})$ (in)	1.924989	0.30834	1.35503
frequency $f_3(\vec{X})$ (Hz)	73.25348	70.2082	108.6224

Quantity	Minimization of weight	Minimization of deflection	Maximization of frequency
Constraints: number of active behavior constraints	9[§]	0	4[$]

[§] buckling stress in members 2, 5, 7, 8, 19 and 20 in load condition1 and in members 13, 16 and 24 in load condition 2. [$] buckling stress in members 2, 5, 7 and 8 in load condition1.

The 25-bar truss design considered in Figure 4.4 is a benchmark example and does not represent a practical case. Hence, in the present work, a new 25-bar truss design is formulated (with modifications to the existing truss) to represent a design closer to a practical case. The new truss is shown in Figure 4.5. The mean diameter (d_i) to thickness (t_i) ratio for each member of the new 25-bar truss is fixed to 20. The optimization problem formulation for the new truss is similar to the original truss (given by Eq. (4.22 – 4.26)) with the buckling stress $p_i(X)$ for the new 25-bar truss design, for d_i/t_i = 20, is given by

$$p_i(X) = \frac{2.5\pi E A_i}{l_i^2} \tag{4.36}$$

It is to be noted that Eq. 4.36 is derived similar to Eq. 4.27 using d_i/t_i = 20.

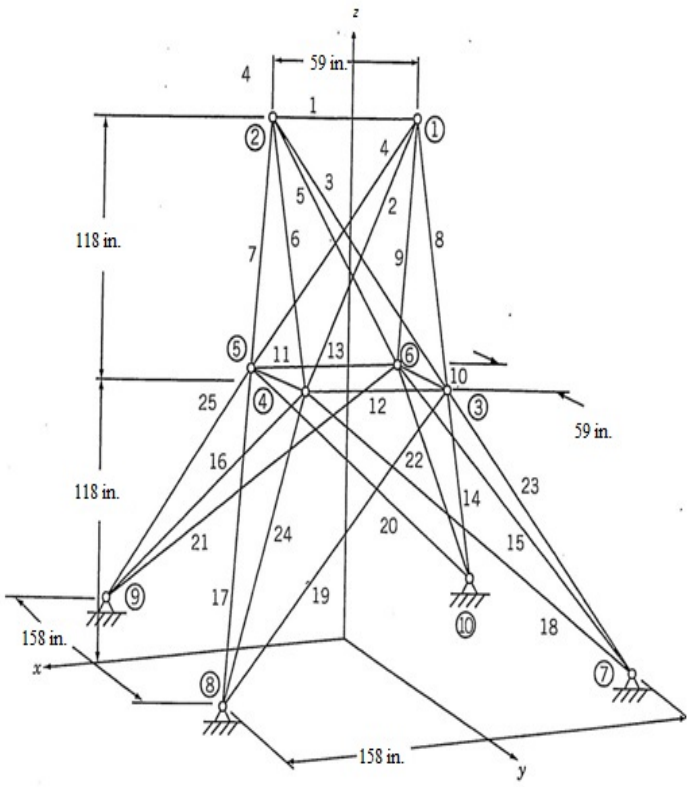

Figure 4.5 New Twenty-five bar space truss

In the new design, the upper and lower bounds for the design variables (areas) are taken as 5 in^2 and 1 in^2 respectively. For any area of cross-section of member i, the mean diameter and thickness of the member are given by $d_i = \sqrt{\frac{20}{\pi} A_i}$ and $t_i = \sqrt{\frac{1}{20\pi} A_i}$ .The load conditions are given in Table 4.17 and the member areas are grouped as given in Table 4.14. The nodal coordinates for the new 25 bar truss are given in Table 4.20. The new 25-bar truss optimization problem is solved using the ML and ACO approaches.

Table 4.20 Coordinates for the new 25 bar truss

Node	x (in)	y (in)	z (in)
1	-29.5	0.0	118.0
2	29.5	0.0	118.0
3	-29.5	29.5	59.0
4	29.5	29.5	59.0

Node	x (in)	y (in)	z (in)
5	29.5	-29.5	59.0
6	-29.5	-29.5	59.0
7	-79.0	79.0	0.0
8	79.0	79.0	0.0
9	79.0	-79.0	0.0
10	-79.0	-79.0	0.0

4.2.1 Multilevel multi-objective optimization of the new 25-bar truss

In the multi-level deterministic formulation of the new 25-bar truss (Figure 4.5), two levels are considered. These two levels are specified as

a) System level: Design variables are areas and the objective function is a combination of weight, deflection and frequency and is obtained using the modified game theory approach previously discussed (section 2.2.2). Constraint is that stress in each member is less than the allowable stress.

b) Component level: Design variables are mean diameter and thickness of the cross section of the bars. Constraint is the Euler buckling constraint. Objective function is obtained by taking the summation of the squares of the difference between the areas (fixed) obtained from system level and the areas calculated using the thickness and mean diameter (design variables in component level).

Formulation used in the multi-level process is given below:

<u>System level problem:</u>

Minimize $f(X) = \sum_{l=1}^{3} c_l \, f_{nl}(X)$ (4.37)

Where c_l represents the weight assigned to each of the objective (taken as 0.8, 0.1 and 0.1 for l = 1, 2, and 3 respectively) and $f_{nl}(X)$ represents the normalized objective function for weight, deflection and frequency (Eq. (2.9)).

Subject to

$\sigma_{ij}(X) \leq 40000\ psi$ (tension and compression) ; $i = 1,2,\ldots,25;\ j = 1,2$ (4.38)

and $X = \{A_i\}$; $i = 1,2,\ldots,25$ (4.39)

Component level problem:

Minimize $f(X) = \sum_{i=1}^{25}(A_i - \pi d_i t_i)^2$ (4.40)

Subject to

$\sigma_{ij}(X) \leq p_i(X)$; $i = 1,2,\ldots,25;\ j = 1,2$ (4.41)

and $X = \{d_i, t_i\}$; $i = 1,2,\ldots,25$ (4.42)

Algorithm/Procedure

1. Find the areas to minimize the combined objective function with allowable stress constraint.
2. Find the mean diameter for each member with constraint as the buckling constraint and objective function as the square of the difference in areas obtained from the design variables in the two levels.
3. Calculate the areas from the mean diameter (and the corresponding thickness) obtained in step 2 and check for convergence with areas in step 1. Stop if converged. Else take the calculated areas as the initial values and

4. Repeat steps 1 to 3 until convergence. The convergence criterion used in this example is based on the change in the system level objective function value during consecutive cycles (iterations between the two levels).

Table 4.21 Convergence results of multi-level multi-objective optimization of the new 25-bar truss

cycle[$]	f^* (system level)	weight (lb) (component level)	deflection (in) (component level)	frequency (Hz) (component level)
1	0.1326	588.8250	1.3444	52.1827
2	0.1491	610.7532	1.3012	52.8434
3	0.1165	670.2452	1.2189	60.0270
4	0.1021	637.0586	1.2568	57.3962
5	0.1003	651.8492	1.2347	58.4533
6	0.0998	647.8943	1.2325	57.6134
7	0.0984	639.7831	1.2469	57.1084
8	0.0975	619.0975	1.2823	55.0390
9	0.0972	626.4161	1.2696	55.8419
10	0.0972	627.2229	1.2685	55.9373

[$] iteration between the two levels; f^* - optimum value

Table 4.22 Optimum design vectors at each cycle in the multi-level multi-objective optimization of the new 25 bar truss

cycle[$]	optimum design vectors at system level and component level	
1	x^*	{1.0000, 1.4952, 1.4952, 1.0000, 1.0000, 1.0000, 1.4952, 1.4952}
	d^*	{ 2.5219, 3.7180, 3.7382, 2.5218, 2.5288, 2.8543, 3.6890, 3.5232}
2	x^*	{1.0000, 1.0000, 1.8178, 1.0000, 1.0000, 1.0000, 1.0000, 1.0000}
	d^*	{ 2.5218, 3.6932, 3.9231, 2.5224, 2.5311, 2.9517, 3.6995, 3.5097}
3	x^*	{ 1.0000, 1.9903, 2.2014, 1.0000, 1.0000, 1.0000, 1.0000, 1.9903}
	d^*	{ 2.5218, 3.8682, 3.7276, 2.5218, 2.5218, 2.9489, 3.6752, 3.6565}
4	x^*	{1.0000, 1.0000, 1.0000, 1.0000, 1.0000, 1.0000, 1.0000, 3.3481}
	d^*	{2.5220, 3.7591, 3.7078, 2.5218, 2.5221, 2.9352, 3.6495, 4.6445}
5	x^*	{1.0000, 1.0000, 1.5748, 1.0000, 1.0000, 1.0000, 1.0000, 2.8156}
	d^*	{2.5219, 3.7456, 3.7180, 2.5219, 2.5221, 2.8755, 3.6623, 4.2488}

cycle[$]	optimum design vectors at system level and component level	
6	x^*	{1.0000, 1.3056, 1.2943, 1.0000, 1.0000, 1.0000, 1.0000, 3.0222}
	d^*	{2.5223, 3.7609, 3.7269, 2.5218, 2.5218, 2.8915, 3.6569, 4.4200}
7	x^*	{1.0000, 1.3718, 1.3940, 1.0000, 1.0000, 1.0000, 1.0000, 2.8896}
	d^*	{2.5222, 3.7842, 3.7559, 2.5218, 2.5218, 2.8903, 3.6600, 4.3233}
8	x^*	{1.0000, 1.1856, 1.4845, 1.0000, 1.0000, 1.0000, 1.0000, 2.7674}
	d^*	{2.5218, 3.7429, 3.7659, 2.5218, 2.5218, 2.9028, 3.6662, 4.2242}
9	x^*	{1.0000, 1.1877, 1.3865, 1.0000, 1.0000, 1.0000, 1.0000, 2.3631}
	d^*	{2.5218, 3.7321, 3.7669, 2.5218, 2.5218, 2.9176, 3.6764, 3.9134}
10	x^*	{1.0000, 1.1849, 1.3748, 1.0000, 1.0000, 1.0000, 1.0000, 2.5082}
	d^*	{2.5218, 3.7360, 3.7624, 2.5218, 2.5218, 2.9136, 3.6723, 4.0288}

[$] iteration between the two levels; x^* - system level areas in in^2; d^* - component level mean diameters in in

The convergence results of multi-objective multi-level optimization for the new 25-bar space truss are as shown in Table 4.21 and Table 4.22. Table 4.21 gives the convergence values of each of the objective function for each iteration during the multi-level process. It is evident that it takes 10 iterations for the multi-objective problem to converge. It can be seen that the optimum objective function values of the weight, deflection and frequency at the end of 10 iterations in the ML process are 627.22 lb, 1.2685 in and 55.93 Hz respectively. Also, bucking stress constraints in members 2, 5, 7, 8, 19 and 20 are active for load condition 1. Optimum design vectors in each iteration are given in Table 4.22.

4.2.2 Ant colony optimization of the new 25-bar truss

In this section, the new 25-bar truss optimization problem is solved using the ACO approach. Initially, single objective optimization of each of the three objectives is solved using SQP (by treating all the design variables as continuous) and ACO (by treating all the design variables as discrete). The results obtained by both methods are given in Table 4.23 and Table 4.24. In the case of SQP, the minimum weight obtained is 588.0126 lb and the minimum deflection obtained is 0.5673 in and the maximum frequency obtained is 68.4845 Hz. The corresponding values for ACO are 618.2454 lb, 0.5653 in and 69.0329 Hz. Thus, the SQP method reduces the weight by 5.2 % when compared to the ACO method. This is as expected because SQP uses continuous variables and hence better solutions. The difference in the minimum deflection and maximum frequency obtained by SQP and ACO is negligible. For minimization of weight using SQP, buckling constraints in members 2, 5, 7, 8, 19 and 20 in load condition1 and in members 16 and 24 in load condition 2, are active. In ACO, buckling constraints in members 2, 5, 7, 8, 19 and 20 in load condition1 are active. For maximization of frequency, buckling constraints in members 2 and 5 in load condition1 are active in SQP and buckling constraints in members 2, 5, 7 and 8 are active in load condition1 in ACO. The discrete design variable set used for ACO is given by S = {1.0, 1.4, 1.8, 2.2, 2.6, 3.0, 3.4, 3.8, 4.2, 4.6, 5.0}. Thus, each of the design variables is permitted to take values from the set S. A colony size of 50 ants is used and the convergence is achieved in about 1150 iterations for minimization of weight, 250 iterations for minimization of deflection and 550 iterations for maximization of frequency as shown in Figure 4.6, Figure 4.7 and Figure 4.8 respectively. In SQP, the number of iterations and the number of objective function

evaluations for each objective are 7, 2, 51 and 182, 52, 1547 respectively. The initial design vector for SQP is taken as the lower bound values of the design variables and there are no active constraints at the initial design. In ACO, the initial design vector is chosen randomly.

Table 4.23 Results of single objective optimization of the new 25-bar truss (SQP)

Quantity	Initial Design	Minimization of weight	Minimization of deflection	Maximization of frequency
Design variables: (in^2)				
x_1	1.0	1.0000	1.0000	1.2019
x_2	1.0	2.1722	5.0000	2.1942
x_3	1.0	2.1963	5.0000	2.1808
x_4	1.0	1.0000	2.5253	4.9999
x_5	1.0	1.0000	5.0000	4.9999
x_6	1.0	1.2751	5.0000	4.9301
x_7	1.0	2.1390	5.0000	3.8760
x_8	1.0	1.9433	5.0000	5.0000
Objective functions:				
weight $f_1(\vec{X})$ (lb)	320.3812	588.0126	1540.6097	1157.7150
deflection $f_2(\vec{X})$ (in)	2.8262	1.3461	0.5673	1.0591

Quantity	Initial Design	Minimization of weight	Minimization of deflection	Maximization of frequency
Design variables: (in^2)				
frequency $f_3(\vec{X})$ (Hz)	54.1321	52.1163	56.6731	68.4845
Constraints:				
number of active behavior constraints	0	8[§]	0	2[$]

[§] buckling stress in members 2, 5, 7, 8, 19 and 20 in load condition1 and in members 16 and 24 in load condition 2.
[$] buckling stress in members 7 and 8 in load condition1.

Table 4.24 Results of single objective optimization of the new 25-bar truss (ACO)

Quantity	Minimization of weight	Minimization of deflection	Maximization of frequency
Design variables: (in^2)			
x_1	1.0	1.0	1.0
x_2	2.2	5.0	2.2
x_3	2.2	5.0	2.2
x_4	1.0	5.0	3.0
x_5	1.0	5.0	1.8
x_6	1.4	5.0	5.0
x_7	2.2	5.0	3.4
x_8	2.2	5.0	5.0

Quantity	Minimization of weight	Minimization of deflection	Maximization of frequency
Objective functions:			
weight $f_1(\vec{X})$ (lb)	618.2454	1584.0491	1127.08913
deflection $f_2(\vec{X})$ (in)	1.2992	0.5653	1.0629
frequency $f_3(\vec{X})$ (Hz)	54.0229	56.9705	69.0329
Constraints:			
number of active behavior constraints	6[§]	0	4[§]

[§] buckling stress in members 2, 5, 7, 8, 19 and 20 in load condition1.
[$] buckling stress in members 2, 5, 7 and 8 in load condition1.

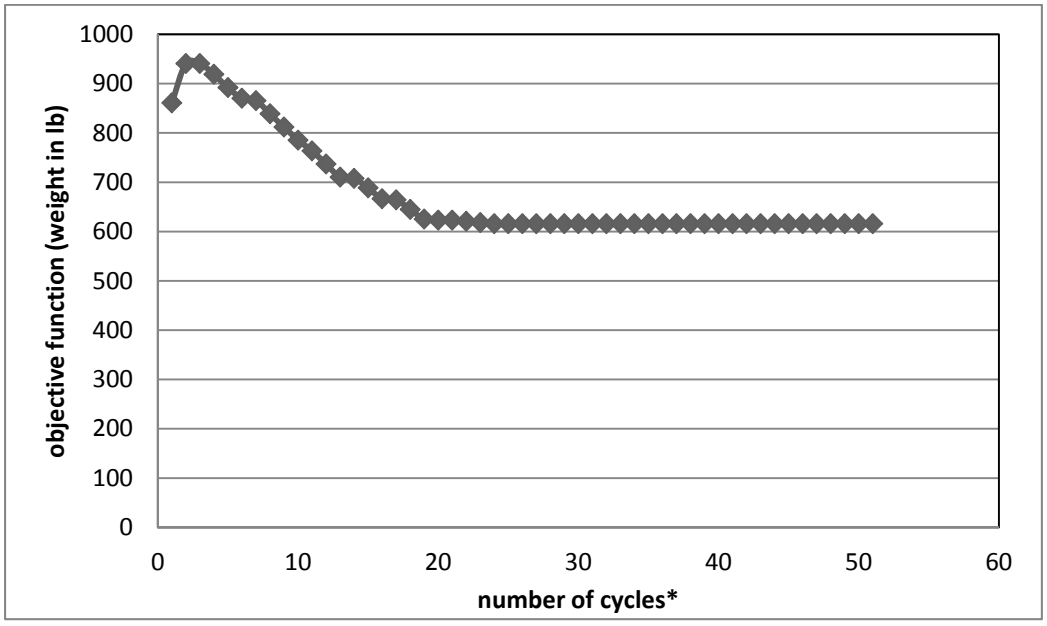

*cycle = number of iterations/number of ants; number of ants = 50

Figure 4.6 Convergence history for minimum weight of the new 25 bar truss

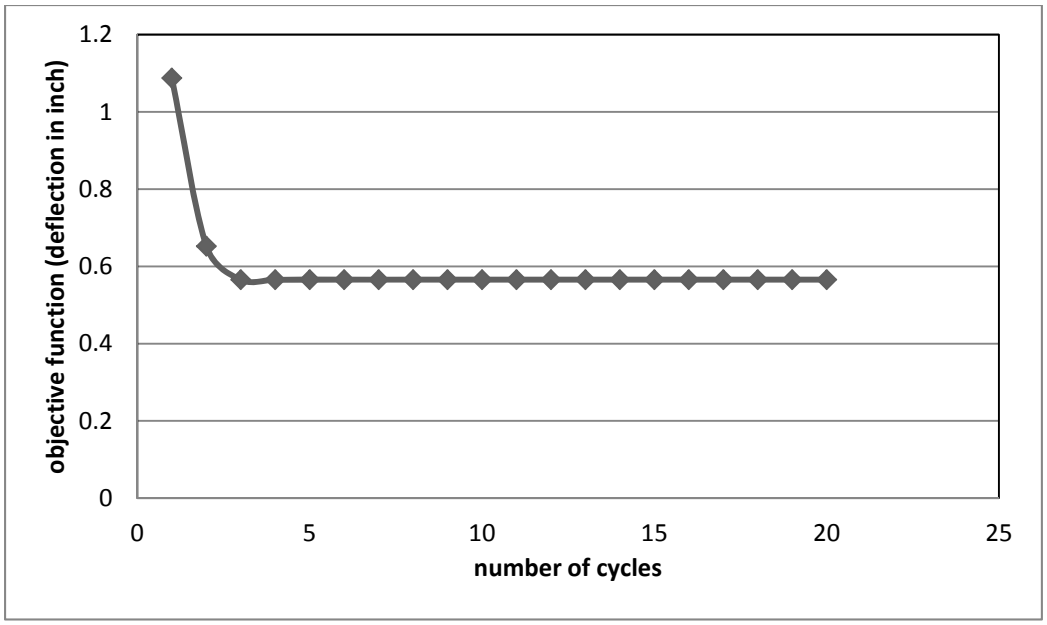

*cycle = number of iterations/number of ants; number of ants = 50

Figure 4.7 Convergence history for minimum deflection of the new 25 bar truss

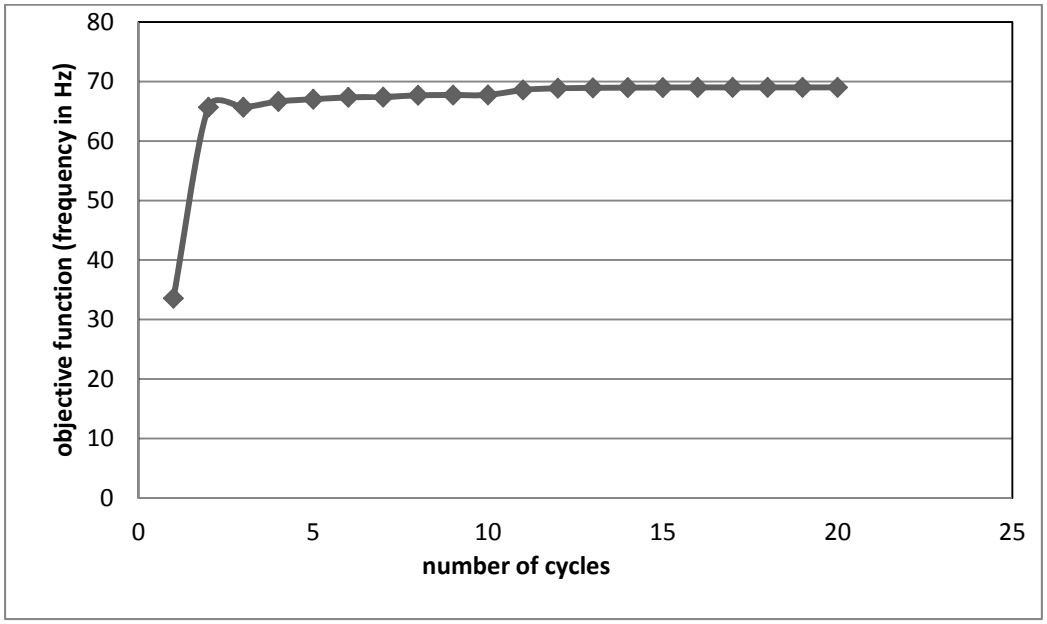

*cycle = number of iterations/number of ants; number of ants = 50

Figure 4.8 Convergence history for maximum frequency of the new 25 bar truss

Multi-objective optimization problem of the new 25-bar truss is solved using SQP and ACO. The results are given in Table 4.25. The minimum weight obtained by SQP is 618.9315 lb whereas the minimum weight obtained by ACO is 640.1884 lb. Hence, the

SQP solution resulted in a lighter truss by 3.48 %. The maximum frequency obtained by SQP is 55.8035 Hz whereas the maximum frequency obtained by ACO is 56.3163 Hz. Hence, both the methods result in almost the same frequency. The minimum deflection obtained by ACO is 1.2598 in and the minimum deflection obtained by SQP is 1.2795 in. Hence, the ACO solution resulted in a decrease in minimum deflection by 1.30 % when compared to the SQP solution. Also, the buckling stress constraints in members 2, 5, 7, 8, 19 and 20 in load condition1 and in member 16 in load condition 2 are active in case of SQP. In ACO, the buckling constraints in members 2, 5, 7, 8, 19 and 20 are active in load condition1. For ACO, a colony size of 50 ants was used. The discrete variable set used in ACO is S = {1.0, 1.4, 1.8, 2.2, 2.6, 3.0, 3.4, 3.8, 4.2, 4.6, 5.0}. The convergence is achieved in 1200 iterations as shown in Figure 4.9.

Table 4.25 Comparison of results of multi-objective optimization of the new 25-bar truss

Quantity	SQP		ACO*
	Initial design	Optimum design	
Design variables: (in^2)			
x_1	1.0	1.0000	1.0
x_2	1.0	2.1959	2.2
x_3	1.0	2.1791	2.2
x_4	1.0	1.0000	1.0
x_5	1.0	1.0000	1.0
x_6	1.0	1.2524	1.4

Quantity	SQP		ACO*
	Initial design	Optimum design	
x_7	1.0	2.1166	2.2
x_8	1.0	2.5555	2.6
Objective functions:			
weight $f_1(\vec{X})$ (lb)	320.3812	618.9315	640.1884
deflection $f_2(\vec{X})$ (in)	2.8262	1.2795	1.2598
frequency $f_3(\vec{X})$ (Hz)	54.1387	55.8035	56.3163
Constraints:			
number of active behavior constraints	0	7[§]	6[&]

* initial design vector is chosen randomly in ACO
[§] buckling stress in members 2, 5, 7, 8, 19 and 20 in load condition1 and 16 in load condition 2.
[&] buckling stress in members 2, 5, 7, 8, 19 and 20 in load condition1.

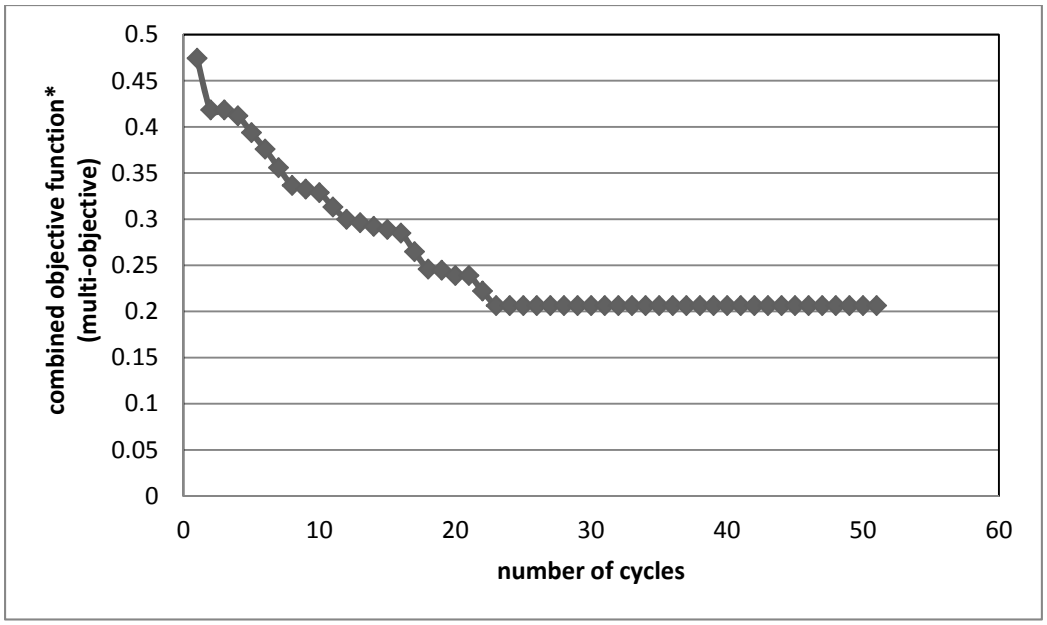

*combined objective is calculated using Eq. (2.29) with normalized individual objectives

Figure 4.9 Convergence history for multi-objective ACO of the new 25 bar truss

Different sets of weights are considered in the multi-objective ACO optimization to study the effect of the influence of weights on the final solution. Results are given in Table 4.26. Three sets of weights are considered as w_1, w_2 and w_3 which represent the importance of the three objectives, weight, deflection and frequency respectively (Eq. 2.29). The discrete set used in ACO is S = {1.0, 1.4, 1.8, 2.2, 2.6, 3.0, 3.4, 3.8, 4.2, 4.6, 5.0} and a colony size of 50 ants is used. It is evident from Table 4.26 that the minimum weight obtained is 640.1884 lb when w_1 is 0.8 and the minimum weight obtained is 1108.173 lb when w_1=0.2. This is as expected, because with an increase in the value of w_1, preference is given to the objective (weight) and hence better solution. Similarly, a maximum value of frequency (68.9776 Hz) is obtained when w_3 is 0.6. The number of iterations for convergence in the three cases is 1150, 1100 and 1000 respectively. These results validate the present ACO approach for solving multi-objective optimization problems.

Table 4.26 Results of multi-objective ACO of the new 25-bar truss using different sets of weights

Quantity	Sets of weights		
	w_1=0.8;w_2=0.1;$w3$=0.1	w_1=0.4;w_2=0.4;$w3$=0.2	w_1=0.2,w_2=0.2;$w3$=0.6
Design variables: (in^2)			
x_1	1.0	1.0	1.0
x_2	2.2	2.6	2.2
x_3	2.2	3.0	2.2
x_4	1.0	1.0	2.2
x_5	1.0	1.0	1.0
x_6	1.4	1.4	5.0
x_7	2.2	2.2	3.4
x_8	2.6	5.0	5.0
Objective functions:			
weight $f_1(\vec{X})$ (lb)	640.1884	832.5799	1108.173
deflection $f_2(\vec{X})$ (in)	1.2598	0.9606	1.0629
frequency $f_3(\vec{X})$ (Hz)	56.3163	61.9974	68.9776
number of active behavior constraints	6[§]	2[&]	4[$]

[§] buckling stress in members 2, 5, 7, 8, 19 and 20 in load condition1.
[&] buckling stress in members 19 and 20 in load condition1.
[$] buckling stress in members 2, 5, 7 and 8 in load condition1.

Sensitivity of the ACO results to variation in the discrete variable sets is also studied. Two discrete sets each with 15 values of the design variables are considered (Table 4.27). Results obtained by the two discrete sets are given in Table 4.28. A colony size of 50 ants is considered. It is evident from the table, that the discrete set *S2* resulted in a lighter truss when compared to discrete set *S1*. Also, there is an increase in the maximum frequency in the discrete set *S2*. The minimum deflection in the case of discrete set *S1* is less than the minimum deflection in the case of *S2*. Also, the same set of buckling constraints is active in both the cases. It is observed that with increase in the number of values in the discrete variable set, the solution is more accurate and the constraints are tighter in ACO and the ACO solution is closer to the solution obtained by SQP which uses continuous variables.

Table 4.27 Discrete variable sets in ACO

S1	{ 1.0, 1.2, 1.5, 1.7, 2.0, 2.2, 2.5, 2.7, 3.0, 3.5, 3.7, 4.0, 4.5, 4.7, 5}
S2	{ 1.0, 1.2, 1.4, 1.8, 2.0, 2.2, 2.4, 2.8, 3.2, 3.4, 3.8, 4.2, 4.4, 4.8, 5}

Table 4.28 Results of multi-objective ACO of the new 25-bar truss using different discrete variable

Quantity	Discrete Set *S1*	Discrete Set *S2*
Design variables (in^2)		
x_1	1.0	1.0
x_2	2.5	2.2
x_3	2.5	2.2

Quantity	Discrete Set *S1*	Discrete Set *S2*
x_4	1.0	1.0
x_5	1.0	1.0
x_6	1.5	1.4
x_7	2.5	2.2
x_8	2.5	2.4
Objective functions:		
weight $f_1(\vec{X})$ (lb)	689.93	626.95
deflection $f_2(\vec{X})$ (in)	1.1456	1.2795
frequency $f_3(\vec{X})$ (Hz)	53.99	53.21
Constraints:		
number of active behavior constraints	6[§]	6[&]

[§] buckling stress in members 2, 5, 7, 8, 9, and 10 in load condition1.
[&] buckling stress in members 2, 5, 7, 8, 9, and 10 in load condition1.

Performance of ACO is studied by varying the size of the ant colony keeping the maximum number of cycles fixed. Three different colony sizes of 25, 50 and 100 ants are considered. The convergence results are shown in Figure 4.10, Figure 4.11 and Figure 4.12. It can be seen that for the minimization of weight (objective), a colony size of 50 ants converges to the optimum in about 20 cycles while a colony size of 25 ants converges to the optimum value in 23 cycles. The colony size of 100 ants did not

converge until the maximum number of cycles. Also, the starting vector is chosen randomly in each case. For the minimization of deflection, as a special case, the same starting vector is chosen. The results are shown in Fig 2. In this case, the colony size of 25 ants performed better with convergence in 6 cycles. The colony with 50 ants converged in 8 cycles. The colony of 100 ants converged in 9 cycles. Convergence of frequency is shown in Fig. In this case, the results are closer because all the different ant colonies take about the same number of cycles to converge.

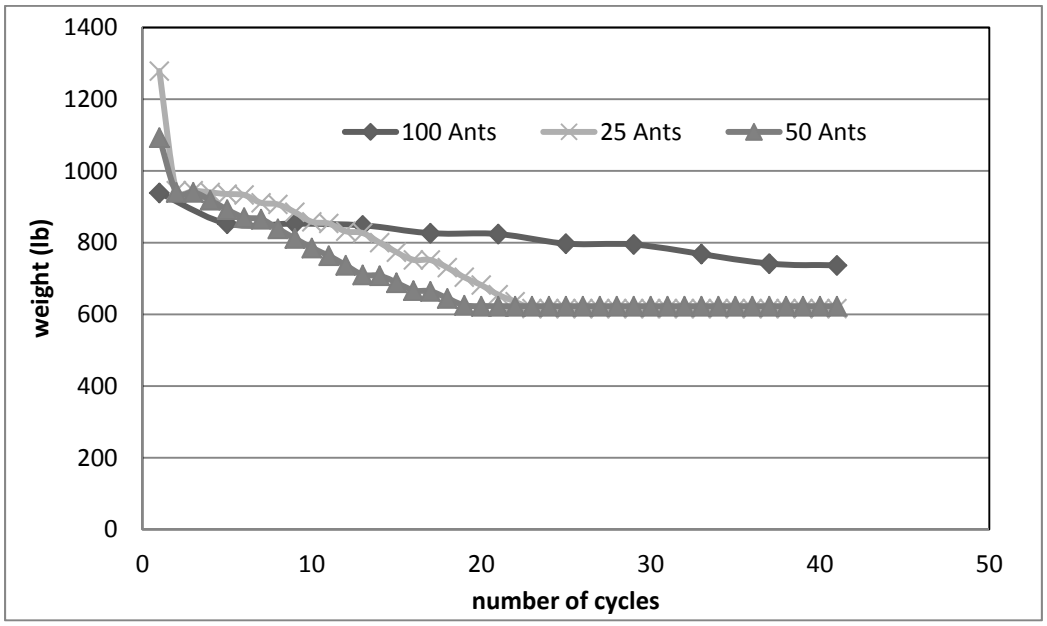

Figure 4.10 Convergence of minimum weight with changes in the number of ants for the new 25 bar truss

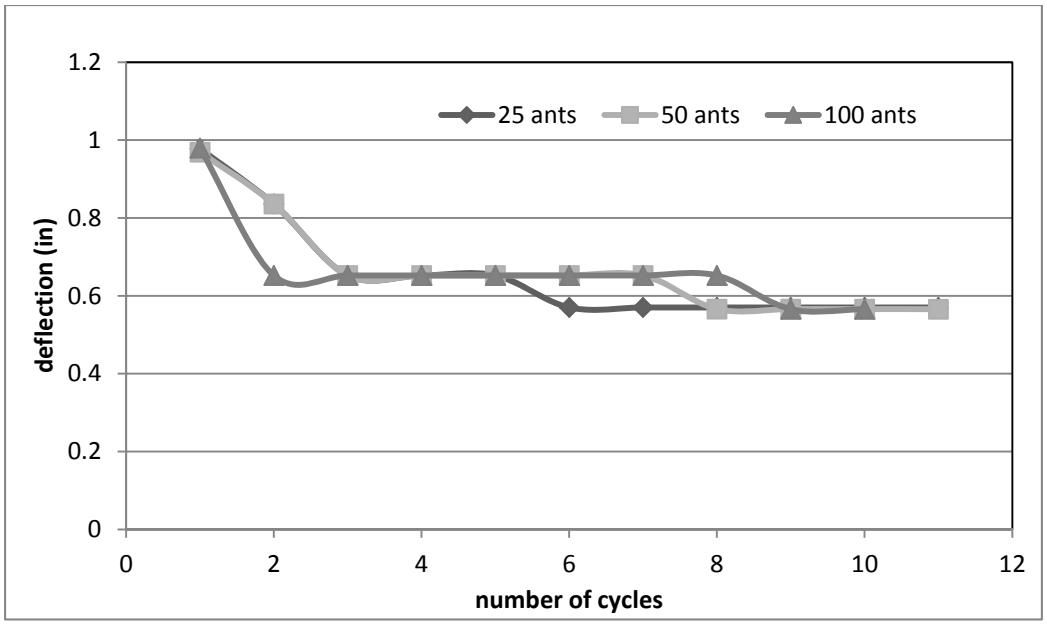

Figure 4.11 Convergence of minimum deflection with changes in the number of ants for the new 25 bar truss

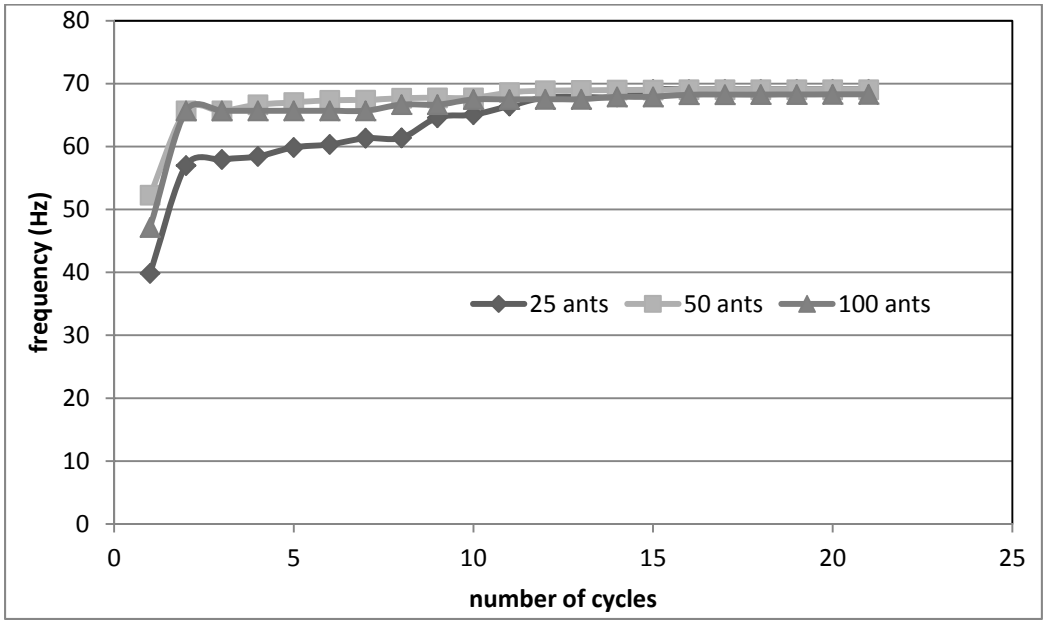

Figure 4.12 Convergence of maximum frequency with changes in the number of ants for the new 25 bar truss

4.2.3 Multi-objective ant colony optimization using modified game theory of the new 25-bar truss

In this section, ant colony optimization method is used to solve the multi-objective optimization problem of the 25 bar truss using modified game theory approach. The problem is given as:

Minimize $f(X) = FC - S$ (4.43)

where $FC = \sum_{l=1}^{3} c_l f_{nl}(X)$ and (4.44)

$S = \prod_{l=1}^{n}[1 - f_{nl}(X)]$ (4.45)

Where c_l represents the weight assigned to each of the objective and $f_{nl}(X)$ represents the normalized objective function for weight, deflection and frequency (Eq. (2.9)).

Subject to

$\sigma_{ij}(X) \leq 40000\ psi$ (tension and compression) ; $i = 1,2,\dots,25;\ j = 1,2$ (4.32)

$\sigma_{ij}(X) \leq p_i(X)\ ;\ i = 1,2,\dots,25;\ j = 1,2$ (4.46)

where $X = \{A_i\}\ ;\ i = 1,2,\dots,25.$ (4.47)

The results obtained by the multi-objective ant colony optimization using modified game theory are given in Table 4.29. As seen from the table, the minimum weight obtained by ACO is 810.9083 lb, the minimum deflection obtained is 1.0078 in and the maximum frequency obtained is 62.8084 Hz. The results obtained by ACO are compared with those obtained using SQP (using modified game theory). The minimum weight obtained by SQP is 1157.878 lb, the minimum deflection obtained is 0.7086 in and the maximum

frequency obtained is 59.2179 Hz. Hence, the ACO solution resulted in a lighter truss by 29.96%. The tradeoff is with an increase in the minimum deflection in ACO. This is because of the different weights obtained in the modified game theory (*c1*, *c2* and *c3* in Table 4.29. Hence, the modified game theory resulted in a compromise solution. Also, the buckling constraints 2, 5, 19 and 20 in load condition 1 are active in the case of ACO and the buckling constraints 19 and 20 in load condition 1 and 16 in load condition 2 are active in SQP. For SQP, the number of iterations for convergence is 15 and the number of function evaluations is 187. At the starting point in SQP, no constraints are active. For ACO, a colony size of 50 ants is used. The discrete set of design variables used for ACO is the set $S = \{1.0, 1.4, 1.8, 2.2, 2.6, 3.0, 3.4, 3.8, 4.2, 4.6, 5.0\}$. The convergence in ACO is achieved in 37 cycles as shown in Figure 4.13.

Table 4.29 Comparison of results of multi-objective ACO and SQP using modified game theory for the new 25 bar truss

Quantity	SQP (MGT)		ACO (MGT)
	Initial design	Optimum design	
Design variables: (in^2)			
x_1	1.0	1.0000	1.0
x_2	1.0	3.4236	2.2
x_3	1.0	4.1932	3.0
x_4	1.0	1.0000	1.0
x_5	1.0	1.0000	1.0
x_6	1.0	3.1194	1.4
x_7	1.0	3.7876	2.2

Quantity	SQP (MGT)		ACO (MGT)
	Initial design	Optimum design	
x_8	1.0	5.0000	5
C1	0.3	0.1	0.7
C2	0.4	0.8	0.2
C3	0.3	0.1	0.1
Objective functions:			
weight $f_1(\vec{X})$ (lb)	320.3812	1157.878	810.9083
deflection $f_2(\vec{X})$ (in)	2.8262	0.7086	1.0078
frequency $f_3(\vec{X})$ (Hz)	54.1387	59.2179	62.8084
Constraints:			
number of active behavior constraints	0	3[§]	4[&]

[§] buckling stress in members 19 and 20 in load condition1 and 16 in load condition 2
[&] buckling stress in members 2, 5, 19 and 20 in load condition1

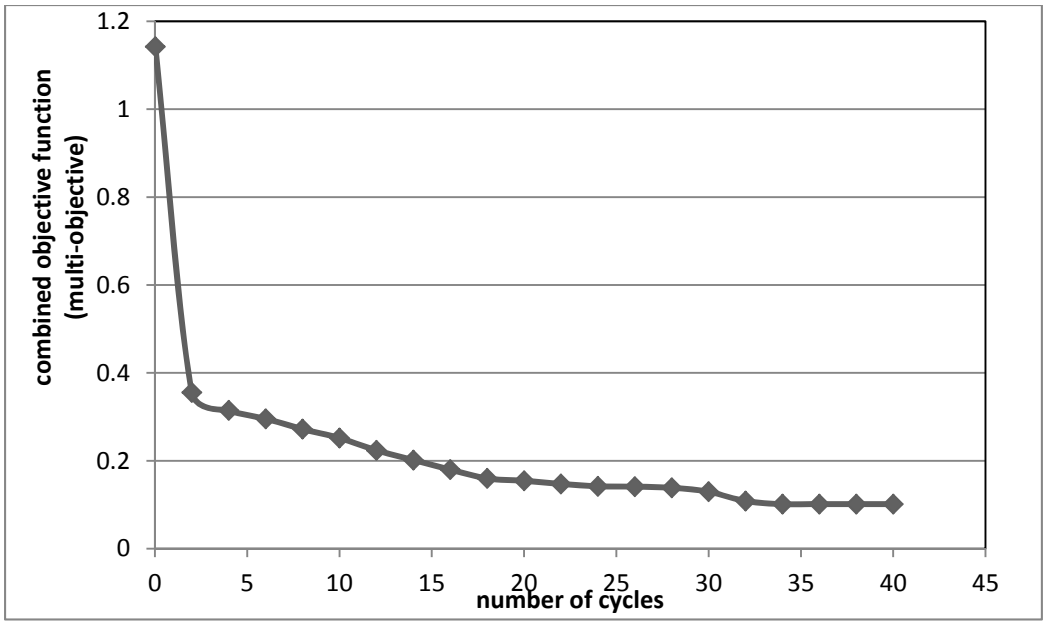

Figure 4.13 Convergence graph for multi-objective ACO using modified game theory for the new 25 bar truss

Table 4.30 Designs for the best 5 ants in multi-objective ACO using modified game theory for the new 25 bar truss

Quantity	Ant 1	Ant 2	Ant 3	Ant 4	Ant 5
Design variables: (in^2)					
x_1	1.0	1.0	1.0	1.0	1.0
x_2	2.6	2.6	2.2	2.2	3.0
x_3	2.6	3.0	3.0	3.0	3.0
x_4	1.0	1.0	1.0	1.0	1.0
x_5	1.0	1.0	1.0	1.0	1.8
x_6	1.8	1.8	1.8	1.4	3.0
x_7	2.2	2.6	2.2	2.2	3.0

Quantity	Ant 1	Ant 2	Ant 3	Ant 4	Ant 5
x_8	5.0	5.0	5.0	5	5.0
c1	0.5	0.6	0.7	0.7	0.5
c2	0.3	0.3	0.2	0.2	0.3
c3	0.2	0.1	1.0	0.1	0.2
Combined objective function $f_1(\vec{X})$	0.1419	0.1385	0.1083	0.1014	0.20157
Constraints:					
number of active behavior constraints	0	0	4[&]	4[$]	0

[&] buckling stress in members 2, 5, 19 and 20 in load condition1
[$] buckling stress in members 2, 5, 19 and 20 in load condition1

Details of the best 5 final designs (corresponding to the best 5 ants) are given in Table 4.30. Among all the designs, the one with minimum combined objective function value is chosen as the final design in ACO. It can be seen from the table, that the design corresponding to ant 4 has the minimum combined objective function value. The design vectors corresponding to each of the final designs, the objective function value and the constant (*c1* ,*c2*, *c3*) obtained in the modified game theory are also listed in Table 4.30.

4.2.4 Multilevel Ant Colony Optimization of 25-bar truss

In this section, a new multi-level ant colony optimization method is developed to solve the 25 bar truss. The new multi-level method consists of two levels and each level solves an optimization problem using the Ant Colony Approach and the SQP approach. For the

25 bar truss, the height and span dimensions of the truss are also considered as design variables in addition to the areas. Hence, a total of 13 design variables are considered. The bounds on the design variables are given in Table 4.31.

In the new multi-level formulation of the 25-bar truss, two levels are considered. These two levels are specified as

a) System level: Design variables are the heights (h_1 and h_2), base dimensions (b_1 and b_2) and the mid span (s_1). Objective function is weight. Constraints are the allowable stress and buckling stress constraints.

b) Component level: Design variables are the areas of cross section of the bars. Objective function is weight. Constraints are the allowable stress and buckling stress constraints.

Formulation used in the multi-level process is given below:

System level problem:

Minimize $f = \sum_{i=1}^{25} \rho A_i l_i$ (4.48)

Subject to

$\sigma_{ij}(X) \leq 40000\ psi$ (tension and compression) ; $i = 1,2,\dots,25;\ j = 1,2$ (4.49)

$\sigma_{ij}(X) \leq p_i(X)$; $i = 1,2,\dots,25;\ j = 1,2$ (4.50)

and $X = \{h_1, h_2, b_1, b_2, s_1\}$; $i = 1,2,\dots,25$ (4.51)

Component level problem:

Minimize $f = \sum_{i=1}^{25} \rho A_i l_i$ (4.52)

Subject to

$\sigma_{ij}(X) \leq 40000\ psi$ (tension and compression) ; $i = 1,2,\ldots,25;\ j = 1,2$ (4.53)

$\sigma_{ij}(X) \leq p_i(X)$; $i = 1,2,\ldots,25;\ j = 1,2$ (4.54)

and $X = \{A_i\}$; $i = 1,2,\ldots,25$ (4.55)

Algorithm/Procedure

1. Find the heights (h_1 and h_2), base dimensions (b_1 and b_2) and the mid span (s_1) to minimize the objective function (weight) with allowable stress and buckling stress constraints using initial trial values for the areas.
2. Find the area of each member to minimize the objective function (weight) with allowable stress and buckling stress constraints using the heights, base dimensions and mid span obtained from step 1.
3. Check for convergence of the objective function in step 1 with that obtained in step 2. Stop if converged. Else take the areas obtained in step 2 as constants in step 1 and
4. Repeat steps 1 to 3 until convergence. The convergence criterion used is the change in the objective function value between the two levels.

The new ML optimization method is used to solve the single objective optimization of minimization of weight, minimization of deflection and maximization of frequency of the 25 bar truss. Both, SQP and Ant Colony Optimization methods are used.

Results obtained by the new ML SQP for minimization of weight are given in Table 4.32 and Table 4.33. Table 4.32 shows the convergence of the design variables for every

iteration between the system and the component levels. From the table it is evident that the convergence in the ML process is achieved in 3 iterations. Variation of the weight at the end of every iteration between the two levels is given in Table 4.33. It is evident that the weight reduced from an initial value of 292.2777 lb to a final minimum value of 181.7240 lb in 3 iterations between the system and the component levels. The convergence is evident with equal values of weight in both the levels at the final design. The total number of function evaluations in SQP is 222 and the total number of iterations for convergence of the ML process is 18. At the initial design, there are no active constraints whereas at the final design, allowable stress constraints in members 7 and 8 for load condition 1 and the buckling constraints in members 1, 2, 5, 19 and 20 for load condition 1 and buckling constraints in member 24 for load condition 2 are active.

Table 4.31 Bounds on the design variables for the 25 bar truss

Design variable	x_1	x_2	x_3	x_4	x_5	x_6	x_7	x_8	x_9	x_{10}	x_{11}	x_{12}	x_{13}
Lower bound	160	144	80	72	60	0.1	0.1	0.1	0.1	0.1	0.1	0.1	0.1
Upper bound	240	216	120	108	90	5.0	5.0	5.0	5.0	5.0	5.0	5.0	5.0

Table 4.32 New Multi-level SQP results for single objective minimization of weight

Iteration	Optimum design vectors at system level and component level	
1	x^*	{218.6693, 144.0000, 80.0000, 95.8379, 60.0000}
	A^*	{0.1059, 1.0047, 0.8670, 0.1000, 0.1000, 0.6310, 1.0479, 0.9927}
2	x^*	{204.7371, 144.0000, 80.0000, 72.0000, 60.0000}
	A^*	{0.1024, 0.7355, 0.6418, 0.1000, 0.1000, 0.4057, 1.0203, 0.8689}
3	x^*	{204.7370, 144.0000, 80.0000, 72.0000, 60.0000}

	A^*	{0.1024, 0.7355, 0.6418, 0.1000, 0.1000, 0.4057, 1.0203, 0.8689}

x^*- system level design vector in in; A^*- component level design vector (areas) in in^2

Table 4.33 New Multi-level SQP results for single objective minimization of weight

Iteration	f^* (system level)	f^* (component level)
1	292.2777	240.5903
2	220.2519	181.7240
3	181.7240	181.7240

f^* - optimum value (weight in lb)

Results obtained by the new ML SQP for minimization of deflection are given in Table 4.34 and Table 4.35. Table 4.34 shows the convergence of the design variables for every iteration between the system and the component levels. From the table it is evident that the convergence in the ML process is achieved in 3 iterations. Variation of the deflection at the end of every iteration between the two levels is given in Table 4.35. It is evident, that the deflection reduced from an initial value of 3.0265 in to a final minimum value of 0.2474 in in 3 iterations between the system and the component levels. The convergence is evident with equal value of deflection in both the levels at the final design. The total number of function evaluations in SQP is 162 and the total number of iterations for convergence of the ML process is 18. No constraints are active in the initial and final designs.

Table 4.34 New Multi-level SQP results for single objective minimization of deflection

Iteration	Optimum design vectors at system level and component level	
1	x^*	{218.6693, 144.0000, 80.0000, 95.8379, 60.0000}
	A^*	{5.0000, 5.0000, 5.0000, 0.4661, 2.6678, 5.0000, 5.0000, 5.0000}
2	x^*	{216.6140, 144.0008, 81.8232, 82.9610, 75.7799}

	A^*	{5.0000, 5.0000, 5.0000, 0.4661, 2.6678, 5.0000, 5.0000, 5.0000}
3	x^*	{214.7465, 144.7412, 81.8854, 72.0000, 84.1482}
	A^*	{5.0000, 5.0000, 5.0000, 0.4661, 2.6678, 5.0000, 5.0000, 5.0000}

x^*- system level design vector in in; A^*- component level design vector (areas) in in^2.

Table 4.35 New Multi-level SQP results for single objective minimization of deflection

Iteration	f^* (system level)	f^* (component level)
1	3.0265	0.6055
2	0.3396	0.3396
3	0.2474	0.2474

f^* - optimum value (deflection in in)

Results obtained by the new ML SQP for maximization of frequency are given in Table 4.36 and Table 4.37. Table 4.36 shows the convergence of the design variables for every iteration between the system and the component levels. From the table it is evident that the convergence in the ML process is achieved in 7 iterations. Variation of the frequency at the end of every iteration between the two levels is given in Table 4.37. It is evident, that the frequency increased from an initial value of 62.2896 Hz to a final value of 164.2267 Hz in 7 iterations between the system and the component levels. The convergence is evident with equal value of frequency in both the levels at the final design. The total number of function evaluations in SQP is 1821and the total number of iterations for convergence of the ML process is 144. At the initial design, there are no active constraints whereas at the final design, buckling constraints in members 2 and 5 are active for load condition 1.

Table 4.36 New Multi-level SQP results for single objective maximization of frequency

Iteration	Optimum design vectors at system level and component level	
1	x^*	{218.6693, 144.0000, 80.0000, 95.8379, 60.0000}
	A^*	{0.1004, 0.9581, 0.8998, 1.0647, 0.1000, 5.0000, 5.0000, 5.0000}
2	x^*	{215.1449, 144.0000, 84.6827, 72.0000, 64.1295}
	A^*	{0.1000, 0.6669, 0.7550, 0.1000, 0.1051, 5.0000, 3.7996, 5.0000}
3	x^*	{209.4678, 144.0000, 80.0000, 72.0000, 64.8245}
	A^*	{0.1000, 0.6591, 0.7729, 0.1000, 0.1000, 5.0000, 4.0998, 5.0000}
4	x^*	{194.1813, 146.1304, 80.1896, 72.0000, 66.8672}
	A^*	{00.1000, 0.6486, 0.7642, 0.2148, 0.1834, 5.0000, 4.2569, 5.0000}
5	x^*	{178.4132, 156.6992, 80.0000, 72.0000, 67.3553}
	A^*	{0.1060, 0.6604, 0.6876, 0.6965, 0.1000, 5.0000, 5.0000, 5.0000}
6	x^*	{178.3065, 155.6373, 80.0000, 72.0000, 67.3571}
	A^*	{0.1060, 0.6604, 0.6876, 0.7424, 0.1181, 5.0000, 5.0000, 5.0000}
7	x^*	{178.3065, 155.6373, 80.0000, 72.0000, 67.3571}
	A^*	{0.1060, 0.6604, 0.6877, 0.7424, 0.1181, 5.0000, 5.0000, 5.0000}

x^*- system level design vector in in; A^*- component level design vector (areas) in in^2.

Table 4.37 New Multi-level SQP results for single objective maximization of frequency

Iteration	f^* (system level)	f^* (component level)
1	62.2896	104.8622
2	132.9182	143.7044
3	148.8049	150.1132
4	155.4710	158.1940
5	160.5125	163.9858
6	164.1131	164.2267
7	164.2267	164.2268

f^* - optimum value (frequency in Hz)

In the single objective minimization of weight, using the ML ACO approach, the discrete variable set is obtained by taking 20 values equally distributed between the bounds for each design variable (Table 4.38) and the number of ants used for ACO is 50. Results obtained by the new ML ACO for minimization of weight are given in Table 4.39 and Table 4.40. Table 4.39 shows the convergence of the design variables for every iteration between the system and the component levels. From the table, it is evident that the convergence in the ML process is achieved in 3 iterations. Variation of the weight at the end of every iteration between the two levels is given in Table 4.40. It is evident that the weight reduced from an initial value of 294.8969 lb to a final minimum value of 205.4903 lb in 3 iterations between the system and the component levels. The convergence is evident with equal values of weight in both the levels at the final design. At the final design, allowable stress constraints in members 7 and 8 for load condition 1and buckling constraints in members 7, 8, 19 and 20 in load condition1 and member 16 in load condition 2 are active. The convergence in ACO is achieved in 68 cycles (3400 iterations).

Table 4.38 Discrete values for the design variables for 25 bar truss

x_1	{160.0000, 164.2105, 168.4211, 172.6316, 176.8421, 181.0526, 185.2632, 189.4737, 193.6842, 197.8947, 202.1053, 206.3158, 210.5263, 214.7368, 218.9474, 223.1579, 227.3684, 231.5789, 235.7895, 240.0000}
x_2	{144.0000, 147.7895, 151.5789, 155.3684, 159.1579, 162.9474, 166.7368, 170.5263, 174.3158, 178.1053, 181.8947, 185.6842, 189.4737, 193.2632, 197.0526, 200.8421, 204.6316, 208.4211, 212.2105, 216.0000}
x_3	{80.0000, 82.1053, 84.2105, 86.3158, 88.4211, 90.5263, 92.6316, 94.7368, 96.8421,

	98.9474, 101.0526, 103.1579, 105.2632, 107.3684, 109.4737, 111.5789, 113.6842, 115.7895, 117.8947, 120.0000}
x_4	{72.0000, 73.8947, 75.7895, 77.6842, 79.5789, 81.4737, 83.3684, 85.2632, 87.1579, 89.0526, 90.9474, 92.8421, 94.7368, 96.6316, 98.5263, 100.4211, 102.3158, 104.2105, 106.1053, 108.0000}
x_5	{60.0000, 61.5789, 63.1579, 64.7368, 66.3158, 67.8947, 69.4737, 71.0526, 72.6316, 74.2105, 75.7895, 77.3684, 78.9474, 80.5263, 82.1053, 83.6842, 85.2632, 86.8421, 88.4211, 90.0000}
x_6 - x_{13}	{0.1000, 0.3579, 0.6158, 0.8737, 1.1316, 1.3895, 1.6474, 1.9053, 2.1632, 2.4211, 2.6789, 2.9368, 3.1947, 3.4526, 3.7105, 3.9684, 4.2263, 4.4842, 4.7421, 5.0000}

Table 4.39 New Multi-level ACO results for single objective minimization of weight

Iteration	Optimum design vectors at system level and component level	
1	x^*	{168.4211, 151.5789, 90.5263, 102.3158, 67.8947}
	A^*	{0.6158, 3.1947, 0.8737, 0.1000, 0.1000, 0.6158, 0.8737, 2.6789}
2	x^*	{160.0000, 144.0000, 80.0000, 72.0000, 60.0000}
	A^*	{0.3579, 1.3895, 0.6158, 0.1000, 0.1000, 0.3579, 0.8737, 1.3895}
3	x^*	{160.0000, 144.0000, 80.0000, 72.0000, 60.0000}
	A^*	{0.3579, 1.3895, 0.6158, 0.1000, 0.1000, 0.3579, 0.8737, 1.3895}

x^*- system level design vector in in; A^*- component level design vector (areas) in in^2.

Table 4.40 New Multi-level ACO results for single objective minimization of weight

Iteration	f^* (system level)	f^* (component level)
1	294.8969	418.2428
2	353.7359	205.4903
3	205.4903	205.4903

f^* - optimum value (weight in lb)

Table 4.41 New Multi-level ACO results for single objective minimization of deflection

Iteration	Optimum design vectors at system level and component level	
1	x^*	{240.0000, 147.7895, 96.8421, 75.7895, 90.0000}
	A^*	{5.0000, 5.0000, 5.0000, 5.0000, 5.0000, 5.0000, 5.0000, 5.0000}
2	x^*	{160.0000, 193.2632, 80.0000, 72.0000, 90.0000}
	A^*	{5.0000, 5.0000, 5.0000, 5.0000, 5.0000, 5.0000, 5.0000, 5.0000}
3	x^*	{160.0000, 174.3158, 80.0000, 72.0000, 90.0000}
	A^*	{5.0000, 5.0000, 5.0000, 5.0000, 5.0000, 5.0000, 5.0000, 5.0000}

x^*- system level design vector in in; A^*- component level design vector (areas) in in^2.

Table 4.42 New Multi-level ACO results for single objective minimization of deflection

Iteration	f^* (system level)	f^* (component level)
1	1.6110	0.3222
2	0.2251	0.2251
3	0.2231	0.2231

f^* - optimum value (deflection in in)

Results obtained by the new ML ACO for minimization of deflection are given in Table 4.41 and Table 4.42. Table 4.41 shows the convergence of the design variables for every iteration between the system and the component levels. From the table it is evident that the convergence in the ML process is achieved in 3 iterations. Variation of the deflection at the end of every iteration between the two levels is given in Table 4.42. It is evident that the weight reduced from an initial value of 1.6110 in to a final minimum value of 0.2231 in in 3 iterations between the system and the component levels. The convergence is evident with equal values of deflection in both the levels at the final design. At the final design, no constraints are active. The number of ants used in ACO is 50 and the discrete

variable set is obtained by taking 20 values equally distributed between the bounds for each design variable. The convergence in ACO is achieved in 24 cycles (1200 iterations).

Results obtained by the new ML ACO for maximization of frequency are given in Table 4.43 and Table 4.44. Table 4.43 shows the convergence of the design variables for every iteration between the system and the component levels. From the table it is evident that the convergence in the ML process is achieved in 5 iterations. Variation of the frequency at the end of every iteration between the two levels is given in Table 4.44. It is evident that the frequency increased from an initial value of 74.1132 Hz to a final value of 158.8843 Hz in 5 iterations between the system and the component levels. The convergence is evident with equal values of frequency in both the levels at the final design. At the final design buckling constraints in members 2 and 5 for load condition 1 are active. The number of ants used in ACO is 50 and the discrete variable set is obtained by taking 20 values equally distributed between the bounds for each design variable. The convergence in ACO is achieved in 86 cycles (4300 iterations).

Table 4.43 New Multi-level ACO results for single objective maximization of frequency

Iteration	Optimum design vectors at system level and component level	
1	x^*	{189.4737, 162.9474, 113.6842, 87.1579, 88.4211}
	A^*	{0.3579, 0.8737, 1.3895, 1.6474, 0.6158, 5.0000, 3.7105, 5.0000}
2	x^*	{160.0000, 144.0000, 80.0000, 72.0000, 69.4737}
	A^*	{0.3579, 0.8737, 1.1316, 2.6789, 0.1000, 4.4842, 3.9684, 5.0000}
3	x^*	{168.4211, 147.7895, 80.0000, 72.0000, 71.0526}
	A^*	{0.3579, 0.8737, 1.1316, 2.9368, 0.1000, 5.0000, 3.7105, 5.0000}

4	x^*	{168.4211, 147.7895, 80.0000, 72.0000, 72.6316}
	A^*	{0.3579, 0.8737, 0.8737, 2.1632, 0.1000, 4.7421, 3.4526, 5.0000}
5	x^*	{168.4211, 147.7895, 80.0000, 72.0000, 72.6316}
	A^*	{0.3579, 0.8737, 0.8737, 2.1632, 0.3579, 4.7421, 3.7105, 5.0000}

x^*- system level design vector in in; A^*- component level design vector (areas) in in^2.

Table 4.44 New Multi-level ACO results for single objective maximization of frequency

Iteration	f^* (system level)	f^* (component level)
1	74.1132	115.1384
2	150.6809	155.3210
3	155.7106	155.9729
4	156.0388	158.8824
5	158.8824	158.8843

f^* - optimum value (frequency in Hz)

ML ACO results for single objective weight minimization are compared to the ML SQP results in Table 4.45. It is evident from the table that the minimum weight obtained by SQP is 181.7240 lb whereas the minimum weight obtained by ACO is 205.4903 lb. Hence, SQP resulted in a lighter truss by 11.5%. This is as expected because SQP is continuous and ACO is discrete optimization. Both SQP and ACO converged in 3 cycles and the number of active constraints is 8 and 7 respectively.

Table 4.45 Comparison of results for ML ACO and ML SQP for single objective weight minimization

Quantity	SQP		ACO
	Initial design	Optimum design	
Design variables: (in^2) x_1	240	204.7370	160.0000

Quantity	SQP		ACO
	Initial design	Optimum design	
x_2	150	144.0000	144.0000
x_3	110	80.0000	80.0000
x_4	100	72.0000	72.0000
x_5	69	60.0000	60.0000
x_6	0.1	0.1024	0.3579
x_7	0.1	0.7355	1.3895
x_8	0.1	0.6418	0.6158
x_9	0.1	0.1000	0.1000
x_{10}	0.1	0.1000	0.1000
x_{11}	0.1	0.4057	0.3579
x_{12}	0.1	1.0203	0.8737
x_{13}	0.1	0.8689	1.3895
Objective function:			
weight $f_1(\vec{X})$ (lb)	33.3823	181.7240	205.4903
Constraints:			
number of active behavior constraints	0	8	7

ML ACO results for single objective deflection minimization are compared to the ML SQP results in Table 4.46. It is evident from the table that the minimum deflection

obtained by SQP is 0.2474 in whereas the minimum deflection obtained by ACO is 0.2231 in. Hence, ACO resulted in a better solution. Both SQP and ACO converged in 3 cycles and the there are no active constraints in both the cases.

Table 4.46 Comparison of results for ML ACO and ML SQP for single objective deflection minimization

Quantity	SQP		ACO
	Initial design	Optimum design	
Design variables: (in^2)			
x_1	240	214.7465	160.0000
x_2	150	144.7412	174.3158
x_3	110	81.8854	80.0000
x_4	100	72.0000	72.0000
x_5	69	84.1482	90.0000
x_6	0.1	5.0000	5.0000
x_7	0.1	5.0000	5.0000
x_8	0.1	5.0000	5.0000
x_9	0.1	0.4661	5.0000
x_{10}	0.1	2.6678	5.0000
x_{11}	0.1	5.0000	5.0000
x_{12}	0.1	5.0000	5.0000
x_{13}	0.1	5.0000	5.0000

Quantity	SQP		ACO
	Initial design	Optimum design	
Objective function: deflection $f_1(\vec{X})$ (in)	27.28	0.2472	0.2231
Constraints: number of active behavior constraints	0	0	0

ML ACO results for single objective frequency maximization are compared to the ML SQP results in Table 4.47. It is evident from the table that the minimum frequency obtained by SQP is 164.2267 Hz whereas the minimum frequency obtained by ACO is 158.8843 Hz. Hence, SQP resulted in a better solution. This is as expected because SQP is continuous and ACO is discrete optimization. SQP converged in 7 cycles and ACO converged in 5 cycles and the number of active constraints is 2 in both cases.

Table 4.47 Comparison of results for ML ACO and ML SQP for single objective frequency minimization

Quantity	SQP		ACO
	Initial design	Optimum design	
Design variables: (in^2) x_1	240	178.3065	168.4211

Quantity	SQP		ACO
	Initial design	Optimum design	
x_2	150	155.6373	147.7895
x_3	110	80.0000	80.0000
x_4	100	72.0000	72.0000
x_5	69	67.3571	72.6316
x_6	0.1	0.1060	0.3579
x_7	0.1	0.6604	0.8737
x_8	0.1	0.6877	0.8737
x_9	0.1	0.7424	2.1632
x_{10}	0.1	0.1181	4.7421
x_{11}	0.1	5.0000	0.3579
x_{12}	0.1	5.0000	3.7105
x_{13}	0.1	5.0000	5.0000
Objective function:			
frequency $f_1(\vec{X})$ (Hz)	58.54	164.2267	158.8843
Constraints:			
number of active behavior constraints	0	2	2

4.2.5 Multilevel multi-objective ant colony optimization of 25-bar truss using modified game theory

In this section, the multi-level ant colony optimization procedure is used to solve the multi-objective problem using modified game theory. At the system and component levels, the combined objective function is formulated and the optimization problem is solved using the ant colony approach.

Formulation used in the multi-level multi-objective ant colony optimization is given below:

System level problem:

Minimize $f(X) = FC - S$ (4.56)

where $FC = \sum_{l=1}^{3} c_l f_{nl}(X)$ and (4.57)

$S = \prod_{l=1}^{n} [1 - f_{nl}(X)]$ (4.58)

where c_l represents the weight assigned to each of the objective and $f_{nl}(X)$ represents the normalized objective function for weight, deflection and frequency (Eq. (2.9))

Subject to

$\sigma_{ij}(X) \leq 40000\ psi$ (tension and compression) ; $i = 1,2,\ldots,25;\ j = 1,2$ (4.59)

$\sigma_{ij}(X) \leq p_i(X)$; $i = 1,2,\ldots,25;\ j = 1,2$ (4.60)

and $X = \{h_1, h_2, b_1, b_2, s_1\}$; $i = 1,2,\ldots,25$ (4.61)

Component level problem:

Minimize $f(X) = FC - S$ (4.62)

where $FC = \sum_{l=1}^{3} c_l f_{nl}(X)$ and (4.63)

$S = \prod_{l=1}^{n} [1 - f_{nl}(X)]$ (4.64)

where c_l represents the weight assigned to each of the objective and $f_{nl}(X)$ represents the normalized objective function for weight, deflection and frequency (Eq. (2.9))

Subject to

$\sigma_{ij}(X) \leq 40000\ psi$ (tension and compression) ; $i = 1,2,\ldots,25;\ j = 1,2$ (4.65)

$\sigma_{ij}(X) \leq p_i(X)$; $i = 1,2,\ldots,25;\ j = 1,2$ (4.66)

and $X = \{A_i\}$; $i = 1,2,\ldots,25$ (4.67)

Table 4.48 Optimum design vectors at each cycle in the multi-level multi-objective ant colony optimization using modified game theory of 25 bar truss

Iteration	Optimum design vectors at system level and component level	
1	x^*	{227.3684, 212.2105, 84.2105, 106.1053, 78.9474, 0.2000, 0.3000, 0.5000}
	A^*	{0.3579, 1.3895, 1.1316, 0.1000, 0.1000, 5.0000, 5.0000, 5.0000}
2	x^*	{231.5789, 151.5789, 94.7368, 104.2105, 85.2632, 0.1000, 0.7000, 0.2000}
	A^*	{0.3579, 1.1316, 1.3895, 0.3579, 0.1000, 5.0000, 4.2263, 5.0000}
3	x^*	{227.3684, 151.5789, 94.7368, 102.3158, 88.4211, 0.1000, 0.7000, 0.2000}
		{0.3579, 1.1316, 1.3895, 0.3579, 0.1000, 5.0000, 3.7105, 5.0000}

	A^*	
4	x^*	{160.0000, 144.0000, 86.3158, 72.0000, 80.5263, 0.1000, 0.1000, 0.8000}
		{0.3579, 0.8737, 0.8737, 1.3895, 0.6158, 4.7421, 4.4842, 5.0000}
	A^*	
5	x^*	{164.2105, 144.0000, 80.0000, 72.0000, 74.2105, 0.1000, 0.1000, 0.8000}
		{0.3579, 0.8737, 0.8737, 2.1632, 0.3579, 5.0000, 3.9684, 5.0000}
	A^*	
6	x^*	{168.4211, 147.7895, 80.0000, 72.0000, 72.6316, 0.1000, 0.1000, 0.8000}
		{0.3579, 0.8737, 0.8737, 2.1632, 0.3579, 4.7421, 3.7105, 5.0000}
	A^*	
7	x^*	{168.4211, 147.7895, 80.0000, 72.0000, 72.6316, 0.1000, 0.1000, 0.8000}
		{0.3579, 0.8737, 0.8737, 2.1632, 0.3579, 4.7421, 3.7105, 5.0000}
	A^*	

x^*- system level design vector in in; A^*- component level design vector (areas) in in^2.

Table 4.49 Convergence results of multi-level multi-objective ant colony optimization using modified game theory of 25 bar truss

Iteration	f^* (system level)	f^* (component level)
1	0.9310	0.8502
2	0.7661	0.7367
3	0.6697	0.6722
4	0.1119	-0.0459
5	-0.1552	-0.1637
6	-0.1554	-0.1691
7	-0.1691	-0.1691

f^* - optimum value

Results obtained by the multi-level multi-objective ant colony optimization using modified game theory are given in Table 4.48 and Table 4.49. Variation of optimum design vectors at each iteration is given in Table 4.48 and the variation of the objective function in the modified game theory is given in Table 4.49. Convergence of the ML

process is evident with equal value of the objective function in the two levels. As seen from the two tables, the number of iterations for convergence is 7.

4.2.6 Single objective optimization

The single objective optimization of the 25-bar space truss, shown in Figure 4.4, is solved for minimum weight with constraints on elemental stresses and nodal displacements. Note that the load conditions (Table 4.50) and the constraint sets are different from the one described previously. This problem is solved for a comparative study of different optimization methods. The optimization problem can be stated as follows:

Minimize the weight

$$f = \sum_{i=1}^{25} \rho A_i \, l_i \tag{4.68}$$

Stress and displacements constraints are

$$\sigma_i(x) \leq 40000 \, psi \; ; \; i = 1, 2, \ldots, 25 \tag{4.69}$$

$$d_{ij} \leq 0.35 \, in \; ; \; i = 1, 2 \; ; \; j = 1, 2 \tag{4.70}$$

where σ_i indicates the magnitude of stress in element *i* and d_{ij} the displacement of node *i* along direction *j* (*j* = 1 for *x*, 2 for *y*, 3 for *z*). Upper and lower bounds on the design variables are taken as 3.4 in^2 and 0.1 in^2, respectively.

This problem is described in Camp and Bichon (2004) and Rajeev and Krishnamoorthy (1992). The design variables are assumed to be discrete in present ACO approach with the discrete variable set given by $S = \{0.1*i$ where $i=1, 2 \ldots 34\}$. A colony size of 50 ants is used and the convergence is achieved in about 22 cycles. Table 4.51 compares the

present results with those reported by different studies in literature. The ACO resulted in a lighter design by 16.6 % and 13.09 % compared to those of Zhu (1986) and Rajeev and Krishnamoorthy (1992) respectively. The SQP method gave a minimum weight of 468.5 lb. The comparative results indicate that the present ACO is comparable with other approaches.

Table 4.50 Load conditions for 25 bar truss

Node	F_x (lb)	F_y (lb)	F_z (lb)
1	1000	-10000	-10000
2	0	-10000	-10000
3	500	0	0
6	600	0	0

Table 4.51 Comparison of results of minimization of weight of truss

Quantity	Zhu (1986) (discrete)	Rajeev and Krishnamurthy (1992) (discrete)	Camp and Bichon (2004) (ACO) (discrete)	Present work (SQP) (continuous)	Present work (ACO) (discrete)
Design variables: (in^2)					
x_1	0.1	0.1	0.1	0.1000	0.1
x_2	1.9	1.8	0.5	0.1000	0.3
x_3	2.6	2.3	3.4	3.6000	3.4
x_4	0.1	0.2	0.1	0.1000	0.1
x_5	0.1	0.1	1.9	1.9700	1.7
x_6	0.8	0.8	0.9	0.7784	1.1
x_7	2.1	1.8	0.5	0.1501	0.5
x_8	2.6	3.0	3.4	3.9291	3.4
Objective function: weight(lb)	562.93	546.01	485.05	468.50	486.09

Quantity	Zhu (1986) (discrete)	Rajeev and Krishnamurthy (1992) (discrete)	Camp and Bichon (2004) (ACO) (discrete)	Present work (SQP) (continuous)	Present work (ACO) (discrete)
$f(\vec{X})$					

This chapter applies the developed multi-level and ant colony approaches to structural engineering example problems. Multi-level uncertainty models and multi-objective ant colony optimization models are considered. Results indicate the validity of the methods. Next chapter considers the application in Mechanical Engineering problems.

CHAPTER 5 - MECHANICAL DESIGN PROBLEMS

In this chapter, benchmark examples in mechanical design are considered. These optimization problems are solved using the ant colony and multi-level approaches and the results are compared to those obtained using classical methods. The classical method used to solve these problems is Sequential Quadratic Programming (SQP). Mechanical engineering example problems considered are a gear box and the cylinder block of an internal combustion engine.

5.1 Example 1: Design optimization of a gear box

The volume of the gear box, stress in shaft 1 and stress in shaft 2 are to be minimized subjected to stress, displacement and torque constraints for the gear box shown in Figure 5.1(Huang et al., (2006)). There are 7 design variables and 11 constraints.

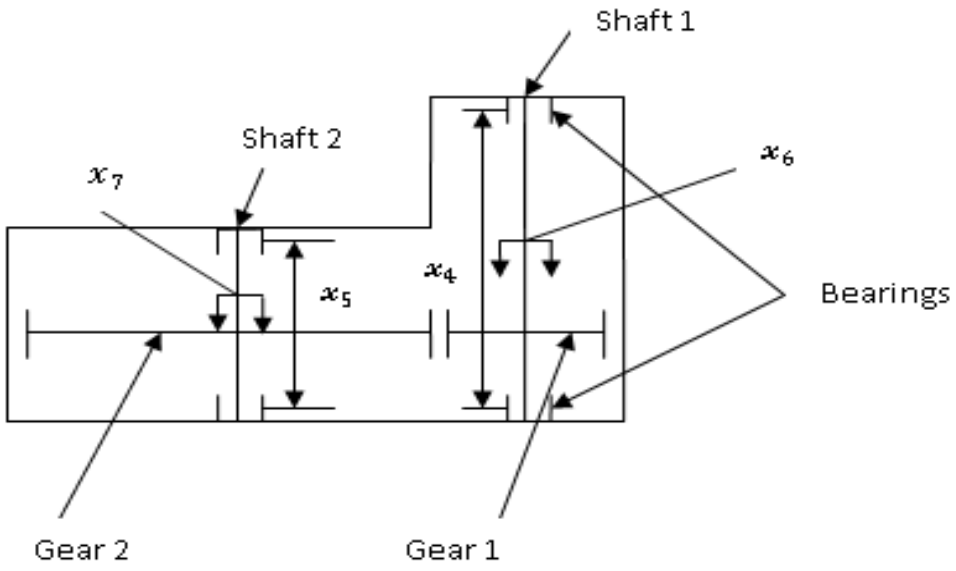

Figure 5.1 Speed reducer / gear box (Huang et al., (2006))

The design variables are the face width of the gears (x_1), teeth module (x_2), number of pinion teeth (x_3), length of shaft 1 between bearings (x_4), length of shaft 2 between bearings (x_5), diameter of shaft 1 (x_6), diameter of shaft 2 (x_7). The problem can be stated as follows:

Minimize the objective functions:

Volume of the gear box

$$f_1(\vec{X}) = 0.7854x_1x_2^2\left(\frac{10x_3^2}{3} + 14.9334x_3 - 43.0934\right) - 1.508x_1(x_6^2 + x_7^2) + 7.4777(x_6^3 + x_7^3) + 0.785(x_4x_6^2 + x_5x_7^2) \quad (5.1)$$

Stress in shaft 1

$$f_2(\vec{X}) = \left[\{(745x_4x_2^{-1}x_3^{-1})^2 + 1.69 \times 10^7\}^{1/2} \Big/ 0.1x_6^3\right] \quad (5.2)$$

Stress in shaft 2

$$f_3(\vec{X}) = \left[\{(745x_5x_2^{-1}x_3^{-1})^2 + 1.575 \times 10^8\}^{1/2} \Big/ 0.1x_7^3\right] \quad (5.3)$$

Subject to

a) Stresses in shafts

$$g_1(X) = \left[\{(745x_4x_2^{-1}x_3^{-1})^2 + 1.69 \times 10^7\}^{1/2} \Big/ 0.1x_6^3\right] \leq 1300 \quad (5.4)$$

$$g_2(X) = \left[\{(745x_5x_2^{-1}x_3^{-1})^2 + 1.575 \times 10^8\}^{1/2} \Big/ 0.1x_7^3 \right] \leq 1100 \quad (5.5)$$

b) Bending and contact stress (in teeth) constraints

$$g_3(X) = 27x_1^{-1}x_2^{-2}x_3^{-3} - 1 \leq 0 \quad (5.6)$$

$$g_4(X) = 397.5x_1^{-1}x_2^{-2}x_3^{-2} - 1 \leq 0 \quad (5.7)$$

c) Transverse displacement (of shafts 1 and 2) constraints

$$g_5(X) = 1.93x_2^{-1}x_3^{-1}x_4^3x_6^{-4} - 1 \leq 0 \quad (5.8)$$

$$g_6(X) = 1.93x_2^{-1}x_3^{-1}x_5^3x_7^{-4} - 1 \leq 0 \quad (5.9)$$

d) Torque constraints

$$g_7(X) = {x_2x_3}/{40} - 1 \leq 0 \quad (5.10)$$

$$g_8(X) = {x_1x_2^{-1}}/{12} - 1 \leq 0 \quad (5.11)$$

$$g_9(X) = 1 - x_1x_2^{-1}/5 \leq 0 \quad (5.12)$$

$$g_{10}(X) = x_4/1.9 - 1.5x_6/1.9 - 1 \leq 0 \quad (5.13)$$

$$g_{11}(X) = x_5/1.9 - 1.1x_7/1.9 - 1 \leq 0 \quad (5.14)$$

5.1.1 Single-objective ant colony optimization

In this section, single objective optimization of each of the three objectives is solved using SQP (by treating all the design variables as continuous) and ACO (by treating all the design variables as discrete). The objective function for the single objective

optimization problem is to minimize the volume of the gear box (Eq. 5.1) with constraints as stress, displacement and torque constraints (Eq. 5.4 - Eq. 5.14). The results obtained by both methods are given in Table 5.1 and Table 5.2. In SQP, the minimum volume obtained is 2770.6 cm^3 and the minimum stress in shaft 1 is obtained as 1300 kgf/cm^2 (12.7×10^7 N/m^2) and the minimum stress in shaft 2 is obtained to be 1004.0 kgf/cm^2 (9.8×10^7 N/m^2). The corresponding values for ACO are 2869.2 cm^3, 1144.0 kgf/cm^2 (11.2×10^7 N/m^2) and 1004.0 kgf/cm^2 (9.8×10^7 N/m^2)[@]. Thus, the SQP method reduces the weight by 3.55 % and the minimum stress in shaft 1 by 13.9 % when compared to the ACO method. This is as expected because SQP uses continuous variables and hence better solutions. The minimum stress in shaft 2 is the same in both cases. For minimization of volume using SQP, torque constraints 9, 11 and in stress constraint in shaft are active. In ACO, torque constraints 9 and 11 are active. For minimization of stress in shaft 1, torque constraints 9 and 10 are active are active in both SQP and ACO. The discrete set of design variables used for ACO is a set of 6 values distributed between the bounds of the corresponding design variables. A colony size of 25 ants is used and the convergence is achieved in about 8 cycles for minimization of volume, 6 cycles for minimization of stress in shaft 1 and 6 cycles for minimization of stress in shaft 2, as shown in Figure 5.2, Figure 5.3 and Figure 5.4. In SQP, the number of iterations and the number of objective function evaluations for each objective are 7, 8, 7 and 59, 64, 56 respectively. Also, the results obtained by the SQP and ACO approaches for single objective minimization of volume of the gear box are compared to those available in

[@] The problem formulation, originally given by Huang et al., (2006), contained empirical/experimental constants valid in Kgf and cm2 units. As such, the optimization study was conducted in the same units, and the results are reported in the same units with their equivalent values in SI units indicated in parentheses.

literature. The comparative results are given in Table 5.3. The minimum volume of the gear box obtained by Ray (2003) is 2996 cm^3 and the present ACO algorithm gives a minimum volume of 2869.2 cm^3. Hence, there is a reduction in the minimum volume by about 4.23 % by using ACO. The reason for the improvement of the optimum objective value can be attributed to tighter (more critical) torque constraints in ACO compared to that of Ray (2003). The SQP gives better result than ACO (3.56 %). This is because of two active torque constraints and active stress constraint in shaft 1.

Table 5.1 Results of single objective optimization of the gear box (SQP)

Quantity	Initial Design	Minimization of volume	Minimization of stress in shaft 1	Minimization of stress in shaft 2
Design Variables:				
x_1 (cm)	2.6	3.5	3.6	3.6
x_2 (cm)	0.8	0.7	0.72	0.72
x_3 (integer)	23	17	23	23
x_4 (cm)	7.9	7.3	7.75	7.9
x_5 (cm)	7.6	7.4	7.6	7.95
x_6 (cm)	3.6	3.1623	3.9	3.6
x_7 (cm)	5.0	5.0	5.0	5.5
Objective Functions:				
volume $f_1(\vec{X})$ (cm^3)	4061.5	2770.6	4439.7	4652.9
stress 1 $f_2(\vec{X})$ (kgf/cm^2)@	881.12	1300	693.03	881.13

Quantity	Initial Design	Minimization of volume	Minimization of stress in shaft 1	Minimization of stress in shaft 2
stress 2 $f_3(\vec{X})$ (kgf/cm^2)	1004.01	1004.01	995.64	754.31
Constraints:				
number of active behavior constraints	0	3[§]	2*	2[$]

[@]1kgf/cm^2=9.8×10^{7}N/m^2;† $bounds$ $(2.6 \le x_1 \le 3.6; 0.7 \le x_2 \le 0.8; 17 \le x_3 \le 28; 7.3 \le x_4, x_5 \le 8.3; 2.9 \le x_6 \le 3.9; 5 \le x_7 \le 5.5)$; [§] torque constraints 9, 11 and stress constraint in shaft 1; * torque constraints 9 and 10; [$] torque constraints 9 and 11

Table 5.2 Results of single objective optimization of the gear box (ACO)

Quantity	Minimization of volume	Minimization of stress in shaft 1	Minimization of stress in shaft 2
Design variables:			
x_1 (cm)	3.6	3.6	3.6
x_2 (cm)	0.7	0.72	0.72
x_3 (integer)	17	28	28
x_3 (cm)	8.3	8.1	8.3
x_4 (cm)	8.3	8.3	8.1
x_5 (cm)	3.3	3.9	3.9
x_6 (cm)	5.0	5.5	5.5
Objective functions:			
volume $f_1(\vec{X})$ (cm^3)	2869.2	6115.0	6112.7

Quantity	Minimization of volume	Minimization of stress in shaft 1	Minimization of stress in shaft 2
stress 1 $f_2(\vec{X})$ (kgf/cm^2)	1144.0	693.0	693.0
stress 2 $f_3(\vec{X})$ (kgf/cm^2)	1004.0	754.3	754.3
Constraints:			
number of active behavior constraints	2[§]	2*	2[$]

[@]1kgf/cm^2=9.8×10^{7}N/m^2;† *bounds* ($2.6 \le x_1 \le 3.6; 0.7 \le x_2 \le 0.8; 17 \le x_3 \le 28; 7.3 \le x_4, x_5 \le 8.3; 2.9 \le x_6 \le 3.9; 5 \le x_7 \le 5.5$); [§] torque constraints 9 and 11; * torque constraints 9 and 10; [$] torque constraints 9 and 11.

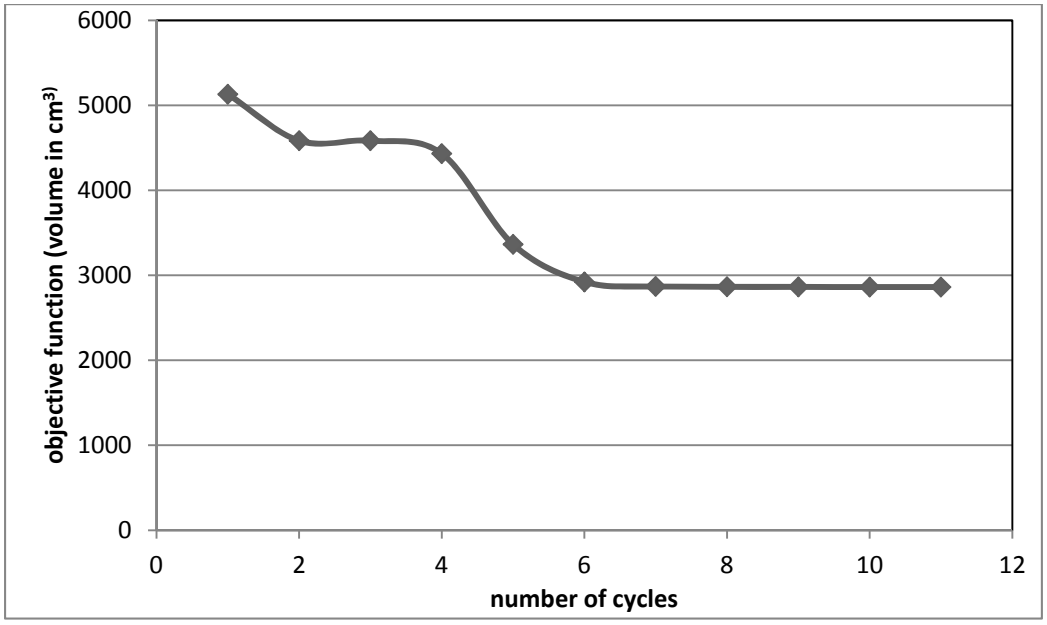

*cycle =number of iterations/number of ants; number of ants = 25

Figure 5.2 Convergence history for minimum volume of the gear box

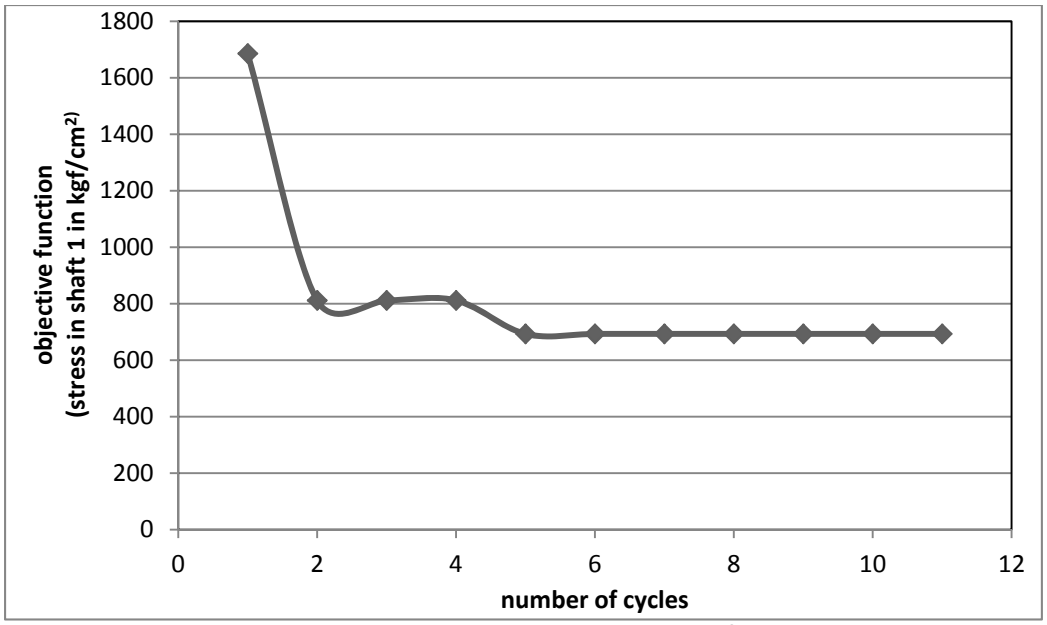

*cycle =number of iterations/number of ants; number of ants = 25; @1kgf/cm^2=9.8×10^{7}N/m^2

Figure 5.3 Convergence history for minimum stress in shaft 1 of the gear box

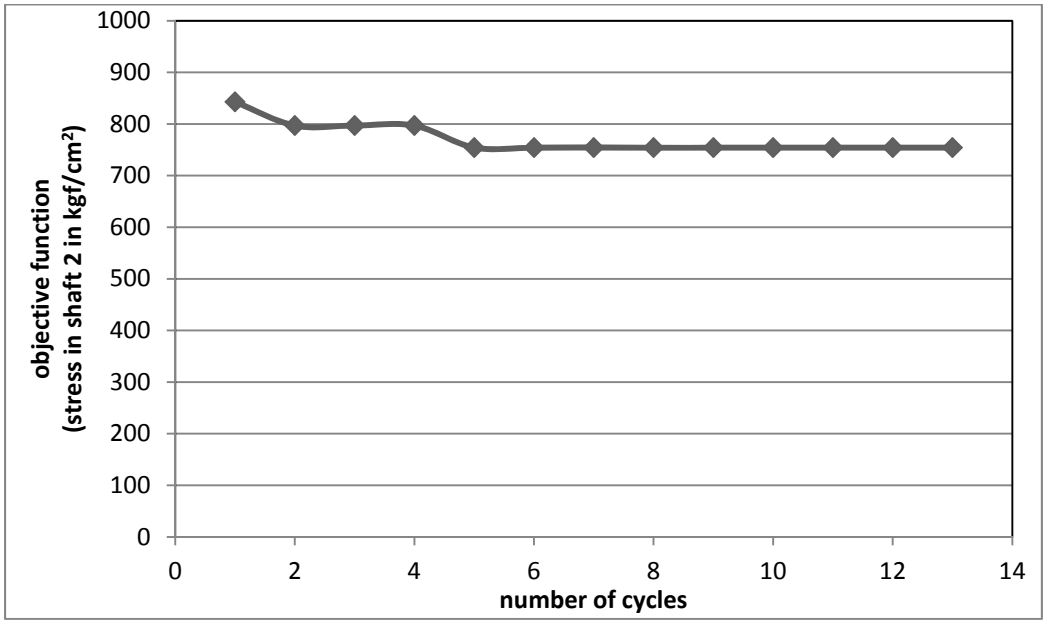

*cycle =number of iterations/number of ants; number of ants = 25; @1kgf/cm^2=9.8×10^{7}N/m^2

Figure 5.4 Convergence history for minimum stress in shaft 2 of the gear box

Table 5.3 Comparison of results of minimization of volume of gear box

Quantity	Ray (2003)	SQP (continuous variables)	ACO (discrete variables)
Design variables:			
x_1 (cm)	3.5	3.5	3.6
x_2 (cm)	0.7	0.7	0.7
x_3 (integer)	17	17	17
x_4 (cm)	7.3	7.3	8.3
x_5 (cm)	7.8	7.4	8.3
x_6 (cm)	3.3	3.1623	3.3
x_7 (cm)	5.3	5.0	5
Objective function:			
volume $f(\vec{X})$ (cm^3)	2996	2770.6	2869.2
Constraints:			
number of active behavior constraints	1[§]	3[£]	2[$]

† $bounds$ $(2.6 \leq x_1 \leq 3.6; 0.7 \leq x_2 \leq 0.8; 17 \leq x_3 \leq 28; 7.3 \leq x_4, x_5 \leq 8.3; 2.9 \leq x_6 \leq 3.9; 5 \leq x_7 \leq 5.5)$; [§] torque constraint; [£] torque constraints 9, 11 and stress in shaft 1; [$] torque constraints 9 and 11

5.1.2 Multi objective ant colony optimization using weighted sum approach

Multi-objective optimization problem of gear box is solved using SQP and ACO using weighted sum approach. The problem is defined as

$$\text{Minimize } f(X) = \sum_{l=1}^{3} c_l f_{nl}(X) \tag{5.15}$$

Where c_l represents the weight assigned to each of the objective (taken as 0.8, 0.1 and 0.1 for l = 1, 2, and 3 respectively) and $f_{nl}(X)$ represents the normalized objective function for volume, stress in shaft 1 and stress in shaft 2 (Eq. (2.9)).

The constraints are stress, displacement and torque constraints defined by Eq. 5.4 to Eq. 5.14. The results are given in Table 5.4. The minimum volume obtained by SQP is 3310.7 cm^3 whereas the minimum volume obtained by ACO is 3354.4 cm^3. Hence, the SQP solution resulted in a lighter truss by 1.32 %. The minimum stresses in shafts 1 and 2 obtained by SQP and ACO are the same. Also, the torque constraints 9, 10 and 11 are active in both cases. For ACO, a colony size of 25 ants is used. The discrete set of design variables used for ACO is a set of 6 values distributed between the bounds of the corresponding design variables. The convergence is achieved in 12 cycles as shown in Figure 5.5.

Also, the results of multi-objective optimization of the gear box problem are compared with those available in literature in Table 5.4. Huang et al., (2006) used a fuzzy approach with continuous design variables, to solve the multi-objective gear box optimization problem. A relevant set of their results is presented in Table 5.4 along with those obtained in present work (using both SQP and ACO approaches). A direct comparison is not possible between the various sets of results shown. The results of the fuzzy approach indicate the optimum design vector and the corresponding objective functions with a satisfaction (membership) level of 0.8 (less than one), and the results of SQP denote the optimum design vector and the corresponding objective functions which are expected to be equal or better than those obtained with ACO. The results are presented for an order-of-magnitude type of comparison. It can be seen from the results shown in Table 5.4 that the minimum volume obtained by the ACO is less than the volume reported by Huang et al., (2006) by 2.1 %. One of the stresses (stress in shaft 2) remained almost the same and the stress in shaft 1 decreased.

Table 5.4 Comparison of results of multi-objective optimization of the gear box

Quantity	SQP	ACO	Huang et al., (2006)
Design variables:			
x_1 (cm)	3.5	3.6	3.5
x_2 (cm)	0.7	0.7	0.71
x_3 (integer)	17	17	18
x_4 (cm)	7.75	7.9	8.24
x_5 (cm)	7.95	8.1	8.23
x_6 (cm)	3.9	3.9	3.61
x_7 (cm)	5.5	5.5	5.4
Objective functions:			
volume $f_1(\vec{X})$ (cm^3)	3310.71	3354.43	3425.1
Stress 1 $f_2(\vec{X})$ (kgf/cm^2)	693.03	693.03	879.8
Stress 2 $f_3(\vec{X})$ (kgf/cm^2)	754.31	754.31	797.6
Constraints:			
number of active behavior constraints	3[§]	3[&]	0

[@]$1kgf/cm^2=9.8\times10^7N/m^2$;† ons $(2.6 \le x_1 \le 3.6; 0.7 \le x_2 \le 0.8; 17 \le x_3 \le 28; 7.3 \le x_4, x_5 \le 8.3; 2.9 \le x_6 \le 3.9; 5 \le x_7 \le 5.5)$;[§] torque constraints 9, 10, 11; [&] torque constraints 9, 10, 11.

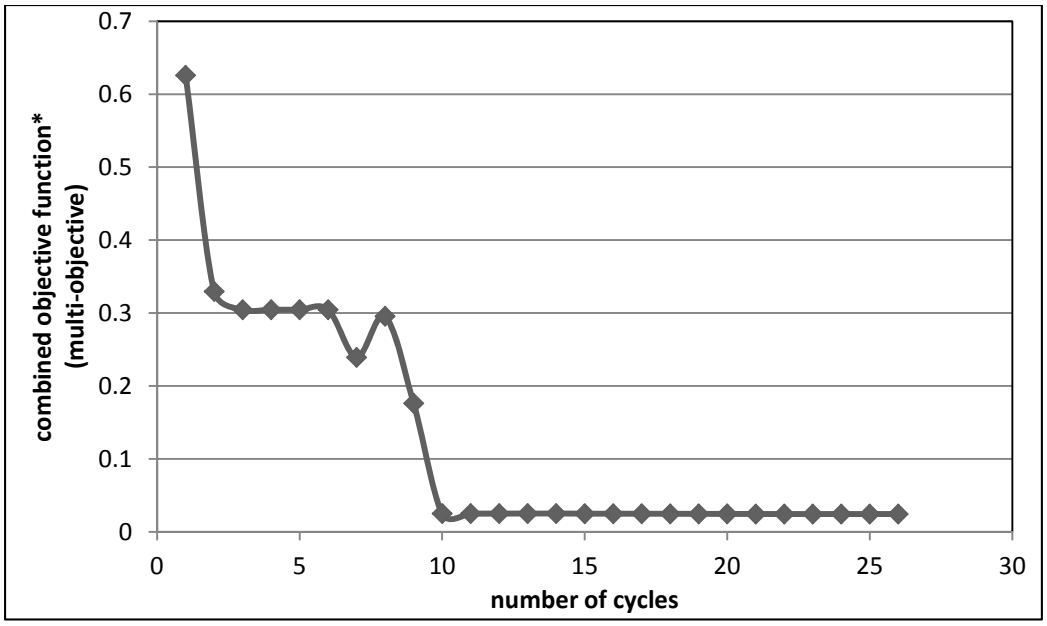

*combined objective is calculated using Eq. (2.29) with normalized individual objectives

Figure 5.5 Convergence history for multi-objective ACO of the gear box

Performance of ACO is studied by varying the size of the ant colony keeping the maximum number of cycles fixed. Three different colony sizes of 25, 50 and 75 ants are considered. The convergence results are shown in Figure 5.6, Figure 5.7 and Figure 5.8. It can be seen that for the minimization of volume (objective), a colony size of 25 ants converges to the optimum in about 8 cycles while a colony size of 50 ants converges to the optimum value in 6 cycles. The colony size of 75 ants converges to about 10 cycles. But in all the cases, the converged volume is different. The minimum volume is obtained with 25 ants. Also, the starting vector is chosen randomly in each case. For the minimization of stress in shaft 1, the colony size of 25 and 50 ant size colonies converge in about 5 cycles. The colony with 75 ants converged in 7 cycles. Convergence of stress in shaft 2 is shown in Figure 5.8. In this case, 25 and 50 ant size colonies take 5 cycles to converge while the colony with 75 ants converges in 13 cycles.

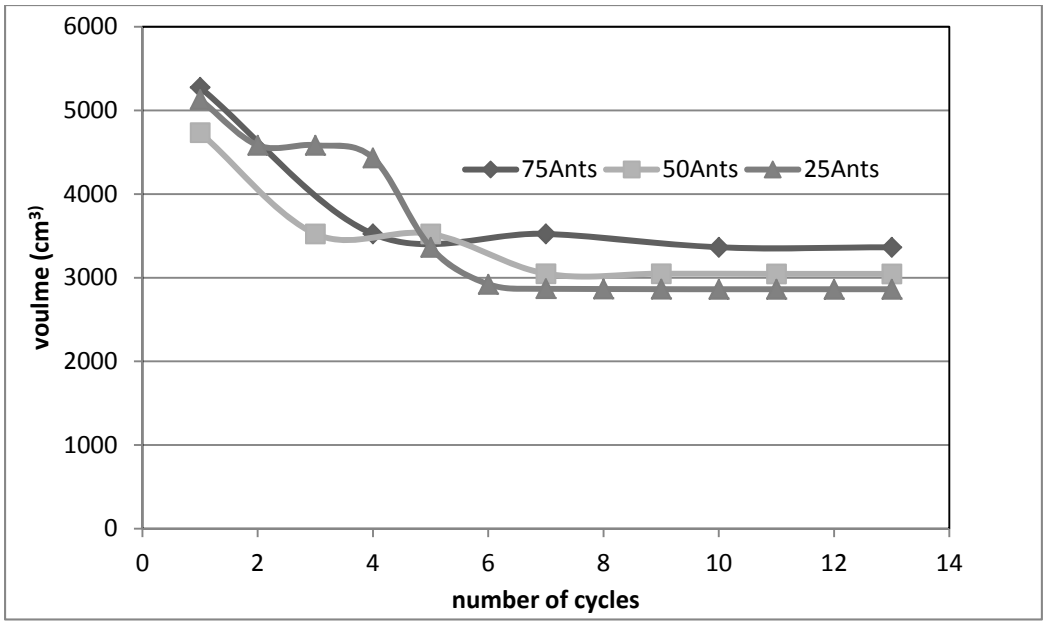

Figure 5.6 Convergence of minimum volume with changes in the number of ants for the gear box

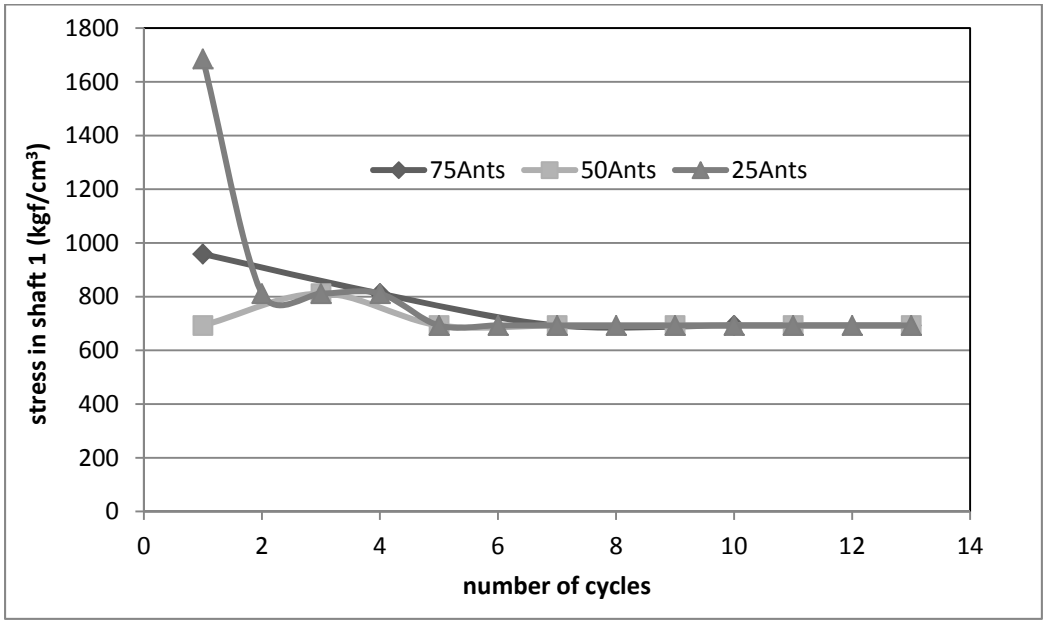

@1kgf/cm^2=9.8×10^{7}N/m^2

Figure 5.7 Convergence of stress in shaft 1with changes in the number of ants for the gear box

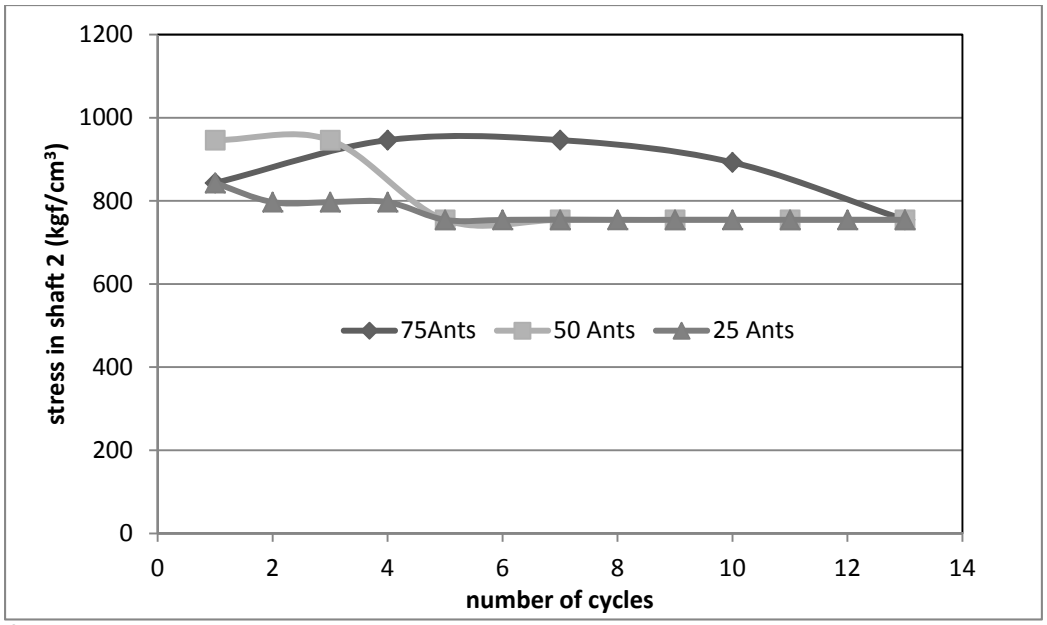

@1kgf/cm^2=9.8×10^{7}N/m^2

Figure 5.8 Convergence of stress in shaft 2 with changes in the number of ants for the gear box

5.1.3 Multi-objective ant colony optimization using modified game theory approach

In this section, ant colony optimization method is used to solve the multi-objective optimization problem of the gear box using modified game theory approach. The multi-objective problem is defined as

$$\text{Minimize } f(X) = FC - S \tag{5.16}$$

$$\text{where } FC = \sum_{l=1}^{3} c_l f_{nl}(X) \text{ and} \tag{5.17}$$

$$S = \prod_{l=1}^{n} [1 - f_{nl}(X)] \tag{5.18}$$

Where c_l represents the weight assigned to each of the objective and $f_{nl}(X)$ represents the normalized objective function for volume, stress in shaft1 and stress in shaft (Eq. (2.9)).

The constraints are stress, displacement and torque constraints defined by Eq. 5.4 to Eq. 5.14. The results obtained by the multi-objective ant colony optimization using modified game theory are given in Table 5.5. As seen from the table, the minimum volume obtained by ACO is 3890.46 cm^3, the minimum stress in shaft 1 is 1143.92 kgf/cm^2 (11.2 $\times 10^7$ N/m^2) and the minimum stress in shaft 2 is 797.00 kgf/cm^2 (7.8 $\times 10^7$ N/m^2). The results obtained by ACO are compared with those obtained using SQP (using modified game theory). The minimum volume obtained by SQP is 3310.70 cm^3, the minimum stress in shaft 1 is 693.03 kgf/cm^2 (6.7 $\times 10^7$ N/m^2) and the minimum stress in shaft 2 is 754.31 kgf/cm^2 (7.3 $\times 10^7$ N/m^2). Hence, the SQP solution resulted in a lesser volume by 14.13 %. The stresses in shaft 1 and shaft 2 also decreased by 39.42 % and 5.3 % respectively. Hence, the SQP resulted in a better solution in all the three objectives when compared to ACO. Also, the torque constraints 9, 10 and 11 are active in the case of SQP and the torque constraints 9 and 11 are active in ACO. For SQP, the number of iterations for convergence is 12 and the number of function evaluations is 132. The discrete set of design variables used for ACO (with 25 ants) is a set of 6 values distributed between the bounds. The convergence in ACO is achieved in 10 cycles as shown in Figure 5.9.

Table 5.5 Comparison of results of multi-objective ACO and SQP using modified game theory for the gear box

Quantity	SQP (MGT)		ACO* (MGT)
	Initial design	Optimum design	
Design variables: x_1 (cm)	2.7	3.5	3.6

Quantity	SQP (MGT)		ACO* (MGT)
	Initial design	Optimum design	
x_2 (cm)	0.73	0.7	0.7
x_3 (integer)	25	17	21
x_4 (cm)	7.3	7.75	8.1
x_5 (cm)	7.6	7.95	7.9
x_6 (cm)	3.6	3.9	3.3
x_7 (cm)	5.3	5.5	5.4
C1	0.3	0.1	0.4
C2	0.3	0.25	0.4
C3	0.4	0.65	0.2
Objective functions:			
volume $f_1(\vec{X})$ (cm^3)	4264.51	3310.70	3890.46
stress 1, $f_2(\vec{X})$ (kgf/cm^2)	881.12	693.03	1143.92
stress 2, $f_3(\vec{X})$ (kgf/cm^2)	842.97	754.31	797.00
Constraints:			
number of active behavior constraints	1	3[§]	2[&]

[@]$1kgf/cm^2=9.8\times10^7 N/m^2$

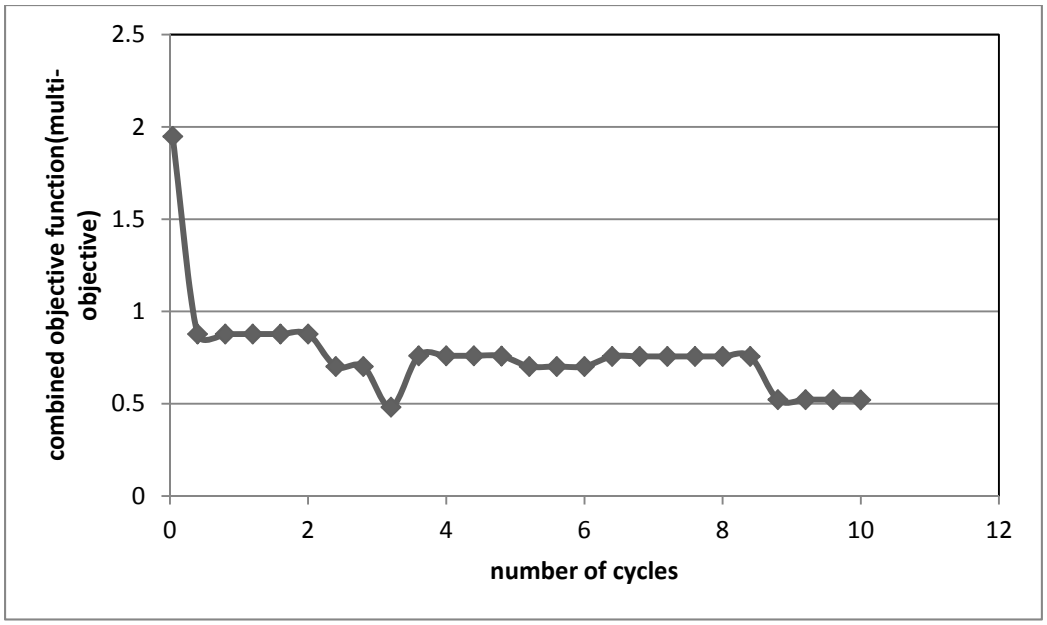

Figure 5.9 Convergence graph for multi-objective ACO using modified game theory for the gear box

Table 5.6 Designs for the best 5 ants in multi-objective ACO using modified game theory for the gear box

Quantity	Ant 1	Ant 2	Ant 3	Ant 4	Ant 5
Design variables:					
x_1(cm)	3.2	3.4	3.6	3.6	3.2
x_2 (cm)	0.72	0.72	0.7	0.7	0.72
x_3 (integer)	24	24	24	21	24
x_4 (cm)	8.3	8.3	8.1	8.1	8.3
x_5 (cm)	7.9	7.9	8.1	7.9	7.9
x_6 (cm)	3.3	3.3	3.3	3.3	3.1
x_7	5.4	5.4	5.4	7.4	5.4

Quantity	Ant 1	Ant 2	Ant 3	Ant 4	Ant 5
c1	0.4	0.4	0.4	0.4	0.4
c2	0.4	0.4	0.4	0.4	0.4
c3	0.2	0.2	0.2	0.2	0.2
Combined objective function $f_1(\vec{X})$	0.7019	0.7599	0.7561	0.5205	0.8773
Constraints:					
number of active behavior constraints	0	1[&]	1[$]	1[§]	0

[&] torque constraint 7; [$] torque constraint 9; [§] torque constraint 7

Details of the best 5 final designs (corresponding to the best 5 ants) are given in Table 5.6. Among all the designs, the one with minimum combined objective function value is chosen as the final design in ACO. It can be seen from the table, that the design corresponding to ant 4 has the minimum combined objective function value with torque constraint 7 as active constraint. In this problem, all the constants (*c1*, *c2* and *c3*) converged to the same values of 0.4, 0.4 and 0.2 respectively.

5.2 Example 2: Design optimization of combustion chamber of an internal combustion engine

To illustrate multi-level multidisciplinary design optimization framework with uncertainties, the design of an internal combustion engine combustion chamber is proposed. The problem is detailed in Papalambros and Wilde (2000). The model is based on fundamental thermodynamic relations and assumes some empirical data. A flat head

design is considered as shown in Figure 5.10. The model has five design variables. They are the cylinder bore (b), compression ratio (c_r), exhaust valve diameter (d_e), intake valve diameter (d_i), and the engine's revolutions per minute at peak power (w). The objective is to maximize the break power per unit engine displacement. The constraints represent the fuel economy and packaging specifications. The mathematical optimization problem is given as

$$\text{Minimize } f(c_r, w, b, d_i) = K_0\, w[FMEP(c_r, w, b) - P_0 \eta_t(c_r, b)\eta_v(w, d_i)] \tag{5.19}$$

Subject to the following constraints

a) Constraint for the bore wall thickness is given

$$g_1(b) = b - P_1 \leq 0 \tag{5.20}$$

b) Constraint for the engine height

$$g_2(b) = P_2 - b \leq 0 \tag{5.21}$$

c) Constraint for the valve structure

$$g_3(b, d_i, d_e) = d_i + d_e - K_3 b \leq 0 \tag{5.22}$$

d) Constraint for the ratio of minimum valve diameter

$$g_4(d_i, d_e) = K_4 d_i - d_e \leq 0 \tag{5.23}$$

e) Constraint for the ratio of maximum valve diameter

$$g_5(d_i, d_e) = d_e - K_5 d_i \leq 0 \tag{5.24}$$

f) Constraint for the maximum Mach index

$$g_6(w, d_i) = P_3 w - d_i^2 \leq 0 \tag{5.25}$$

g) Constraint for the knock-limited compression

$$g_7(c_r, b) = c_r - \ 13.2 + 0.045b \ \leq 0 \tag{5.26}$$

h) Constraint for the maximum torque convertor rpm

$$g_8(w) = w - K_7 \leq 0 \tag{5.27}$$

i) Constraint for the fuel economy

$$g_9(c_r, b) = P_4 - 0.8595(1 - c_r^{-0.33}) + S_v(c_r, b) \leq 0 \tag{5.28}$$

where all the variables are positive and $P_i(i = 0,1, \ldots ,4)$, $K_i(i = 0,2,3,4,5,7)$ are parametric values given in Papalambros and Wilde (2000). FMEP represents the friction mean effective pressure, η_t and η_v are the thermal and volumetric efficiencies, S_v is the surface to volume ratio and *s* is the stroke length. It is to be noted that complete formulations and other parameters not shown in these equations, are detailed in Papalambros and Wilde (2000).

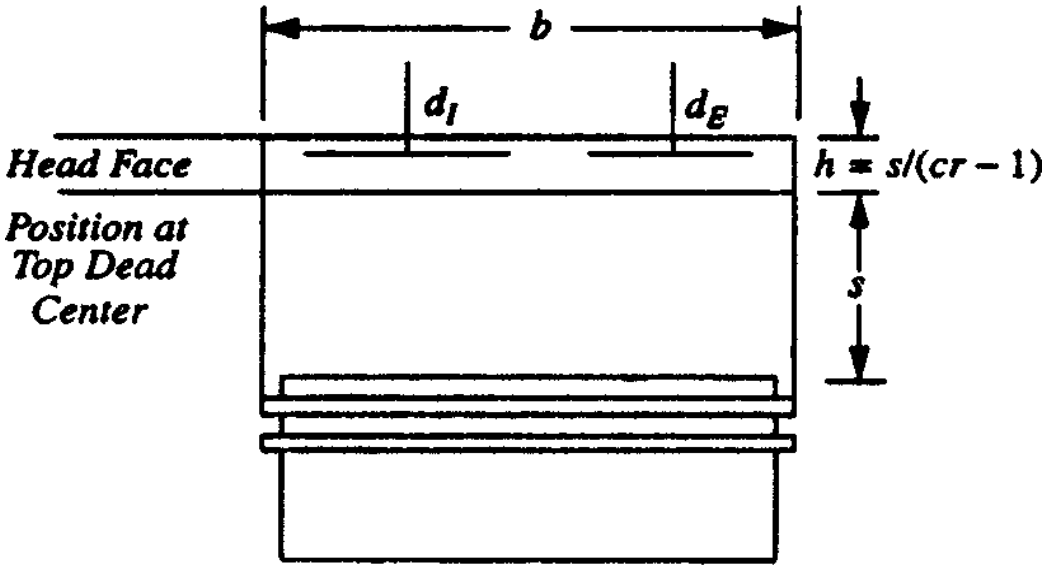

Figure 5.10 Combustion chamber (Papalambros and Wilde (2000))

5.2.1 Multi-level formulation (approach 1)

The multilevel formulation of the model is based on defining two sub-problems (disciplines), namely, the geometry sub-problem and the thermodynamics sub-problem as shown in Figure 5.11. Each sub-problem has its own design variables and constraints along with the common system level shared design variables. The objective of the sub-problem is to minimize the discrepancy function. At the system level the objective is to minimize the negative specific power and assign target values to the shared variables. The coordination between levels is obtained by repeated iterations between both levels to satisfy the equality constraints.

Formulation used in the multi-level process is given below:

System level problem:

Minimize $f(Y) = -\text{power}$ (5.29)

subject to

$$Y - X^g = 0; \tag{5.30}$$

$$Y - X^t = 0; \tag{5.31}$$

$$\text{where } Y = \begin{Bmatrix} b \\ d_i \\ d_e \\ c_r \\ w \end{Bmatrix} \tag{5.32}$$

Component level problem (geometry discipline):

$$\text{Minimize } f(X^g) = (b^* - b^g)^2 + ({d_i}^* - {d_i}^g)^2 \tag{5.33}$$

subject to

$$g_1(b) = b - P_1 \leq 0 \tag{5.34}$$

$$g_2(b) = P_2 - b \leq 0 \tag{5.35}$$

$$g_3(b, d_i, d_e) = d_i + d_e - K_3 b \leq 0 \tag{5.36}$$

$$g_4(d_i, d_e) = K_4 d_i - d_e \leq 0 \tag{5.37}$$

$$g_5(d_i, d_e) = d_e - K_5 d_i \leq 0 \tag{5.38}$$

$$\text{where } X^g = \begin{Bmatrix} b \\ d_i \\ d_e \end{Bmatrix} \tag{5.39}$$

Component level problem (thermodynamics discipline):

$$\text{Minimize } f(X^t) = ({c_r}^* - {c_r}^t)^2 + (w^* - w^t)^2 \tag{5.40}$$

subject to

$$g_6(w, d_i) = P_3 w - d_i^2 \leq 0 \tag{5.41}$$

$$g_7(c_r, b) = c_r - \ 13.2 + 0.045b \ \leq 0 \tag{5.42}$$

$$g_8(w) = w - K_7 \leq 0 \tag{5.43}$$

$$g_9(c_r, b) = P_4 - 0.8595(1 - c_r^{-0.33}) + S_v(c_r, b) \leq 0 \tag{5.44}$$

where and $X^t = \begin{Bmatrix} b \\ d_i \\ c_r \\ w \end{Bmatrix}$ (5.45)

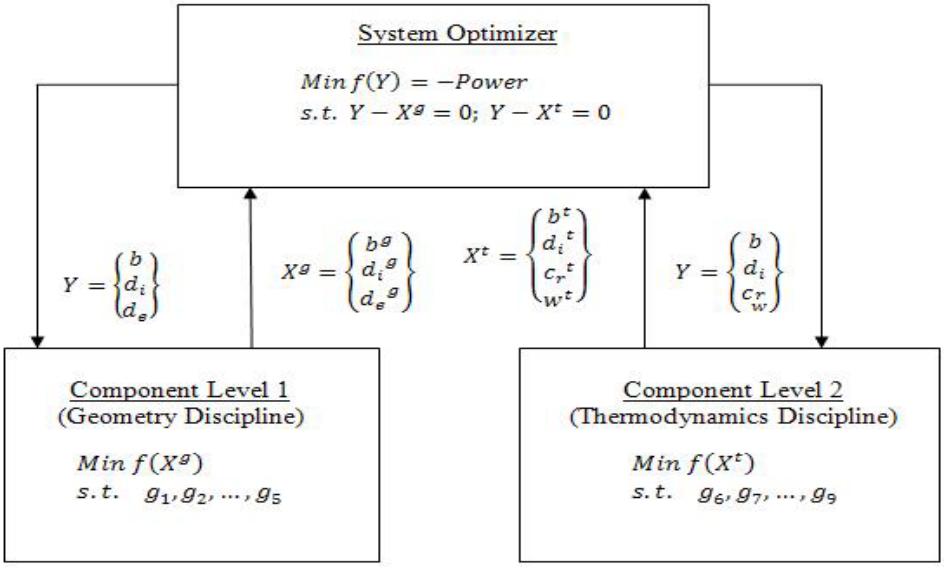

Figure 5.11 Multi-level combustion chamber design

5.2.2 Multi-level stochastic formulation

To account for stochastic uncertainty in the engine's chamber design, the two level formulations ares made similar to the previous deterministic case but with modifications. The design variables in this case are considered as the random variables. The standard

deviation of the random variables is assumed to be about 1% of the mean value and the constraints are satisfied with 0.95 probability level. The procedure described in the earlier section is used to convert the stochastic optimization problem into an equivalent deterministic optimization using the chance constrained optimization. In this case, the system level objective is the combined specific power obtained by considering the mean and standard deviation of the design variables. The target variables are assigned and matched by the equality constraints. At the sub-problem levels, the objective is to match the shared variables while satisfying the discipline specific constraints. Also, it is to be noted that the constraints are stochastic as opposed to deterministic.

5.2.3 Multi-level interval formulation

For interval based multi-level optimization, the mathematical formulation for the multilevel system is based on the interval analysis and optimization. The design variables at both levels are intervals. For the optimization, the minimum and maximum values of each of the five initial design variables (b, d_i, d_e, c_r, w) are taken as the design variables in the interval formulation. Hence, a total of 10 design variables are used to minimize the mean specific power using interval calculations. Also, extra sets of discipline specific constraints are obtained because of the minimum and maximum values. The results obtained for deterministic, stochastic and interval optimizations are tabulated in Table 5.7, Table 5.10 and Table 5.11 respectively. For each of the three cases, the deterministic, stochastic and interval approaches, the results were obtained using different starting points chosen randomly. It was found that, the starting point did not have much influence on the converged designs. It is to be noted that in all the three cases, SQP method is used to solve the optimization problems in each level.

Table 5.7 Results of deterministic optimization (single and multilevel)

Quantity	Initial Design	Bounds		Optimum Design	
		Lower	Upper	Single level*	Multi-level **
Design variables:					
b (cm)	75	70	90	83.33	83.34
d_i (cm)	27	25	50	37.33	37.35
d_e (cm)	35	25	50	30.99	30.99
c_r	6.5	6	12	9.45	9.45
w (rpm)	5200	5000	6500	6070	6071
Objective function: (power in bhp)	25.03	17.47	77.55	55.65	55.71

* $(g_1, g_3, g_4 \text{ and } g_7)$ are active at optimum point; converged in 7 iterations and 48 function evaluations.

** $(g_1, g_3, g_4 \text{ and } g_7)$ are active at optimum point; converged in 8 iterations and 56 function evaluations.

Table 5.8 Convergence results of the deterministic multi-level optimization

cycle	f^* (system level)	$f^{(0)}$ (geometry component)	f^* (geometry component)	$f^{(0)}$ (thermodynamics component)	f^* (thermodynamics component)	Power (bhp)
1	38.3339	20.3536	11.2397	5.6924	5.4213	34.5738
2	52.3522	78.1485	0.1440	26.4289	2.1245	49.6936
3	61.3554	162.6573	5.2880	36.9312	5.8486	53.6992
4	65.4466	250.8627	10.0033	37.1671	6.4904	55.709

f^* - optimum value ; $f^{(0)}$ - initial value

Table 5.9 Optimum design vectors at each cycle in the deterministic multi-level optimization

cycle	optimum design vectors at system level and component levels	
1	x^*	{75.3218, 31.5000, 35.0000, 8.3838, 5000}
	x_1^*	{ 78.4165, 32.7895, 31.5348}
	x_2^*	{ 75.3218, 31.5000, 6.0000, 4802}
2	x^*	{79.2809, 34.6952, 30.3124, 9.6467, 5653}

cycle	optimum design vectors at system level and component levels	
	x_1^*	{ 79.2809, 34.6952, 30.3124}
	x_2^*	{ 78.9628, 34.9022, 9.6467, 5653}
3	x^*	{81.3488, 36.4514, 30.2547, 9.5816, 6065}
	x_1^*	{ 81.3488, 36.4514, 30.2547}
	x_2^*	{ 80.4088, 38.5500, 9.5816, 6065}
4	x^*	{83.3300, 37.3391, 30.9915, 9.4524, 6071}
	x_1^*	{ 83.3300, 37.3391, 30.9915}
	x_2^*	{ 83.2808, 40.5015, 9.4524, 6071}

x^*- system level design vector ; x_1^*- component level (geometry) design vector; x_2^*- component level (geometry) design vector

Table 5.10 Results of stochastic multi-level optimization

Quantity	Initial Design	Bounds		Optimum Design
		Lower	Upper	Multi-level **
Design variables:				
b (cm)	75	70	90	82.46
d_i(cm)	27	25	50	34.32
d_e(cm)	35	25	50	30.19
c_r	6.5	6	12	9.86
w (rpm)	5200	5000	6500	5128
Combined objective function* (bhp)	25.03	17.47	77.55	48.27

*linear sum of mean and standard deviation of power (Eq. 3.6)

** (g_1, g_3, g_4 and g_7) are active at optimum point; converged in 7 iterations with 46 function evaluations.

Table 5.11 Results of interval multi-level optimization

Quantity	Initial Design (intervals)	Bounds		Optimum Design
		Lower	Upper	Multi-level * (intervals)
Design variables:				
b (cm)	[75 85]	70	90	[84.75 88.88]
d_i(cm)	[26 35]	25	50	[39.51 39.59]
d_e(cm)	[30 37]	25	50	[31.03 32.49]
c_r	[6.1 6.7]	6	12	[6.92 8.22]
w (rpm)	[4800 5400]	5000	6500	[5512 6457]
Objective function: (interval of power in bhp)	[21.98 44.29]	17.47	77.55	[50.97 57.53]

*(g_1, g_3, g_4 $and g_7$) are active at optimum point; converged in 24 iterations and 461 function evaluations

Table 5.7 shows the results obtained by the deterministic case with one level and two level optimizations. The single level optimization results are shown to validate the bi-level procedure described in present work. The details of the iterative procedure are given in Table 5.8 and Table 5.9. It can be seen that both the algorithms converge to the same design. The bi-level algorithm requires slightly more number of function evaluations and iterations for its convergence. Three of the geometry constraints **(**g_1, g_3, g_4**)** are active indicating that the valve and engine geometry are tightly constrained. Also, the thermodynamics constraint related to knocking **(**g_7**)** is active. The power obtained by the multi-level deterministic approach is 55.7 bhp and lies in the interval result with lower value of 50.97 bhp and upper value of 57.53 bhp. As expected the brake power obtained by the stochastic optimization is slightly lower because of the design feasibility. Also, the mean and standard deviation values in stochastic multi-level optimization at the initial

design are 24.73 bhp and 0.294 bhp. The corresponding values for the final design are 47.69 bhp and 0.574 bhp respectively. The same set of constraints is active within tolerances in all the three cases. Deterministic and stochastic algorithms took almost the same number of iterations and objective function evaluations for convergence. But, interval optimization algorithm took about three times the number of iterations to converge. This might be because of double the number of design variables and constraints when compared to the deterministic and stochastic designs.

5.2.4 Sensitivity analysis

To further understand the effect of uncertainty on the design optimization, sensitivity analysis of the optimum designs is considered. Variation of the objective function (brake power) with changes in the optimum values of the design variables is studied. In all the three cases, the diameter of the inlet valve was most sensitive to the brake power. This is as expected because the inlet valve design controls the amount of fuel into the combustion chamber in turn influencing the engine power. The variable most insensitive to power was the exhaust valve diameter. As The sensitivity results for the deterministic, stochastic and interval approaches are shown in Figure 5.12, Figure 5.13, Figure 5.14 and Figure 5.15 respectively. As seen in Figure 5.12 for the deterministic design, there is not much variation in the brake power until almost 10% change in the design variable values from the optimum design. But with further increase in the percentage change, the brake power widely varies especially with change in the rpm which could be the operating conditions. This data could be used by the designer for initial designs. For the stochastic design, the change in percentage of the design variables had similar effects as in the deterministic design but with slightly less scatter in the design points. The same is

true for interval optimization results with the lower intervals. The upper interval values of the interval design behaved similar to the deterministic optimization results with more scattered points and sensitivity with the change in design variables.

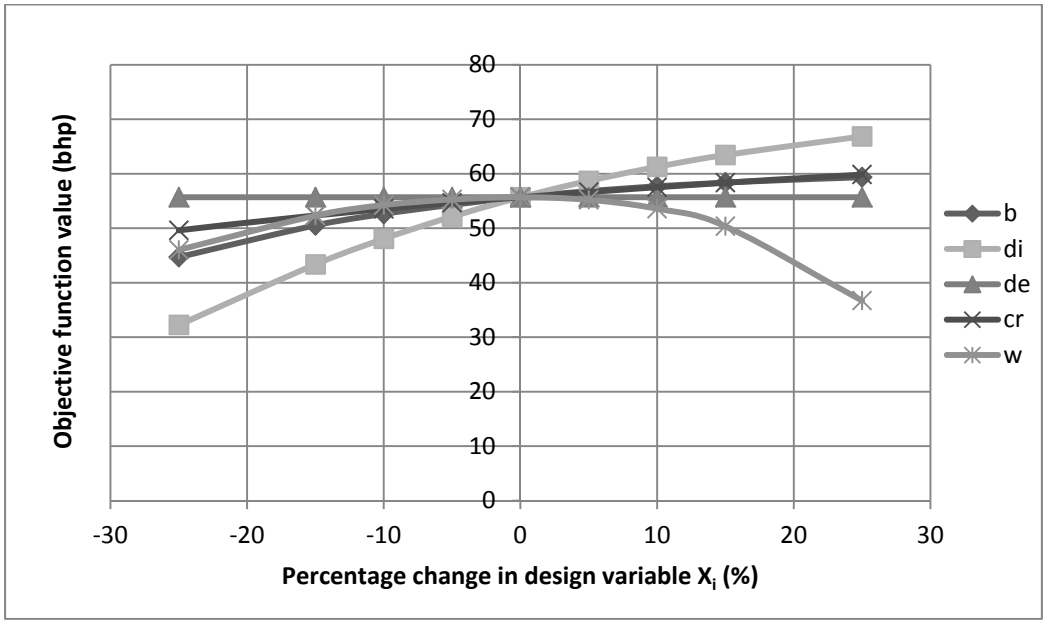

Figure 5.12 Sensitivity of power in deterministic optimization

Also, it is observed that the constraints g_1, g_3, g_4 and g_7 were active until about 10% change in the design variables in the case of deterministic, stochastic and lower interval designs. In the case of upper interval design, g_4 was not active. This is because of the restrictions in the valve diameter ratios. With 15 % change in the design variables, the constraints g_4 and g_7 were no longer active in the case of deterministic and upper interval design. This is because of the knock limited compression with changes in engine rpm. With further increase in percentage change of the design variables, the constraints g_1, g_3, g_4 and g_7 were violated. Hence, the sensitivity results indicate that the designs can be changed until about 15 % changes in the design variables based on the designer's intent.

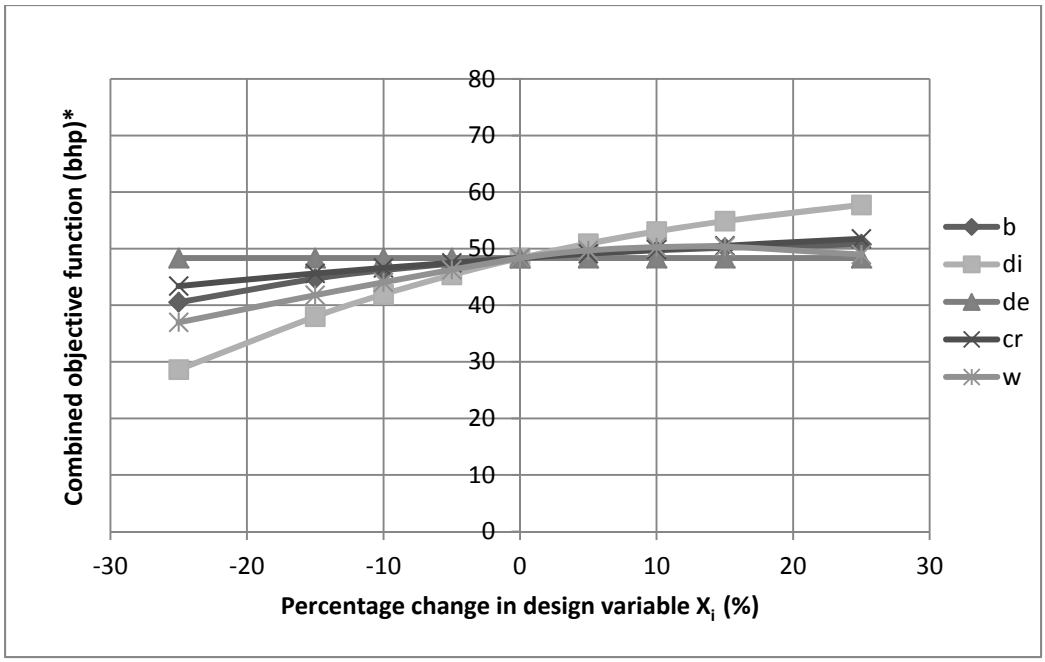

*linear sum of mean and standard deviation of power (Eq. 3.6)

Figure 5.13 Sensitivity of combined power in stochastic optimization

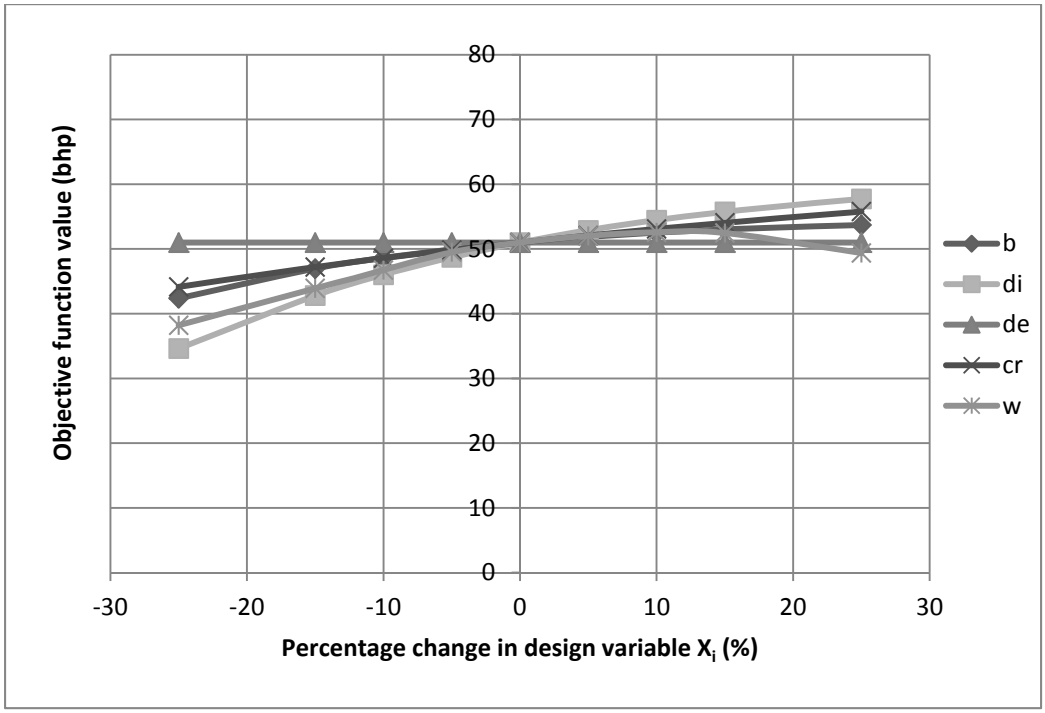

Figure 5.14 Sensitivity of power in interval optimization (lower value of the interval)

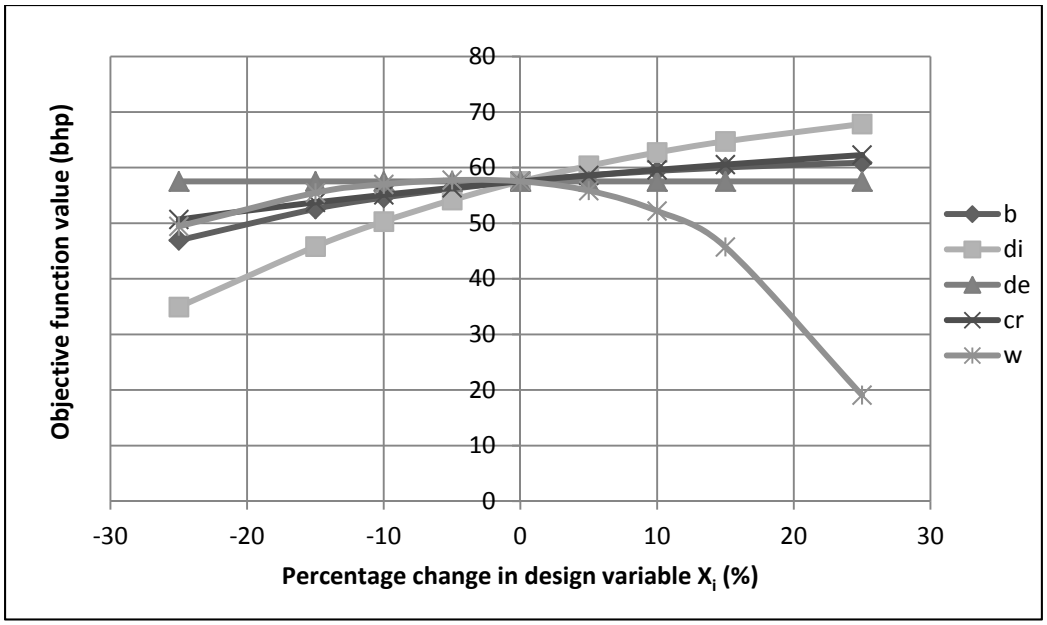

Figure 5.15 Sensitivity of power in interval optimization (upper value of the interval)

5.2.5 Multi-level formulation (approach 2)

The multilevel formulation of the model is based on defining two sub-problems (disciplines), namely, the geometry sub-problem and the thermodynamics sub-problem. Each sub-problem has its own design variables and constraints. The objective is to minimize the negative specific power and the system level assigns target values to the component level variables. The coordination between levels is obtained by repeated iterations between both levels to satisfy the equality constraints at the system level.

Formulation used in the multi-level process is given below:

<u>System level problem:</u>

Minimize $f(Y) = -\text{power}$ (5.46)

subject to

$$Y - X^g = 0; \tag{5.47}$$

$$Y - X^t = 0; \tag{5.48}$$

$$\text{where } Y = \begin{Bmatrix} b \\ d_i \\ d_e \\ c_r \\ w \end{Bmatrix} \tag{5.49}$$

Component level problem (geometry discipline):

$$\text{Minimize } f(X^g) = -power \tag{5.50}$$

subject to

$$g_1(b) = b - P_1 \leq 0 \tag{5.51}$$

$$g_2(b) = P_2 - b \leq 0 \tag{5.52}$$

$$g_3(b, d_i, d_e) = d_i + d_e - K_3 b \leq 0 \tag{5.53}$$

$$g_4(d_i, d_e) = K_4 d_i - d_e \leq 0 \tag{5.54}$$

$$g_5(d_i, d_e) = d_e - K_5 d_i \leq 0 \tag{5.55}$$

$$\text{where } X^g = \begin{Bmatrix} b \\ d_i \\ d_e \end{Bmatrix} \tag{5.56}$$

Component level problem (thermodynamics discipline):

$$\text{Minimize } f(X^t) = -power \tag{5.57}$$

subject to

$$g_6(w, d_i) = P_3 w - d_i^2 \leq 0 \tag{5.58}$$

$$g_7(c_r, b) = c_r - \ 13.2 + 0.045b \ \leq 0 \tag{5.59}$$

$$g_8(w) = w - K_7 \leq 0 \tag{5.60}$$

$$g_9(c_r, b) = P_4 - 0.8595(1 - c_r^{-0.33}) + S_v(c_r, b) \leq 0 \tag{5.61}$$

where and $X^t = \begin{Bmatrix} c_r \\ w \end{Bmatrix}$ (5.62)

Results obtained by the new ML SQP for maximization of bhp are given in Table 5.12 and Table 5.13. Table 5.12 shows the convergence of the design variables for every iteration between the system and the component levels. From the table it is evident that the convergence in the ML process is achieved in 5 iterations. Variation of the power (bhp) at the end of every iteration between the two levels is given in Table 5.13. It is evident that the power increased from an initial value of 38.3339 bhp to a final value of 59.7832 bhp in 5 iterations between the system and the component levels. The convergence is evident with no further change in the value of the maximum bhp after 5 iterations. The total number of function evaluations in SQP is 301 and the total number of iterations for convergence of the ML process is 15. At the initial design, there are no active constraints whereas at the final design, the constraints g_1, g_3, g_4 and g_7 are active.

Table 5.12 New Multi-level SQP results for maximization of power

Iteration	Optimum design vectors at system level and component levels	
1	x^*	{75.3218, 31.5000, 35.0000, 8.3838, 5000}
	x_1^*	{76.8531, 32.2266, 30.8052}

	x_2^*	{9.7132, 5632.4}
2	x^*	{77.4836, 34.8362, 30.8052, 11.4546, 6019.9}
	x_1^*	{78.6219, 35.3510, 29.1193}
	x_2^*	{9.6105, 6067.4}
3	x^*	{79.7673, 38.7062, 29.1193, 12.0000, 6111.0}
	x_1^*	{80.3686, 36.0152, 29.8870}
	x_2^*	{9.3478, 6232.5}
4	x^*	{85.6046, 40.0169, 29.8870, 12.0000, 6394.5}
	x_1^*	{83.3300, 37.3392, 30.9914}
	x_2^*	{9.3478, 6232.5}
5	x^*	{83.3300, 37.3391, 30.9915, 9.1500, 6323.0}
	x_1^*	{83.3300, 37.3391, 30.9915}
	x_2^*	{9.1500, 6323.0}

x^*- system level optimum design vector ; x_1^*- component level (geometry) design vector; x_2^*- component level (geometry) design vector

Table 5.13 New Multi-level SQP results for maximization of power

Iteration	f^* (system level)	f^* (component level) (geometry)	f^* (component level) (thermodynamics)
1	38.3339	40.0594	32.0002
2	52.2336	53.7935	49.4795
3	61.4177	56.5048	57.1115
4	65.2612	59.6064	60.3822
5	59.7832	59.7832	59.7832

f^* - optimum value

Results obtained by the new ML ACO for maximization of power (bhp) are given in Table 5.14 and Table 5.15. Table 5.14 shows the convergence of the design variables for every iteration between the system and the component levels. From the table it is evident that the convergence in the ML process is achieved in 6 iterations. Variation of bhp at the

end of every iteration between the two levels is given in Table 5.15. It is evident that the bhp reduced from an initial value of 9.6706 bhp to a final minimum value of 56.1934 bhp in 6 iterations between the system and the component levels. The convergence is evident with no further change in the value of the maximum bhp after 6 iterations. At the final design, the constraints g_1, g_3, g_4 and g_7 active. The number of ants used in ACO is 25 and the discrete variable set is obtained by taking 20 values equally distributed between the bounds for each design variable. The convergence in ACO is achieved in 44 cycles (1100 iterations).

Table 5.14 New Multi-level ACO results for maximization of power

Iteration	Optimum design vectors at system level and component levels	
1	x^*	{84.7368, 30.2632, 27.6316, 9.7895, 8315.8}
	x_1^*	{82.6316, 35.5263, 30.2632}
	x_2^*	{9.1579, 5000}
2	x^*	{76.3158, 32.8947, 48.6842, 7.2632, 7578.9}
	x_1^*	{82.6316, 35.5263, 31.5789}
	x_2^*	{9.4737, 5000}
3	x^*	{76.3158, 35.5263, 27.6316, 8.2105, 6473.7}
	x_1^*	{82.6316, 35.5263, 31.5789}
	x_2^*	{9.4737, 5736.8}
4	x^*	{78.4211, 39.4737, 25.0000, 8.8421, 5000}
	x_1^*	{82.6316, 35.5263, 31.5789}
	x_2^*	{9.4737, 6105.3}
5	x^*	{86.8421, 39.4737, 25.0000, 12.0000, 5368.4}

	x_1^*	{82.6316, 35.5263, 31.5789}
	x_2^*	{9.1579, 6473.7}
6	x^*	{82.6316, 35.5263, 31.5789, 9.1579, 6105.3}
	x_1^*	{82.6316, 35.5263, 31.5789}
	x_2^*	{9.1579, 6105.3}

x^*- system level optimum design vector ; x_1^*- component level (geometry) design vector; x_2^*- component level (geometry) design vector

Table 5.15 New Multi-level ACO results for maximization of power

Iteration	f^* (system level)	f^* (component level) (geometry)	f^* (component level) (thermodynamics)
1	9.6706	4.9663	39.3903
2	18.8258	28.6240	42.9708
3	45.3467	48.0248	49.9879
4	50.5549	47.2282	57.5009
5	61.4257	54.9891	59.4063
6	56.1934	56.1934	56.1934

In this chapter, mechanical engineering example problems are solved using the multi-level and ant colony approaches. Examples considered are combustion chamber of an internal combustion engine and a speed reducer/gear box. Results obtained are compared to those in literature. Practical application of chiller optimization is reported in the next chapter.

CHAPTER 6 - PRACTICAL APPLICATION – DESIGN OPTIMIZATION OF CHILLER PLANTS

This chapter is concentrated on the application of design optimization in large-scale industrial problems. Chiller plants in the Heating Ventilation and Air Conditioning (HVAC) Systems are considered. A brief introduction of chiller plants is given followed by a literature review. Chiller plant optimization model is formulated and a hybrid solution technique is developed to solve the optimization problem. Case study is performed and the results are analyzed.

6.1 Introductory remarks

Conservation of energy has always been a topic of concern and research. Among the various energy sources, electrical energy is one of the most used forms of energy. Most of the activities people are involved are related to devices that use electric power. The buildings we live in require air conditioning systems. The HVAC systems are among the major power or energy consuming units of a building. Increased emphasis on energy conservation leads to the development of better and optimal ways of using energy. Hence, in this research, optimization of a chiller plant is considered as a practical industrial application.

A chilled water plant is one of the largest electric power consuming units in a typical building in the United States. Depending on the type of facility, a chiller plant can consume electricity ranging from 10% to 50% of the total energy consumption (DOE 2003). Hence, even a small amount of savings in energy (using optimization) would result in a significant savings in cost.

A chiller plant provides the necessary cooling through chilled water to a building. Its main components are chillers, cooling towers, and pumps, which are often grouped together to form the condenser loop and the chilled water loop. Figure 6.1 shows a schematic of a typical chiller plant (HVAC system). The condenser loop consists of chiller condensers, pumps, cooling towers and fans. Similarly, the major components of the chilled water loop are the chiller evaporators and chilled water pumps. The performance of a chiller plant is usually given as kw/ton which indicates the ratio of electric power consumed to the required input load.

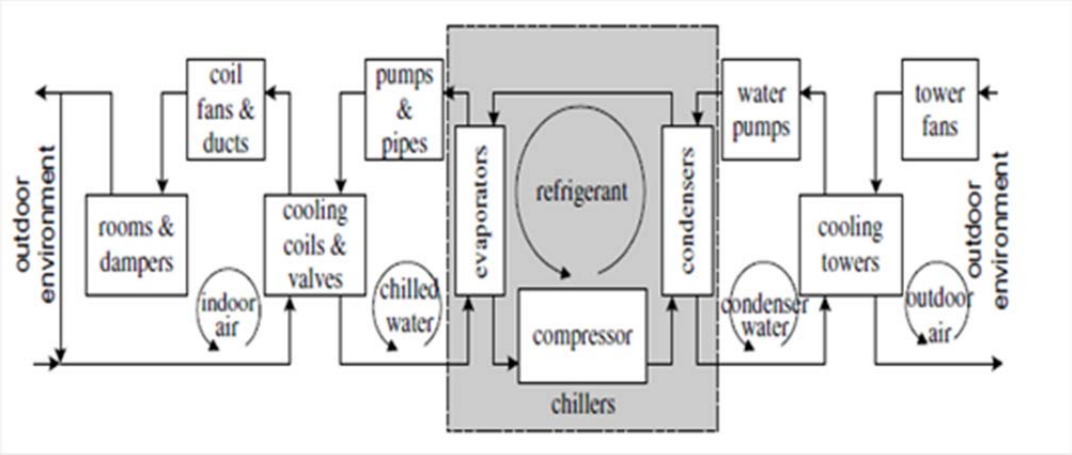

Figure 6.1 Schematic of a HVAC system (Lu et al., (2004))

6.2 Literature review

The aspects of energy conservation and optimal control of chiller plants have been considered by many researchers in literature (Chang (2007), Chang (2009), Wang and Ma (2008)). Some of the works emphasized the study of individual component efficiencies and others have targeted on partial systems. Some works elaborate on the condenser loop (Braun and Doderrich (1990), Shelton and Joyce (1991), Kirsner (1996)) while others have emphasized the chilled water loop (Kirsner (1998), Braun et al., (1989), Olson and

Liebman (1990), Chang (2007)). Most of the chiller plants are either controlled manually or automatically by adjusting the temperature or pressure settings (Hartman (2006, 2007), Christopher (2010)). Also, in a chiller plant, chillers consume a major fraction of the power, and are the most expensive components. Hence, optimizing the performance of chillers is crucial for power and ultimately the cost savings. The pioneering work in this area was done by Hartmann with the promotion of variable speed drive chillers, pumps and cooling tower fans (Hartman (2001, 2005)). This work was followed by Yu and Chan (2009) and Zheng and Wang (2009). The overall system performance of the chiller plants was studied by Austin (1993) and Flake (1998).

The various methodologies used for the optimization and control of chiller plants can broadly be classified as enumeration-based and simulation based methods. The enumeration based optimization (Austin (1991), Bellenger et al., (1996), Avery (2001)) is based on an exhaustive simulation or monitoring based on the entire performance map of the system. This method, by default, involves no mathematical optimization techniques. Using this methodology, Avery (2001) suggested ways to improve the generally accepted and practiced primary/secondary loop systems. It was shown that by making physical changes to the plant like installing temperature and pressure sensors and valves at certain places would increase the efficiency of the plant. Bellenger et al., (1996) developed a spreadsheet based chiller optimization model using manufacturer's data. This uses a systems approach in selecting cost-efficient chillers based on the chiller performance data, cooling tower and the pumping system. Recently, Hydeman and Zhou (2007) used a parametric analysis technique to optimize the control sequence of chilled water plants. A spreadsheet based optimization tool was created for a chiller plant by Morris and Blaine

(2008). The interactions between the components were modeled considering the plant's response to load and outside air conditions. A set of quick look-up tables were created which could help the operators to run the plant efficiently. This study involved no mathematical optimization techniques and was a basic model.

The simulation based methods, on the other hand, use systems optimization theory with mathematical formulations. Olson and Liebman (1990) used a heuristic search and sequential quadratic programming to solve the chiller plant problem. In this study, the optimization is mainly focused on the sequence of operation of the equipment but not on the performance levels of the equipment. Later, Sun and Reddy (2005) have used sequential quadratic programming based method to design optimal heating and cooling systems for buildings. The study uses a two stage optimization approach for the chiller plant. The global optimization of an overall HVAC system is studied by Lu et al., (2004, 2005). In their work, the basic chiller plant model developed by Stoecker (1975) has been modified, and the component interactions are shown. The artificial neural networks are used to determine the set points of components wherever required. This developed model is optimized using genetic algorithms by Lu et al., (2004). The artificial neural networks might rely too much on the input data for training and are often unable to extrapolate beyond the calibration range. Ma and Wang (2011) present a model-based supervisory and optimal control strategy based on genetic algorithms. System performance is predicted using simplified models based on recursive least squares estimation. Genetic algorithms sometimes have the limitation of convergence issues because of the evolution from a bad result. Multiple chiller management for dynamic loading is researched by Beghi et al., (2011). A multi-phase genetic algorithm model is used to simultaneously

solve the optimal chiller loading and optimal chiller sequencing problems. Chang et al., (2005), solved the optimal chiller sequencing problem using the branch and bound and the Lagrangian method of optimization. Only the chillers were considered in the studies but not the entire chiller plant.

Most studies in literature use either the enumeration based models or the simulation based models. The enumeration based models have no mathematical basis while the simulation based models might not span the entire performance of the components and sometimes lead to infeasible solutions. Also, in enumeration based models, there is no validity for the results, unless the changes are physically made to the plant. In order to overcome these difficulties, a novel formulation technique, combining the two methods has been developed in this study. This method uses the performance map of the equipment (to build the models and ensure the spanning of the entire feasible region) along with the systems optimization theory (using a hybrid optimization method) to optimize chiller plants. With this model, the effects/results could be predicted before actual changes are implemented in the plant. A preliminary software model is developed which could be directly installed in the HVAC plant for energy savings.

Chiller plant optimization is a mixed-integer programming problem and hence continuous optimization strategies cannot be implemented directly. This is addressed in literature using two different types of optimization: operation mode optimization (which defines the set of equipment to be operated as discrete/integer optimization) and the set points optimization (which computes the optimal values of the design variables for minimum power consumption as continuous optimization). This two stage optimization is computationally expensive and requires both stages to be converged for the overall plant

optimization. Hence, in present study, a hybrid algorithm is developed which overcomes the drawbacks of the two stage optimization. This algorithm uses only one optimization problem to be solved instead of two optimizations for the set point and the operation modes. One of the robust and proven classical optimization techniques-the sequential quadratic programing (SQP) - has been combined with a modified branch and bound method (B&B) of integer optimization (Rao, 2009) to solve the chiller plant optimization model.

6.3 Algorithm steps for chiller plant optimization

- Simulation of the system
- Formulation of the optimization problem
- Solution of the optimization problem using SQP and modified B & B method

The flowchart of the chiller plant optimization procedure is given in Figure 6.2. Initially, regression models for the components, the chiller, the cooling tower fans and the pumps are generated (Details are given in section 6.7). The chiller plant optimization problem is formulated based on the generated models. As stated earlier, the solution procedure for the chiller plant optimization problem involves two main stages. In the first stage the optimization problem is solved using SQP, assuming all the variables to be continuous in nature. Once the optimum solution to stage one is obtained, the design variables are checked for discreteness (integer in this case). If the condition is satisfied, then the program is terminated and the results printed. Else, the next stage of the algorithm is implemented which involves the branch and bound method with modifications. The discrete variable is set for lower and upper bound integers based on the results obtained in the continuous optimization (stage one). In this way, two sub problems for

optimization are formed. These sub problems have the same objective and constrains as the initial problem except for an extra equality constraint. Then the two sub problems are solved using SQP. At each stage the branching (dividing into sub problems) is continued until an infeasible solution is found. Each time, the best feasible solution obtained until then is updated and the branching and bounding and the SQP optimization is continued until the optimum solution is obtained.

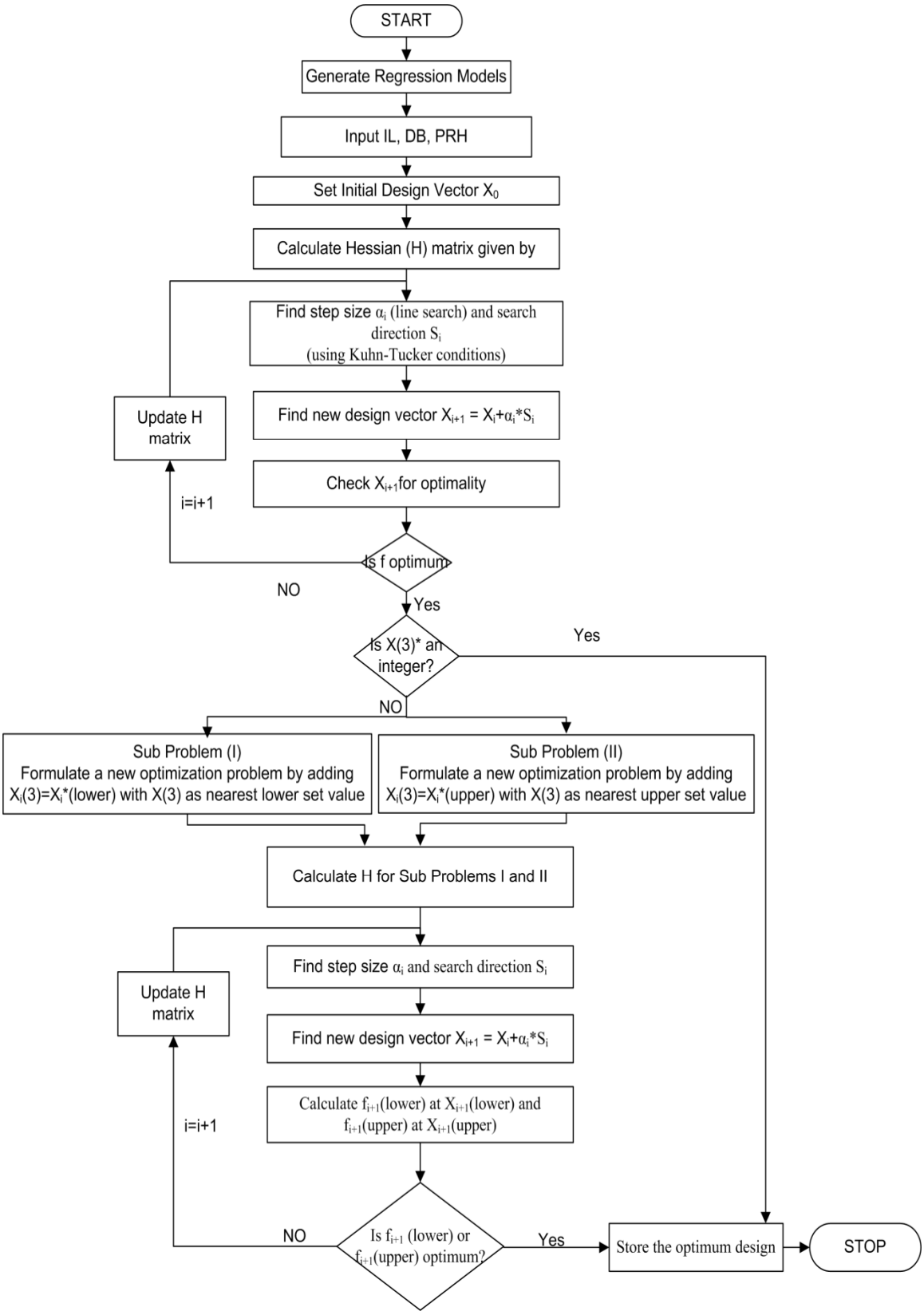

Figure 6.2 Flowchart for the chiller plant optimization (hybrid solution method)

6.3.1 Simulation of the system: Developing multivariable regression models

The chiller plant model simulation involves developing multivariable regression models for the system. These regression models are developed based on thermodynamics, heat transfer, energy and mass balance relations. For the model generation, dependent and independent variables are recognized. In general, the system performance of the chiller and the total plant are identified as the dependent variables. Independent variables are identified as the percentage load of the chiller (PL_{ch}), the mass flow rate of fluid (water) into the condenser (G_w), the condenser entering fluid temperature (T_{ce}), wet bulb temperature (WBT), the percentage speed of the fan (PS_f).

6.3.1.1 Chiller Model

The energy model of a chiller is usually based on the coefficient of performance (COP) of the chiller (Browne and Bansal (1998)). The COP is a function of the Partial Load Rate or the percentage load (PL_{ch}) and the entering temperatures of the fluid in the evaporator and the condenser. In the present model, system performance (SP) of the chiller, defined as $1/COP$, is taken as a function of percentage load of the chiller (PL_{ch}) and the condenser entering water temperature (T_{ce}) in the form

$$SP = A_1 + a_1(PL_{ch}) + a_2(T_{ce}) + a_3(PL_{ch})^2 + a_4(T_{ce})^2 + a_5(PL_{ch})(T_{ce}) + a_6(PL_{ch})^3 \quad (6.1)$$

Power consumed (P_{ch}) by the chiller is calculated as

$$P_{ch} = SP * PL_{ch} * L_r/100 \quad (6.2)$$

Thus, given the condenser entering fluid temperature and the percentage load at which the chiller operates, the present chiller model can predict the required power consumption of the chiller. In this model, the dependent variable is chiller power and the independent variable are the percentage load and the condenser entering fluid temperature. The maximum rated load (L_r) is based on the type of chiller.

6.3.1.2 Cooling tower fan model

The power consumed by a fan (P_{ctf}) is dependent on its speed (rpm) and is taken as

$$P_{ctf} = constant * (rpm)^3 \tag{6.3}$$

6.3.1.3 Pump model

The pump power (P_p) is modeled as

$$P_p = G_w * H/k_c \tag{6.4}$$

where H is assumed to be a function of the flow rate G_w, and k_c is treated as a constant. Hence, P_p becomes a function of flow rate G_w only. Based on the regression analysis of the manufacturer's data, the model for pump is chosen as

$$P_p = C + d_1 * G_w + d_2 * (G_w)^2 + d_3 * (G_w)^3 \tag{6.5}$$

The mathematical basis of the regression models and the values of the coefficients ($a_1, a_2, \ldots a_n$ and d_1, d_2, d_3) are given in section 6.7.

6.4 Chiller plant optimization problem formulation

For the overall chiller plant optimization, the objective is to minimize the total power consumed by the main components. The main energy consuming components in a chiller

plant are the chillers, pumps and the cooling tower fans. In this study, the condenser water loop is considered for optimization of power based on the input load requirement and the outside air temperatures. Design variables are the number of chillers, percentage load of the chillers, condenser entering water (fluid) temperature and the percentage of cooling tower fan speed. The problem can be expressed as

$$\text{Min } f(\vec{X}) = P_{ch}(\vec{X}) + P_p(\vec{X}) + P_{ctf}(\vec{X}) \tag{6.6}$$

$$\text{where} \quad \vec{X} = \begin{Bmatrix} PL_{ch} \\ T_{ce} \\ nch \\ PS_f) \end{Bmatrix} \tag{6.7}$$

with the following constraints

a) Input load equilibrium constraint

This constraint ensures that the total input load required (as an input variable) matches with the load obtained for the optimum number of chillers and the percentage loading of each chiller and the maximum capacity of the chiller.

$$IL(\vec{X}) = (nch)(PL_{ch}) * Ch_{max}/100 \tag{6.8}$$

where Ch_{max} is the maximum chiller capacity

b) Energy balance in chiller and cooling tower

The temperature of the water entering into the chiller (condenser) is equated to the temperature of the water leaving the cooling tower. This is essential for energy balance.

$$T_{ce} = C_0 + c_1(G_w) + c_2\left(PS_f\right) + c_3(T_{wb}) + c_4(\Delta T) + c_5(G_w)^2 + c_6\left(PS_f\right)^2 + c_7(\Delta T)^2 \quad (6.9)$$

where T_{wb} is the wet bulb temperature of the outside air. ΔT is the difference in temperature of water entering and leaving the condenser and $C_0, c_1, c_2, \ldots, c_7$ are constants determined by the regression models.

The design variables have to be limited to certain bounds of operation based on the overall chiller plant and the equipment specifications indicated by the manufacturer. In this problem, the bounds are specified as

$$40 \leq PL_{ch} \leq 100 \quad (6.10)$$

$$1 \leq nch \leq 4 \quad (6.11)$$

$$60 \leq T_{ce} \leq 85 \quad (6.12)$$

$$30 \leq PS_f \leq 100 \quad (6.13)$$

6.5 Illustrative example

To investigate the validity of the optimization model developed, a typical chiller plant (Figure 6.3) is considered. The sample plant is a water cooled HVAC system and it consists of 4 centrifugal chillers with Variable Flow Devices (VFD) and 4 cooling towers with two cells each. The maximum cooling capacity (tonnage) for each of the chillers is 1500 tons. The system consists of 4 condenser water pumps and 4 chilled water pumps. The rated mass flow rate of water being circulated through each condenser pump is 4500gpm. The assumptions made in the formulation are: the condenser pumps have variable flow rates, evaporator leaving fluid temperature is 40°F, cooling tower fans blow

air at 100% speed, maximum number of cooling towers are operated for a given number of chillers operating, cooling towers can handle water flow rates greater than 80% of their maximum capacity and the fluid flow rate is constant on the condenser side.

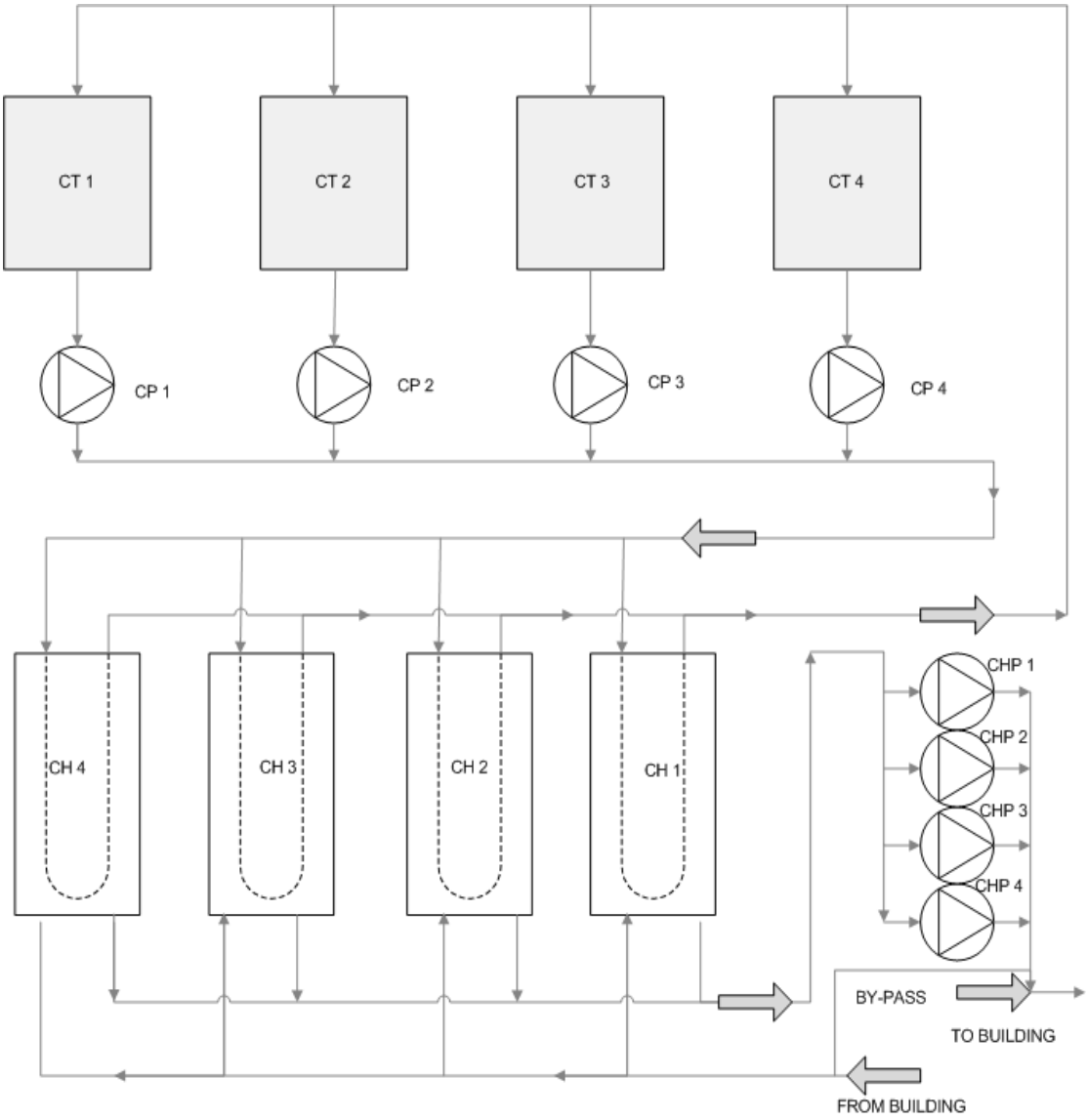

Figure 6.3 Layout of a typical chiller plant (ESI Consulting Engineers (2012))

Table 6.1 shows a sample chiller part load performance data (based on the American Society of Heating Refrigeration and Air Conditioning Engineers (ASHRAE) standards). It basically gives the power consumed by the chiller at different percentage loads, the

entering and leaving fluid temperatures at that point for both the condenser and the evaporator of the chiller. It also gives the pressure drop and the evaporator flow rate at that point. It is evident that the data is based on intervals of 10% of part load. In order to find the exact performance of the chiller at any load condition and temperature, the regression models are developed based on the manufacturer's data. Similarly, the cooling tower performance at different temperature ranges is shown in Figure 6.4.

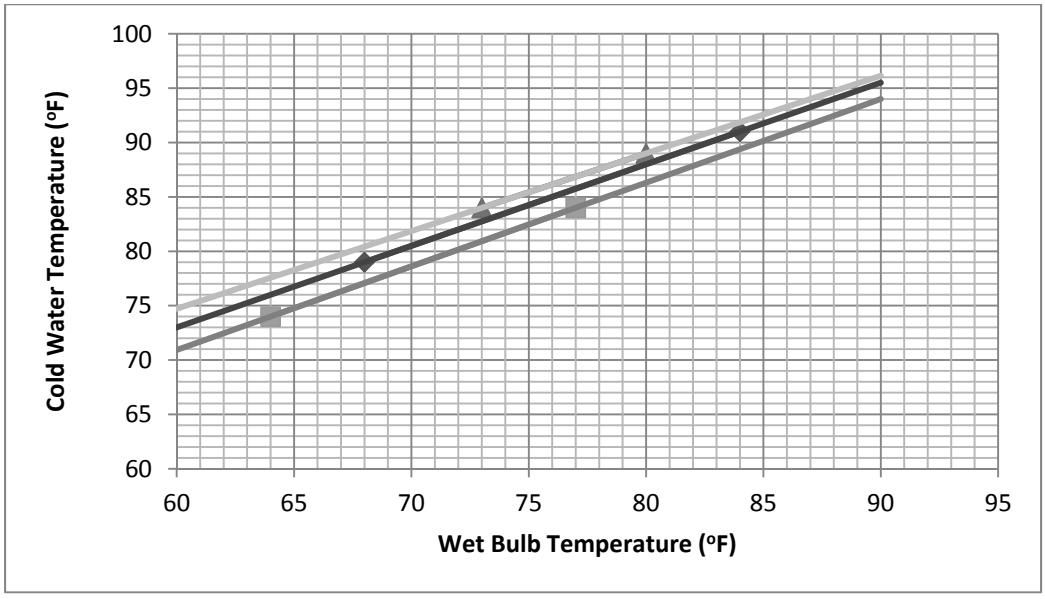

Figure 6.4 Typical cooling tower performance (ESI Consulting Engineers (2012))

Table 6.1 Typical chiller performance (ESI Consulting Engineers (2012))

Part Load (%)	Load (Ton)	Input Power(kW)	EEFT (°F)	ELFT (°F)	Evaporater Pressure Drop	Flow (gpm)	CEFT (°F)	CLFT (°F)	SP (KW/TR)
100	1500	524	55.98	40	25	2250	60	68.72	0.3493
90	1350	460	55.98	40	20.8	2025	60	67.83	0.3407
80	1200	364	55.98	40	16.9	1800	60	66.89	0.3033
70	1050	305	55.98	40	13.4	1575	60	66.01	0.2905
60	900	260	55.98	40	10.2	1350	60	65.15	0.2889
50	750	218	55.98	40	7.4	1125	60	64.28	0.2907
40	600	187	55.98	40	4.7	900	60	63.44	0.3117
30	450	165	55.98	40	2.7	675	60	62.61	0.3667
20	300	131	50.64	40	2.7	675.9	60	61.76	0.4367
15	225.6	114	48	40	2.7	675.9	60	61.33	0.5053

EEFT – Evaporator Entering Fluid Temperature ELFT – Evaporator Leaving Fluid Temperature C – Condenser

6.6 Results

Sample input data is collected from the sample chiller plant for a certain amount of time and the optimization algorithm developed in present study is used to simulate the results. Four different sets of input load, dry bulb temperature and percentage relative humidity are considered as input conditions for optimization and the results are given in Table 6.3 and Table 6.4. Since the plant has four chillers, the data points are taken to span the cases of two, three, and four chiller usage. It can be seen that when the load is 1812 Tons, the optimization results show that two chillers are to be run at 60.4% load. When two chillers are run for a water flow rate condition of 80% or more, two cooling towers and one cell have to be operating to maximize the efficiency of the towers. Also, it can be seen that the fan speed should be 65.7% of maximum speed to maintain 68.2°F for the condenser water supply. Similarly, for the other cases, the number of chillers and fan speed and other optimal operating conditions are obtained based on the input conditions. Table 6.4 also shows the energy (KW) consumed by the chillers, the cooling towers and the condenser water pumps and the system performance.

The optimization results for a particular sample load condition of 2647 tons are shown in Table 6.2. The initial design represents the actual current operating conditions in the plant. It is seen that the objective function value (the power consumed in KW) is reduced from 2412.42 KW to about 2009.77 KW. So, the power savings of about 402.65 KW (16.69%) is possible with optimization for this particular input load. Similar savings can be expected for other load conditions (for the dynamically changing load conditions) in the actual chiller plant.

Table 6.2 Optimization results for input load condition of 2647 tons

Quantity	Initial Design	Bounds		Optimum Design
		Lower	Upper	
Design Variables:				
PL_{ch} (%)	58.80	40	100	58.80
T_{ce} (°F)	78.00	60	85	72.68
nch (integer)	3	1	4	3
PS_f (%)	100	30	100	68.04
Objective: (Total power in KW)	2412.42	646.56	644.02	2009.77

# of iterations to converge is 19; # of function evaluations is 252

The power consumed by the chiller during the optimum and normal modes of operation is shown in Figure 6.5 for three different load conditions. It is seen that the average is 475 KW for the normal mode while the optimum design averages at 375 KW. Hence, there is an average savings of about 100 KW (about 21%) in the chiller with the optimum design.

Table 6.3 Optimum design variable values for different input load conditions

Input load (ton)	DBT (°F)	PRH (%)	nch integer	PL_{ch} (%)	T_{ce} (°F)	PS_f (%)
1812	66.4	81.8	2	60.4	68.20	65.74
2647	78.1	62.4	3	58.8	72.68	68.04
3108	83.2	62.8	4	51.8	76.66	70.21
5040	92.8	57.6	4	84.0	84.15	75.26

Table 6.4 Optimum power consumed at different input load conditions

Chiller Power (KW)	Fan Power (KW)	Condenser Pump Power (KW)	Chill Water Pump Power (KW)	System Performance
332.35	52.98	160.20	350	0.7215
376.85	82.21	272.01	525	0.8369
387.75	103.22	511.41	700	1.0201
748.64	127.14	511.41	700	0.9351

In addition, the variation of one of the design variables, the percentage of fan speed, is shown graphically (Figure 6.6) for the normal and optimal modes. Savings are quite evident because of the speeds. Also, the pump power consumption is shown in Figure 6.7 for the three load cases. The energy consumed by each of the components, chillers, cooling tower fans and the pumps are shown in the bar charts of Figure 6.8 and Figure 6.9. Figure 6.8 corresponds to the normal modes of operation while Figure 6.9 corresponds to the optimal modes of operation as proposed in this study. These results can be used for analysis to decide on the type and quantity of equipment to be purchased while a new plant is installed. This information could also be used to decide on the modifications to be made on an existing plant in order to achieve power savings based on the equipment maps and performances. It can be seen from Figure 6.8 and Figure 6.9 that the chillers are the main power consuming units followed by the pumps and then the cooling tower fans. This shows that by optimizing the number of chillers and operating them at the optimal load conditions, the energy savings could be maximized in certain cases.

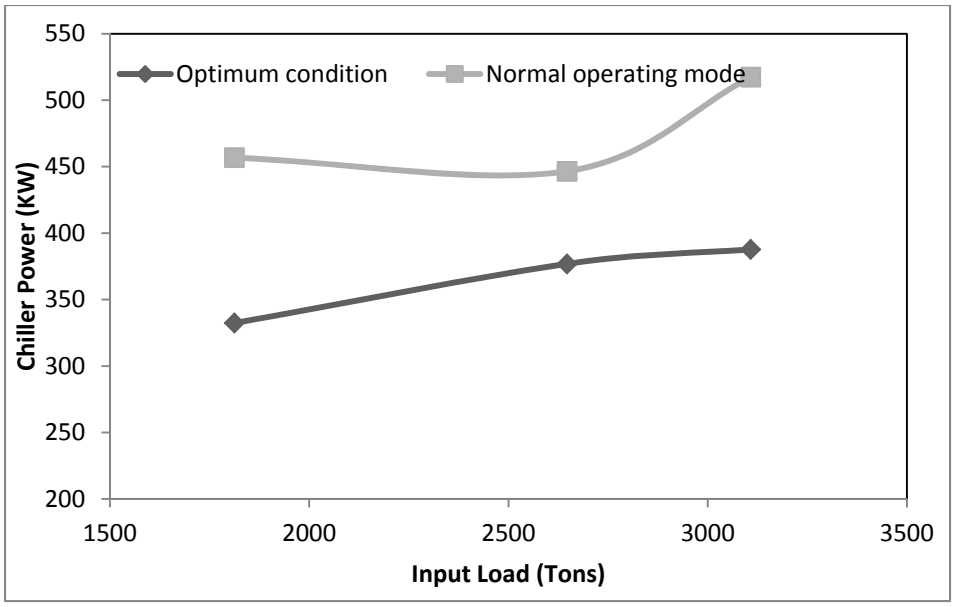

Figure 6.5 Chiller power consumption in normal and optimal modes

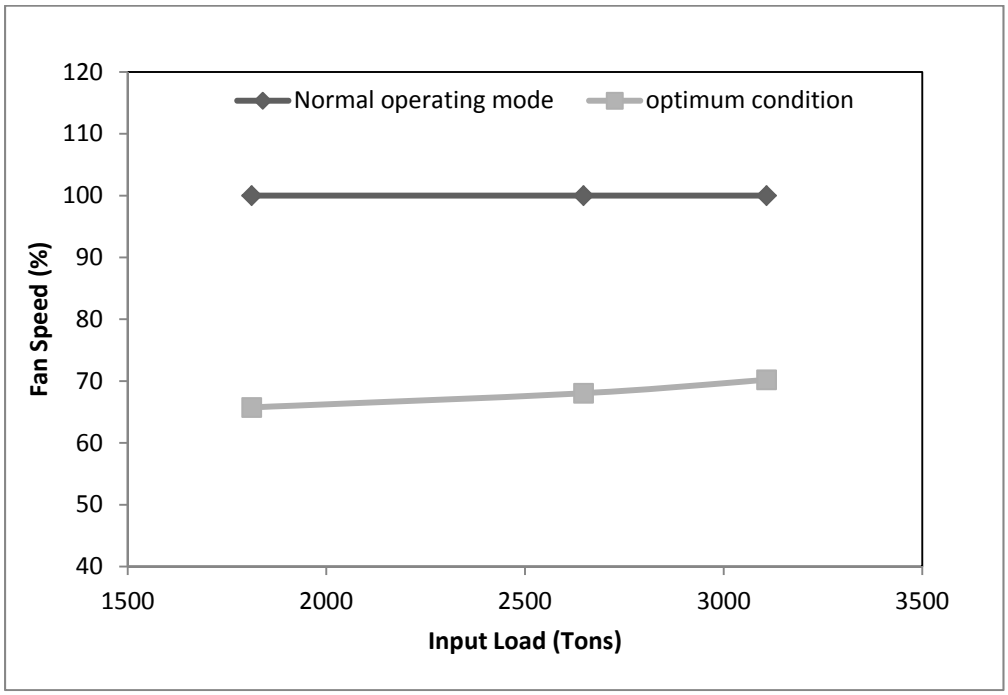

Figure 6.6 Fan speed variation in normal and optimal modes

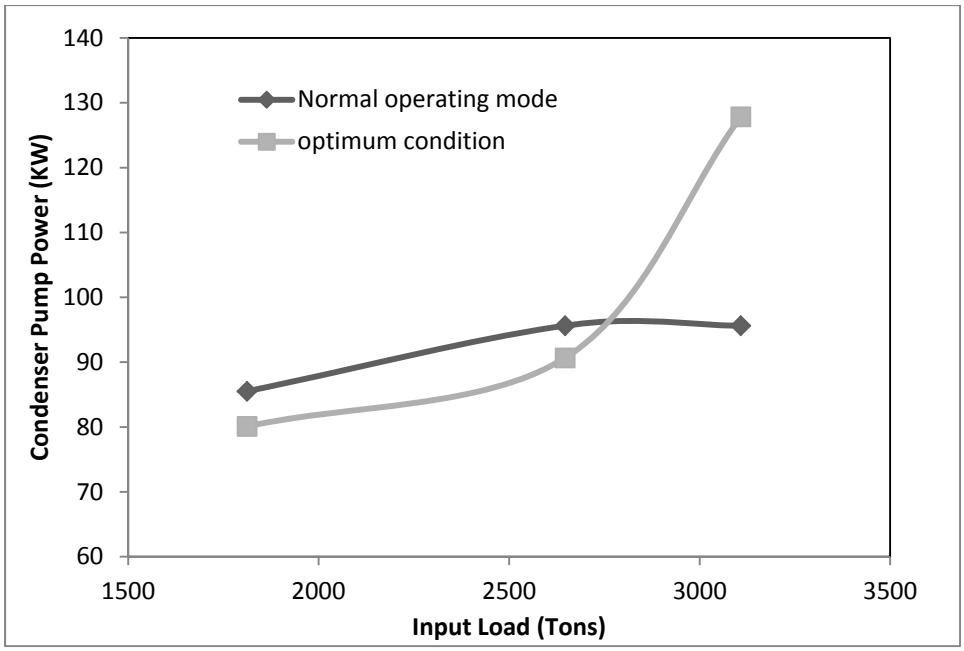

Figure 6.7 Variation of pump power in normal and optimal modes

An important factor in the chiller plant operation is the condenser entering water temperature which in normal operating cycle (without optimization) is set to a constant value by the operator, either manually or automatically. But, in present study, this parameter is also varied and its optimal value is found by the algorithm. The simulation results are shown in Figure 6.10. Figure 6.11 shows the variation of chiller power consumption for different time intervals. It is evident that the chiller power curve has peaks and valleys to accommodate the input load requirement. The chiller power varies from about 300 KW to about 550 KW depending on the tonnage. This large variation in the power accounts for the savings due to the VFD's on the chillers which allow them to be loaded at different levels. The variation of the cooling tower fan speed based on input conditions is shown in Figure 6.12. From the figure it can be seen that when two chillers operate, the fan speed is about 30% and when 3 chillers operate, the fan speed is higher. This is to adjust to the load conditions and cool down the water in the cooling towers.

The graph in Figure 6.13 compares the system performance of the chiller plant for both normal (actual) and simulated operating modes for a certain time in the winter. It is evident that the optimal mode has a better performance than the normal mode since it has a lower system performance. The lower the value of the system performance, the better is the plant. The average system performance for the normal operating mode is 1.01 kw/ton whereas the optimization results gave an average value of 0.7 kw/ton. This shows the amount of savings in power and subsequently, the operating costs of the chiller plant. The summer data for the chiller plant is also considered because the input load and the outside air conditions differ from the winter data. A typical week in the summer is chosen and the comparison of data corresponding to the normal and the optimal operating modes is shown in Figure 6.14. It is evident that the system performance in the optimal mode of operation is significantly better than that in the normal mode of operation. The savings in all the cases could be attributed mainly to the optimal chiller loading and the number of chillers operated at any instant. Also, the number of cooling tower fans running and their speeds are related to the energy savings. The power consumed by the condenser water pumps also contributes to the savings because the number of pumps operated depends on the number of chillers.

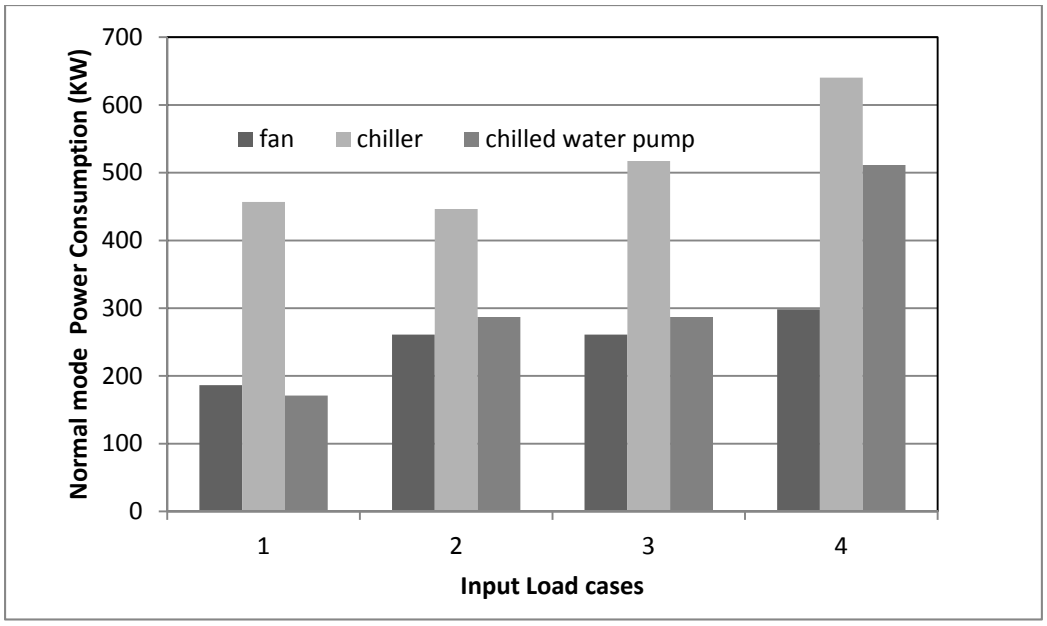

Figure 6.8 Power consumption in the normal mode of operation

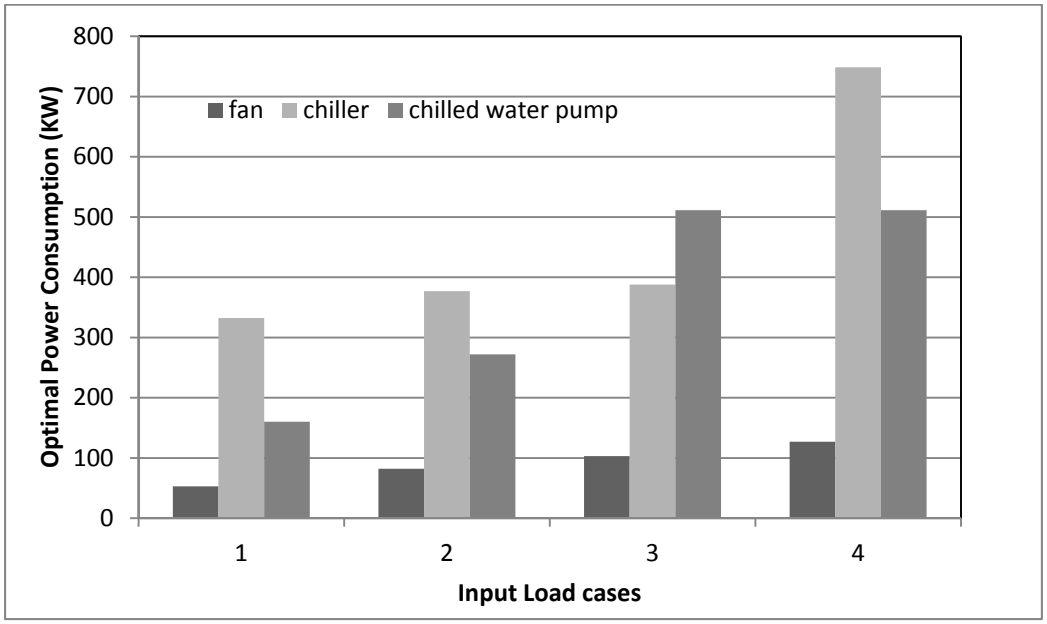

Figure 6.9 Power consumption in the optimum design mode

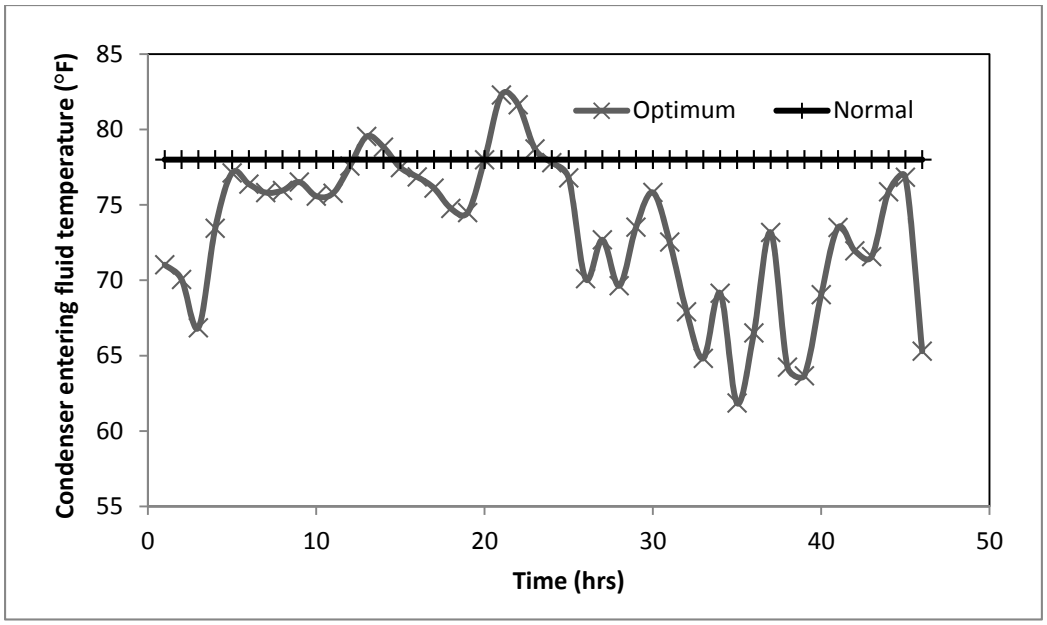

Figure 6.10 Variation of condenser entering fluid temperature with time

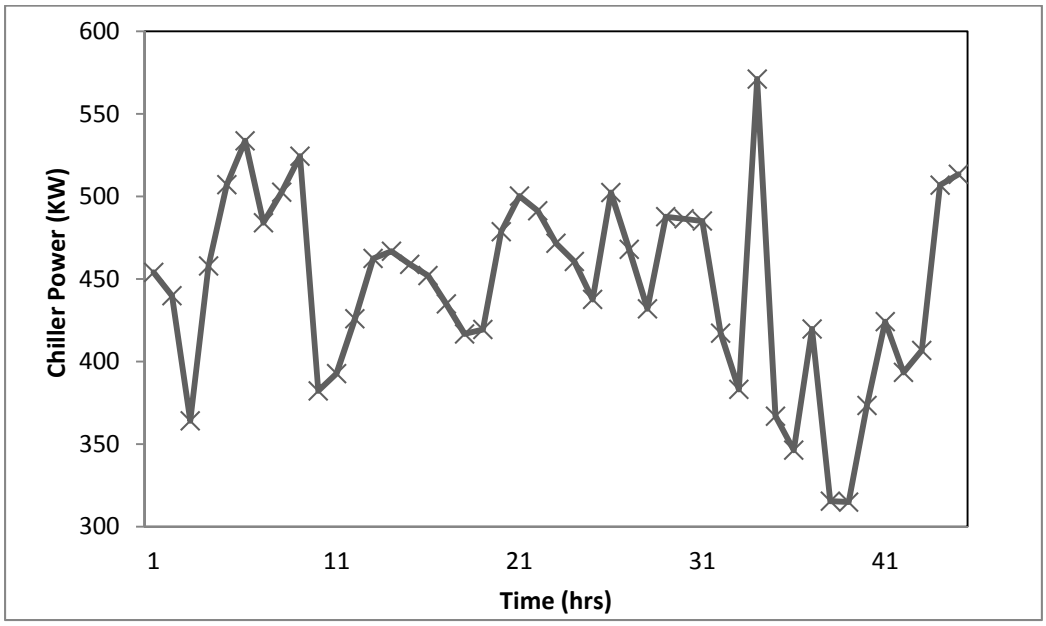

Figure 6.11 Chiller power variation with time

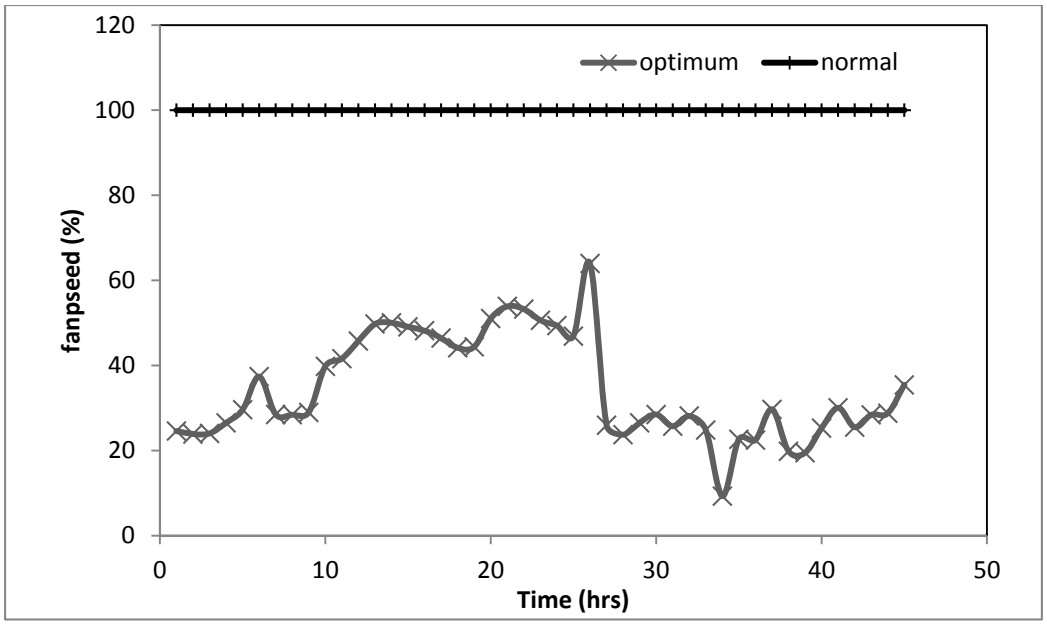

Figure 6.12 Variation of fan speed with time in normal and optimum mode

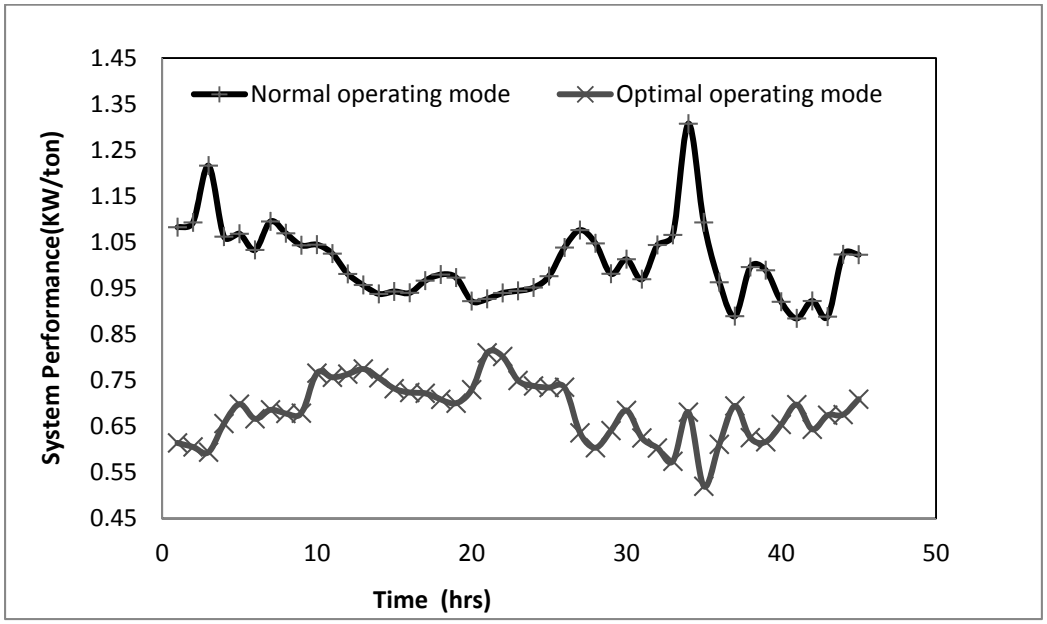

Figure 6.13 Chiller plant system performance in winter

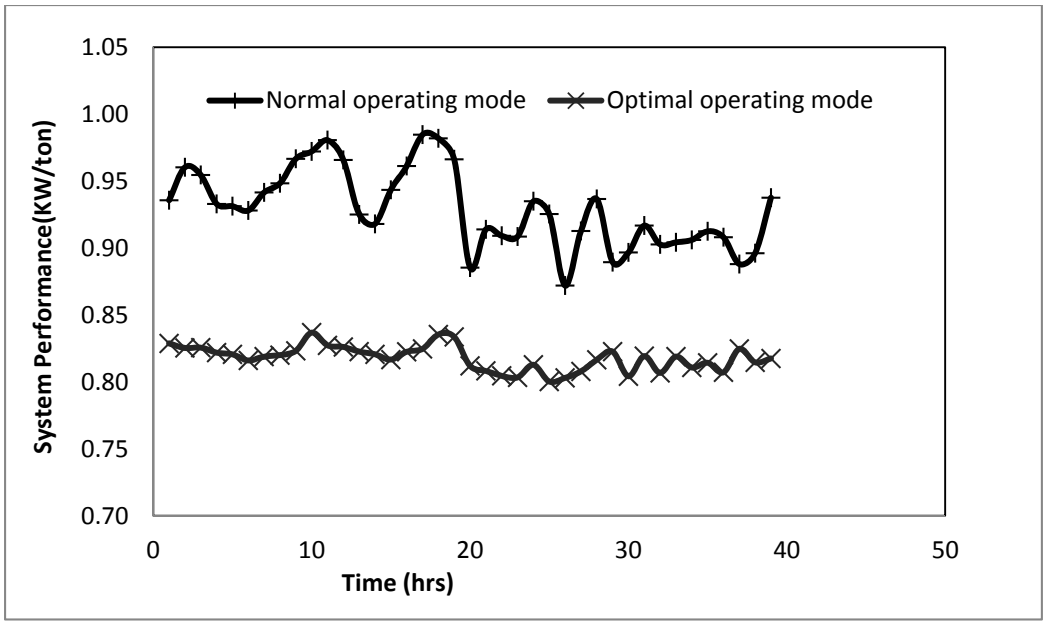

Figure 6.14 Chiller plant system performance in summer

6.7 Details of regression models

Regression Analysis (Rao, (2001)) based models were developed based on the physics of the problem and the actual operating conditions of the chiller plants. Initially, linear models are assumed followed by quadratic and cubic models to achieve the best fit for any specific performance characteristic. The measure of accuracy of the model is indicated by the term *R*, a larger value of *R* implies a more accurate fit.

Chiller Model

Initially, a linear model is considered for regression. The linear model considered for regression is given as

$$SP = A_1 + a_1(PL_{ch}) + a_2(T_{ce}) \tag{6.14}$$

The values of the coefficients are obtained by solving the linear model. The value of A_1 is obtained to be -0.3523, the value of a_1 is obtained to be -0.0023 and the value of a_2 is

obtained to be 0.0136. An *R* value of 0.7694 is obtained. Since, the *R* value is less that about 0.95 (which is considered a reasonably good fit) a quadratic model is assumed. Quadratic model is given by

$$SP = A_1 + a_1(PL_{ch}) + a_2(T_{ce}) + a_3(PL_{ch})^2 + a_4(T_{ce})^2 \quad (6.15)$$

For the quadratic model, the value of A_1 is obtained to be 0.0765, the value of a_1 is obtained to be -0.0120, the value of a_2 is obtained to be 0.0076, the value of a_3 is obtained to be 0.0001 and the value of a_4 is obtained to be 0.000001. An *R* value of 0.9492 is obtained. Since, the *R* value is less that about 0.95 (which is considered a reasonably good fit) a cubic model is assumed for further accuracy. The cubic model assumed is given by

$$SP = A_1 + a_1(PL_{ch}) + a_2(T_{ce}) + a_3(PL_h)^2 + a_4(T_{ce})^2 + a_5(PL_{ch})(T_{ce}) + a_6(PL_{ch})^3 \quad (6.16)$$

For the cubic model, the value of A_1 is obtained to be 0.3093, the value of a_1 is obtained to be -0.0131, the value of a_2 is obtained to be -0.0023, the value of a_3 is obtained to be 0.0003, the value of a_4 is obtained to be 0.0002 and the value of a_5 is obtained to be -0.000001. An *R* value of 0.9902 is obtained. Since, the *R* value is greater than 0.95, the cubic model is considered in the optimization problem formulation.

Pump Model

Initially, a linear model is considered for regression. The linear model considered for regression is given as

$$P_p = C + d_1 * G_w \quad (6.17)$$

The values of the coefficients are obtained by solving the linear model. The value of *C* is obtained to be -48.9641 and the value of d_1 is obtained to be 0.0361. An *R* value of 0.9276 is obtained. Since, the *R* value is less that about 0.95 (which is considered a reasonably good fit) a quadratic model is assumed. Quadratic model is given by

$$P_p = C + d_1 * G_w + d_2 * (G_w)^2 \quad (6.18)$$

For the quadratic model, the value of *C* is obtained to be 44.3844, the value of d_1 is obtained to be -0.0333 and the value of d_2 is obtained to be 0.0000001. An *R* value of 0.9934 is obtained. Although, the *R* value is greater than 0.95 (which is considered a reasonably good fit) a cubic model is assumed for further accuracy. The cubic model assumed is given by

$$P_p = C + d_1 * G_w + d_2 * (G_w)^2 + d_3 * (G_w)^3 \quad (6.19)$$

For the cubic model, the value of *C* is obtained to be -63.08, the value of d_1 is obtained to be 0.080645, the value of d_2 is obtained to be $-3.2*10^{-5}$ and the value of d_3 is obtained to be $4.799*10^{-9}$. An *R* value of 0.9992 is obtained which is very accurate and hence, the cubic model is considered in the optimization problem formulation.

6.8 Discrete optimization using the proposed hybrid method

To demonstrate the effectiveness and convergence of the hybrid branch and bound method, the following standard problem is considered (Beckmann and Kunzi (1980)).

Maximize: $f(\vec{X}) = 120 * x_1 + x_2 \quad (6.20)$

with constraints:

$$4 - x_2 \leq 0 \tag{6.21}$$

$$6.429 - x_1 x_2 \leq 0 \tag{6.22}$$

$$6.429 - x_1^3 x_2 \leq 0 \tag{6.23}$$

$$321.14 - x_2^2 x_1 \leq 0 \tag{6.24}$$

$$0 \leq x_1 \leq 2 \tag{6.25}$$

$$x_1 = 0.1 * k; \quad k = 0, 1, \ldots, 20 \tag{6.26}$$

$$15 \leq x_2 \leq 60; \; x_2 \in \{15, 25, 40, 60\} \tag{6.27}$$

The convergence of the hybrid method is shown in Table 6.5. The branching of the nodes using the proposed hybrid method is shown in detail as a flow-diagram in Figure 6.15.

Table 6.5 Convergence of the hybrid optimization algorithm

Exit flag	*-f(x)*	x_1	x_2	Iterations	function evaluations
1	-101.30	0.63	25.32	11	36
1	-101.76	0.60	29.76	3	12
-2	-97.00	0.60	25.00	1	4
1	-105.24	0.54	40.00	4	15
1	-111.43	0.50	51.43	2	9
-2	-100.00	0.50	40.00	2	7
1	-116.99	0.47	60.00	4	15
-2	-108.00	0.40	60.00	1	4
1	-120.00	0.50	60.00	2	8
1	-112.00	0.60	40.00	2	9
1	-105.41	0.70	21.41	5	18
0	-186.27	1.42	15.00	22	200
-2	-183.14	1.40	15.14	3	10
1	-195.00	1.50	15.00	1	6
1	**-109.00**	**0.70**	**25.00**	**1**	**6**

It is to be noted that Exit flag 1 (Table 6.5) represents that SQP algorithm converged and the solution is feasible, exit flag 2 represents that the SQP algorithm did not converge and the solution is infeasible and exit flag 0 represents the number of iterations exceeded the maximum allowable number of iterations in the SQP algorithm.

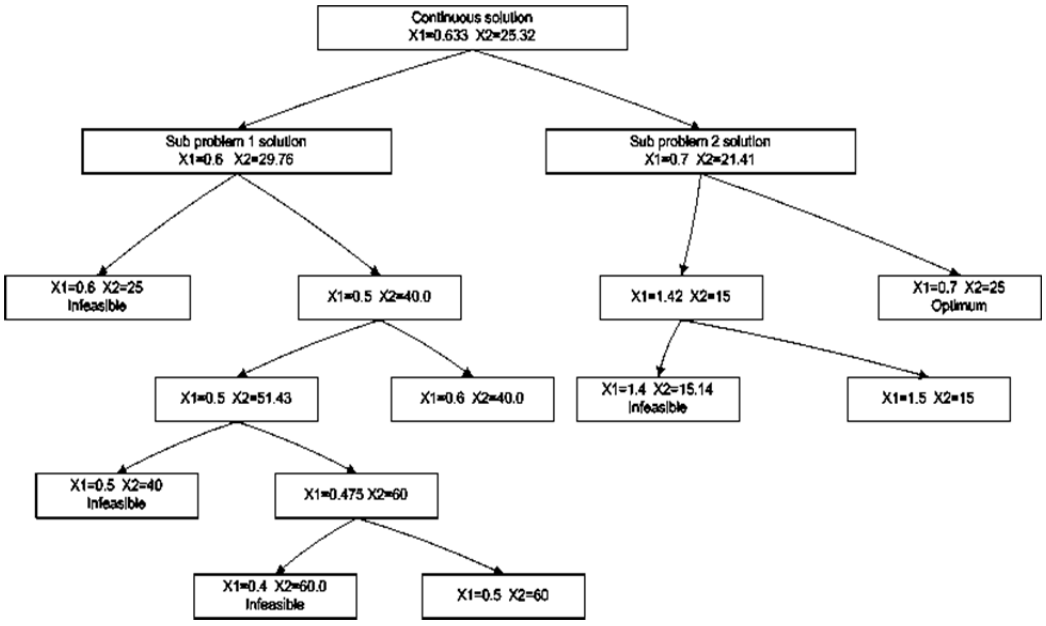

Figure 6.15 Convergence flow-diagram (hybrid optimization method)

An industrial application of chiller plant optimization is considered in this chapter. A novel optimization model is created for the plant and a hybrid optimization technique is developed to solve the model. This application would result in large energy savings in the HVAC industry.

CHAPTER 7 - PRACTICAL APPLICATION - DESIGN OPTIMIZATION OF MICRO-CHANNEL HEAT EXCHANGERS

Optimization of thermal management in micro-electronics is considered in this chapter. A brief introduction and literature review is provided. Design optimization of a novel micro-channel heat exchanger in Low Temperature Co-fired Ceramic (LTCC) is detailed.

7.1 Introductory remarks

Increased device density, switching speeds of integrated circuits and decrease in electronic package size is placing new demands for high power thermal-management. The thermal management system considers the complete thermal path from heat source to the heat sink. It requires optimization of the heat removal by conduction and convection with the lowest possible thermal resistance at all levels of assembly. Depending on the application, a wide range of cooling methods are in use. These include forced air convection, external heat pipes, water cooled heat sinks, immersion cooling and refrigeration cycles.

The conventional method of forced air cooling with passive heat sink can handle heat fluxes up-to 3-5W/cm^2. However, current microprocessors are operating at levels of 100W/cm^2. This demands the usage of novel thermal-management systems. In present research work, a heat exchanger system designed and fabricated by Adluru (2003) is optimized for maximum energy transfer. The design consists of a water-cooling system, with active in-built heat sink and uses vertical free standing silver columns acting as pin fins. These columns are embedded in the Low Temperature Co-fire Ceramic (LTCC) substrate.

7.2 Literature review

Heat transfer in micro-channel heat sinks has been studied for almost three decades now. Tuckerman and Pease (1981) were the first to experimentally study the heat removed using three different micro-channel heat sinks with varying channels heights and widths. Their work was followed by many researchers performing experimental and theoretical studies on micro-channel heat sinks. Kleiner et al., (1995) used a parallel plate-fin heat sink to perform experimental and theoretical investigation in micro-channels. Philips (1990) suggested an analytical model for the estimation of thermal resistance in a micro-channel and validated the model with experiments. Theory based correlations for thermal resistances in micro-channels were reported by Samalam (1989). Numerical simulation of heat transfer in solid and liquid substrate micro-channel heat exchangers was conducted by Weisburg et al., (1992). Manifold micro-channel heat sinks were first proposed by Harpole and Eninger (1991), and numerically studied in Ng and Poh (1999). The studies conclude that the manifold micro-channel heat sinks have a less pressure drop when compared to the conventional micro-channels heat sinks for a fixed flow rate. Different geometries of micro-channels like grooves, pin-fins, dimples and ribs have also been studied by many researchers (Wei and Joshi (2003), Ndao et al., (2009)). A comparative analysis of studies on heat transfer and fluid flow in micro-channels is detailed in Shobhan and Garimella (2001).

Although a lot of research has been going on, in the field of thermal management since early 70's due to tremendous growth in electronic field with increased transistor densities (following Moore's law), decrease in package size and increased power densities, in the initial stages, heat was removed using classical techniques such as surface mounted heat

sinks or forced air convection cooling. Due to the high power density requirement, these classical ways of cooling do not meet the requirements and so new methods of thermal management are to be employed. A brief literature review indicates that no work existed to integrate a micro heat exchanger using silver columns in the substrate itself.

A study in three-dimensional fluid flows and heat transfer in a rectangular micro-channel heat sink are analyzed numerically using water as coolant, was done by Issam Mudawar et al., (2002). In this, the heat sink was made of a 1-cm^2 silicon wafer with micro-channels of width 57 μm and a depth of 180 μm and is separated by a 43-μm wall. A large number of flow channels with characteristic dimensions ranging from 10 to 1000 μm are fabricated in a solid substrate, which usually has high thermal conductivity such as silicon or copper. Figure 7.1 shows the schematic of micro-channel heat sink used and its unit cell. An electronic component is then mounted on the base surface of the heat sink. The heat generated by the component is first transferred to the channels by heat conduction through the solid, and removed by the cooling fluid, which is forced to flow through the channels.

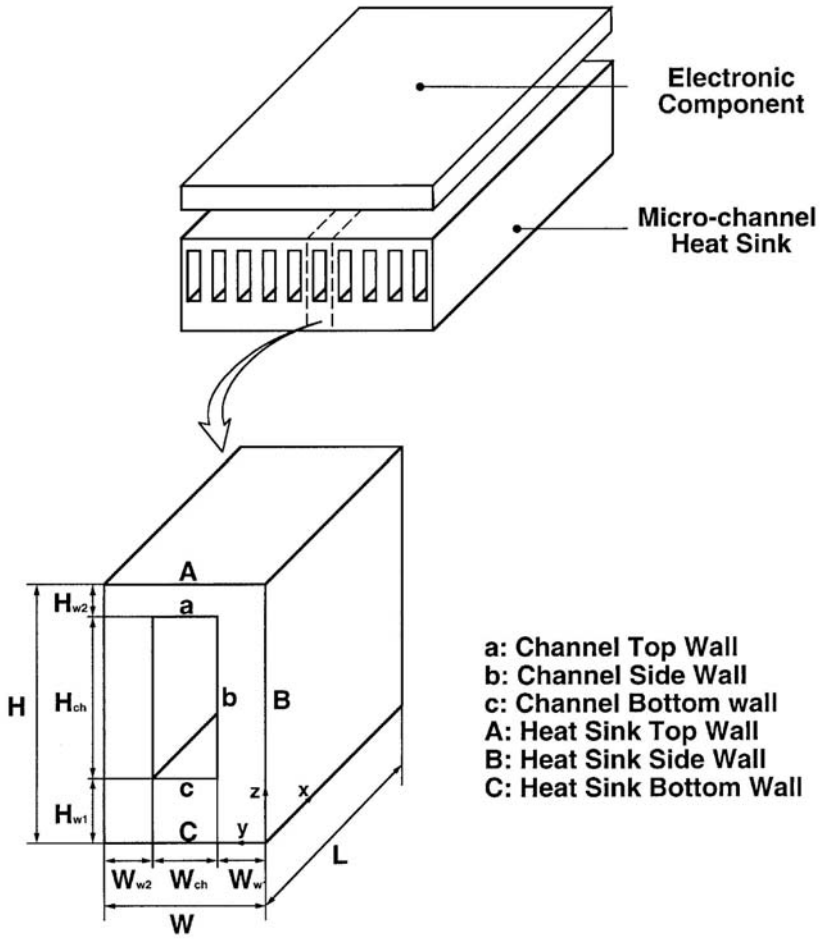

Figure 7.1 Schematic of micro-channel heat sink (Mudawar et al., (2002)).

Micro heat pipe heat spreaders (MHPHS) with three copper foil layers was studied by Kang et al., (2003) to allow liquid and vapor flow separation to reduce viscous shear force. Two wick designs, one using 200 μm wide etched radial groves and other with 100 mesh screens was investigated. The foils were vacuum diffusion bonded to form 31 x 31 x 2.7 mm^3 heat spreader. Thermal performance of the MHPHS was evaluated experimentally in a fan-heat sink CPU test apparatus with a heating area of 13.97 mm x 13.97 mm.

Another study of using micro channels to cool microprocessors by Transmission-Line-Matrix (TLM) technique was done by Belhardj et al., (2003). The Figure 7.2 shows the

packaging structure for heat removal considered in this work. In this structure, the primary mode of heat removal is from the back surface of the silicon die. The die is attached to a heat spreader through an interfacial material, which is either thermal conductive gel or epoxy.

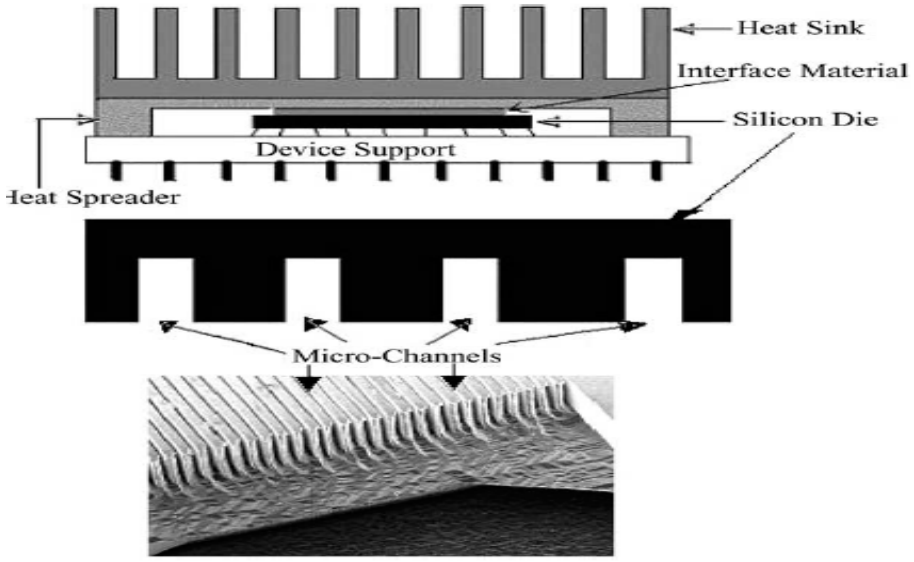

Figure 7.2 Structure with packaging and micro-channels (Belhardj et al., (2003)).

The geometry considered was silicon die 2 mm thick with a surface of 20 x 20 mm^2. Micro-channels of various depths and widths are introduced on the backside of the microprocessor silicon die. These micro channels are micro-machined in the silicon substrate using Micro Electro Mechanical Systems (MEMS) technology. In this study, the TLM technique was used to simulate the effect of micro-channels on the temperature distribution in the active region. To minimize the interface heat resistance various micro-channel and patterns are examined. In this work, the micro channels are filled with the heat spreader material copper or aluminum.

Another similar type of work was done by Kreutz et al., (2000), on Simulation of micro-channel heat sinks for Optoelectronic Microsystems. Water cooled heat sinks are investigated both experimentally and theoretically as model systems to simulate the energy and mass transportation in devices used for cooling of Optoelectronic micro-systems such as diode lasers. The design of micro-channel heat sinks resulted in a decrease of their thermal resistance and of the pressure drop of the coolant allowing an increased heat load of an optoelectronic micro-system.

Another interesting study was done by Jang et al., (2003) on experimental investigation of thermal characteristics for a micro-channel heat sink subjected to an impinging jet, using a micro-thermal sensor array. In this study, a micro-channel heat sink was introduced which is subject to an impinging jet, which has a small pressure drop. It experimentally investigated the heat transfer enhancement of the micro-channel heat sink subject to jet impingement. Temperature distributions at the base of the micro-channel heat sink are measured for evaluating the thermal resistance by using a micro-thermal sensor array.

Zampino (2001) developed the heat pipes embedded into the ceramic substrates that provide a thermal transport mechanism capable of transporting heat over the length of the substrate at an effective thermal conductivity at least ten times higher than typical metals and over 100 times that of the substrate material. The heat pipes described serve to spread heat over a large area, utilizing more of the heat sink if the substrate is bonded to a heat sink material resulting in smaller temperature rise across the substrate. The most powerful use of heat pipe described is in applications where cooling can only be provided along an edge of the substrate (Ravindra (2002)).

Amey (2000) and Ravindra (2002) developed high density thermal vias in Low Temperature Co-fired Ceramics. Their work show that denser thermal vias can be fabricated in the substrates thus reducing the in line resistance of the substrate. These vias also help in efficiently carrying heat on to the surface of the substrate, which can be further removed by a passive heat sink.

From the literature review, it can be concluded that most designs for micro-channel heat exchangers have the heat transferring source surface mounted on the substrate, which means another passive heat sink. Since, thermal management requires optimization of the heat removal by conduction and convection with the lowest possible thermal resistance at all levels of assembly, first it is required to minimize the thermal resistance of the substrate itself. Even though the passive heat sinks are efficient, the resistance of the system increases due to the use of thermal glues or epoxies. Also, most of the heat exchangers were tested for silicon devices. These are expensive when compared to LTCC substrates. Furthermore, it is concluded from the literature review, that fabricating an integrated micro-channel heat-exchanger with freestanding silver (Ag) columns in it, was the first of its kind. Hence, the optimization of such a breakthrough technology has been performed in present research.

7.3 Analytical treatment of the problem

One-dimensional heat transfer relations are used to analyze the heat exchanger model. It gives an estimate of how heat is transferred in the model. The thermal resistance for conduction is defined as L/kA, where L is the length of the thermal path, k is the thermal conductivity of the material, and A is the cross-sectional area through which heat is transferred. For convective heat transfer, the thermal resistance is defined as $1/hA$, where

h is the average convective heat transfer coefficient. The basic thermodynamic, heat transfer and fluid flow relations used for calculations are given as below.

Total heat transferred from the source to the coolant (P_{heat}), is a function of the total thermal resistance (R_{Total}) and the difference in temperature between the two (ΔT). Hence,

$$P_{heat} = \Delta T \big/ R_{Total} \tag{7.1}$$

where the total thermal resistance is calculated as a summation of the conductive and convective resistances and is given by

$$R_{Total} = R_{conduction} + R_{Agpad} + R_{convection} \tag{7.2}$$

Also, the rate of heat transfer ($\dot{Q}$) is calculated as

$$\dot{Q} = h\, A \Delta T_{avg} \tag{7.3}$$

where the convective heat transfer coefficient h is a function of Nusselt number (Nu) and is given by

$$h = \frac{N_u K}{x} \tag{7.4}$$

ΔT_{avg} is calculated using the constant wall source temperature T_1 and the bulk mean temperature of the coolant $T_{bulkmean}$.

$$\Delta T_{avg} = T_1 - T_{bulkmean} \tag{7.5}$$

$T_{bulkmean}$ denotes the average of the inlet (T_{in}) and outlet (T_{out}) temperatures of the coolant.

$$T_{bulkmean} = \frac{T_{in} + T_{out}}{2} \tag{7.6}$$

Energy balance equation gives

$$\dot{m} C_p dT = h(T_1 - T) dA \tag{7.7}$$

where $\dot{m}$ denotes the mass flow rate and C_p is the specific heat of the coolant.

Hence, T_{out} is given by

$$T_{out} = T_1 - (T_1 - T_{in}) e^{-\frac{hA}{mC_p}} \tag{7.8}$$

The pumping power (P_p) is given by

$$P_p = \dot{m} \Delta P / \rho \eta \tag{7.9}$$

where the pressure drop across the system (ΔP), is given by

$$\Delta P = N.f.\frac{L}{D_{eq}}.\frac{V^2}{2}.\rho \tag{7.10}$$

N is the number of Ag columns in a row, f is the friction factor, L is the length of the duct and D_{eq} is the equivalent diameter of the duct, V is the velocity of the coolant and ρ is the density of the coolant and η is the efficiency of the pump.

Figure 7.3 shows the cross sectional schematic of the LTCC heat exchanger and its equivalent thermal resistance network. A constant amount of heat is provided using a heater mounted on top of the copper shim. Silver columns inside the LTCC material form the thermal vias (paths for heat to transfer). Coolant is pumped into the rectangular duct at the center. A silver pad is inserted at the inner surface of the rectangular duct for increasing the heat transfer area. In the figure, T_1 is the temperature at the top surface of the LTCC, T_2 is the temperature at the top surface of the silver pad, and T_3 is the temperature at the bottom surface of the silver pad. $T_{bulkmean}$ is the bulk mean temperature of the coolant.

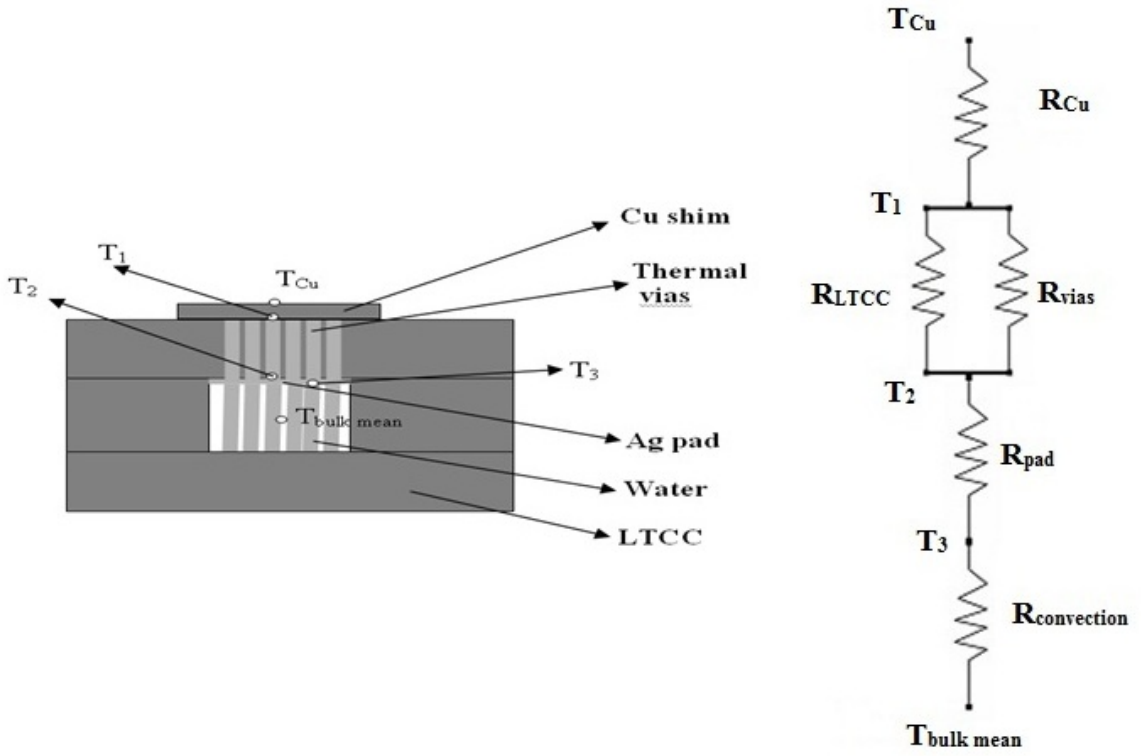

Figure 7.3 Schematic and equivalent thermal resistance network of the LTCC heat exchanger (Adluru, (2003))

7.4 LTCC heat exchanger optimization problem formulation

In the optimization of the LTCC heat exchanger, the main aim is to design an energy efficient heat exchanger configuration based on the maximum possible heat transfer from the source to the heat sink while minimizing the coolant pumping power. In present example, heat source is the top surface of the LTCC sample and the heat sink is the cooling liquid (water). The design variables considered for optimization are diameter of the silver columns (D_{Ag}), pitch of the silver columns (P_{Ag}), height of the duct (h_{dct}), number of silver columns (n_{Ag}) and the mass flow rate of coolant ($\dot{m}_{coolant}$).

The Multi-objective optimization problem can be expressed as

$$\text{Min } f(\vec{X}) = -P_{heat}(\vec{X}) + P_p(\vec{X}) \tag{7.11}$$

$$\text{where} \quad \vec{X} = \begin{Bmatrix} D_{Ag} \\ P_{Ag} \\ h_{dct} \\ n_{Ag} \\ \dot{m}_{coolant}) \end{Bmatrix} \tag{7.12}$$

with the following constraints

Pressure drop across the duct

$$(\Delta P)_l \leq \Delta P \leq (\Delta P)_u \tag{7.13}$$

Volume of silver metal used

$$(V_{Ag})_l \leq V_{Ag} \leq (V_{Ag})_u \tag{7.14}$$

P_{heat} is the amount of heat transferred and P_p is the power consumed by the coolant pump. Design variables have to be limited to certain bounds based on manufacturability and size restrictions. In this problem, the bounds are specified as

$$0.6 \leq D_{Ag} \leq 1.0 \tag{7.15}$$

$$1.5 \leq P_{Ag} \leq 2.5 \tag{7.16}$$

$$1.5 \leq h_{dct} \leq 2.5 \tag{7.17}$$

$$6 \leq n_{Ag} \leq 10 \tag{7.18}$$

$$4.03 \leq \dot{m}_{coolant} \leq 20.5 \tag{7.19}$$

For geometric feasibility, additional geometric constraint is imposed. This constraint ensures that radius of the silver column does not exceed the pitch.

$$\frac{(D_{Ag})}{2} - P_{Ag} \leq 0 \tag{7.20}$$

For a better understanding, the single objective optimization of each of the objectives is solved separately and the results are analyzed.

a) Maximization of heat transfer

$$\text{Min } f(\vec{X}) = -P_{heat}(\vec{X}) \tag{7.21}$$

$$\text{where} \quad \vec{X} = \begin{Bmatrix} D_{Ag} \\ P_{Ag} \\ h_{dct} \\ n_{Ag} \\ \dot{m}_{coolant}) \end{Bmatrix} \tag{7.22}$$

with the following constraints

Pressure drop across the duct

$$(\Delta P)_l \leq \Delta P \leq (\Delta P)_u \tag{7.23}$$

Volume of silver metal

$$(V_{Ag})_l \leq V_{Ag} \leq (V_{Ag})_u \tag{7.24}$$

The design variables have to be limited to certain bounds based on manufacturability and size restrictions. In this problem, the bounds are specified as

$$0.6 \leq D_{Ag} \leq 1.0 \tag{7.25}$$

$$1.5 \leq P_{Ag} \leq 2.5 \tag{7.26}$$

$$1.5 \leq h_{dct} \leq 2.5 \tag{7.27}$$

$$6 \leq n_{Ag} \leq 10 \tag{7.28}$$

$$4.03 \leq \dot{m}_{coolant} \leq 20.5 \tag{7.29}$$

For geometric feasibility, additional geometric constraint is imposed. This constraint ensures that radius of the silver column does not exceed the pitch.

$$\frac{(D_{Ag})}{2} - P_{Ag} \leq 0 \tag{7.30}$$

b) Minimization of pumping power

$$\text{Min } f(\vec{X}) = P_p(\vec{X}) \tag{7.31}$$

where $\vec{X} = \begin{Bmatrix} D_{Ag} \\ P_{Ag} \\ h_{dct} \\ n_{Ag} \\ \dot{m}_{coolant}) \end{Bmatrix}$ (7.32)

The constraints used are given by

Pressure drop across the duct

$$(\Delta P)_l \leq \Delta P \leq (\Delta P)_u \tag{7.33}$$

Volume of silver metal

$$(V_{Ag})_l \leq V_{Ag} \leq (V_{Ag})_u \tag{7.34}$$

The design variables have to be limited to certain bounds based on manufacturability and size restrictions. In this problem, the bounds are specified as

$$0.6 \leq D_{Ag} \leq 1.0 \tag{7.35}$$

$$1.5 \leq P_{Ag} \leq 2.5 \tag{7.36}$$

$$1.5 \leq h_{dct} \leq 2.5 \tag{7.37}$$

$$6 \leq n_{Ag} \leq 10 \tag{7.38}$$

$$4.03 \leq \dot{m}_{coolant} \leq 20.5 \tag{7.39}$$

For geometric feasibility, additional geometric constraint is imposed. This constraint ensures that radius of the silver column does not exceed the pitch.

$$\frac{(D_{Ag})}{2} - P_{Ag} \leq 0 \tag{7.40}$$

c) Minimization of the volume of silver

$$\text{Min } f(\vec{X}) = V_{Ag}(\vec{X}) \tag{7.41}$$

$$\text{where} \quad \vec{X} = \begin{Bmatrix} D_{Ag} \\ P_{Ag} \\ h_{dct} \\ n_{Ag} \\ \dot{m}_{coolant}) \end{Bmatrix} \tag{7.42}$$

Pressure drop across the duct

$$(\Delta P)_l \leq \Delta P \leq (\Delta P)_u \tag{7.43}$$

The design variables have to be limited to certain bounds based on manufacturability and size restrictions. In this problem, the bounds are specified as

$$0.6 \leq D_{Ag} \leq 1.0 \tag{7.44}$$

$$1.5 \leq P_{Ag} \leq 2.5 \tag{7.45}$$

$$1.5 \leq h_{dct} \leq 2.5 \tag{7.46}$$

$$6 \leq n_{Ag} \leq 10 \tag{7.47}$$

$$4.03 \leq \dot{m}_{coolant} \leq 20.5 \tag{7.48}$$

For geometric feasibility, additional geometric constraint is imposed. This constraint ensures that radius of the silver column does not exceed the pitch.

$$\frac{(D_{Ag})}{2} - P_{Ag} \leq 0 \tag{7.49}$$

7.5 Optimization results

Single objective optimization of maximization of heat transfer is considered first. The rate of heat transfer is to be increased while making sure that the pressure drop and volume of silver are within limits. A random initial design is considered with a heat transfer of 34.72W. Since, it is a maximization problem. The objective function is taken with a negative sign for minimization. The results are tabulated in Table 7.1. It is seen that at the optimum design, when the heat transfer is maximum, the diameter of the silver columns is 0.0006 m and pitch is 0.001 m. The duct height and number of columns are active constraints (reaching the upper bounds). This is due to the fact that in order to have the maximum heat transfer from the heat source point to the cooling liquid the material with maximum thermal conductivity is needed. Since, silver is a very good conductor of heat when compared to LTCC material, so the optimization converges to the maximum limits for the silver metal. So, the number of silver columns and duct height reach maximum. It is to be noted that the diameter of silver columns does not reach the maximum because of the geometric feasibility constraint. The maximum heat transferred at this point is 43.64W which evidently lies between 1.25W and 46.42W (lower and upper limits of the design variables).

Table 7.1 Optimization results for maximization of heat transfer

Quantity	Initial Design	Bounds		Optimum Design
		Lower	Upper	
Design Variables:				
D_{Ag} (m)	0.0008	0.0002	0.0010	0.0006
P_{Ag} (m)	0.0016	0.0005	0.0020	0.0010

Quantity	Initial Design	Bounds		Optimum Design
		Lower	Upper	
h_{dct} (m)	0.0020	0.0015	0.0025	0.0025
n_{Ag}	8	4	10	10
$\dot{m}_{coolant}$ (kg/s)	0.00567	0.00487	0.0205	0.0205
Objective function:				
Heat transfer (W)	34.72	1.25	46.42	43.64

Design of a heat exchanger with maximum heat transfer is not the only important objective in a heat exchanger with a cooling fluid passing through it. It is essential to consider the power required to pump the fluid and the type of fluid. In this research, the coolant is fixed to water and so the pumping power of water is considered as an objective function. The second single objective optimization problem minimizes the pumping power subjected to constraints on the volume of silver and geometry of the heat exchanger. In this case, there is no need for pressure drop constraint as the pressure drop indirectly relates to the pumping power. The design variables and the initial design point remain same as in the previous case. The optimum results (Table 7.2) show that the coolant flow rate design variable is active which means optimum $\dot{m}_{coolant}$ value reaches the lower bound. This is because, with minimum pump power, the flow rate has a minimum value for a particular design (with fixed number of silver columns). The optimum number of silver columns is eight and the duct height is at its upper bound because larger height means larger volume for the coolant. Hence, more fluid is to be pumped slowly to minimize the pump power. Also, more fluid stays in the duct and so lesser number of silver columns are needed for cooling.

Table 7.2 Optimization results for minimization of pumping power

Quantity	Initial Design	Bounds		Optimum Design
		Lower	Upper	
Design Variables:				
D_{Ag} (m)	0.0008	0.0002	0.0010	0.0007
P_{Ag}(m)	0.0016	0.0005	0.0020	0.0012
h_{dct} (m)	0.0020	0.0015	0.0025	0.0025
n_{Ag}	8	4	10	8
$\dot{m}_{coolant}$ (kg/s)	0.00487	0.00487	0.0205	0.0049
Objective function:				
Pump power (W)	6.5	3.0	10.0	5.4

Table 7.3 Optimization results for minimization of volume of silver

Quantity	Initial Design	Bounds		Optimum Design
		Lower	Upper	
Design Variables:				
D_{Ag} (m)	0.0008	0.0002	0.0010	0.0006
P_{Ag} (m)	0.0016	0.0005	0.0020	0.0011
h_{dct} (m)	0.0020	0.0015	0.0025	0.0022
n_{Ag}	8	4	10	8
$\dot{m}_{coolant}$ (kg/s)	0.00567	0.00487	0.0205	0.00487
Objective function:				
Volume of silver (m^3)	$99.69*10^{-9}$	$4.68*10^{-9}$	$296.7*10^{-9}$	$73*10^{-9}$

For the cost analysis the volume of silver metal used for cooling becomes an important factor. Hence, the third single objective optimization problem considers the volume of the silver metal subjected to pressure drop and geometric constraints. The results are shown in Figure 7.3. The optimum number of silver columns needed is eight. The coolant flow rate is at its lower bound (0.00487 kg/s). It is no be noted that the diameter and number of silver column variables are not active at the optimum design. After analyzing the results of the single objective optimization problems, the multi-objective optimization problem is formulated. Two objectives are considered for the multi-objective formulation namely, the maximization of heat transfer and the minimization of pumping power. Constraints are the pressure drop, silver volume and geometric constraints.

Table 7.4 Optimization results for combined heat transfer and pumping power

Quantity	Initial Design	Bounds		Optimum Design
		Lower	Upper	
Design Variables:				
D_{Ag} (m)	0.0008	0.0002	0.0010	0.0006
P_{Ag} (m)	0.0016	0.0005	0.0020	0.0010
h_{dct} (m)	0.0020	0.0015	0.0025	0.0025
n_{Ag}	8	4	10	10
$\dot{m}_{coolant}$ (kg/s)	0.00567	0.00487	0.0205	0.018
Objective function:				
Total Power (W)	34.72	1.25	46.42	37.32

The multi-objective optimization problem is solved using a hybrid optimization algorithm using SQP and modified branch and bound method as discussed in Section 6.3 (HVAC optimization). The optimum results are given in Table 7.4. The optimum diameter of silver columns is found to be 0.0006m while the pitch is 0.0010m. Two of the design variables, duct height and the number of silver columns, are at their upper bounds. This means that for maximum heat transfer the duct area is to be maximized and maximum allowable number of silver columns is to be used. Also, the coolant mass flow rate (0.018kg/s) is closer to its maximum value (0.0205kg/s). This validates the results, because the flow rate is proportional to the heat transfer.

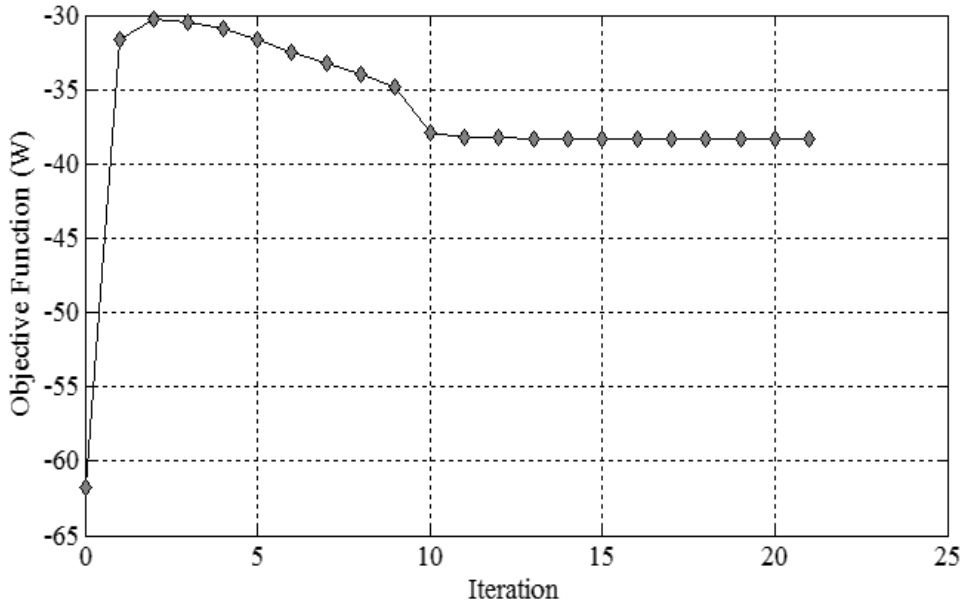

Figure 7.4 Convergence of the objective function

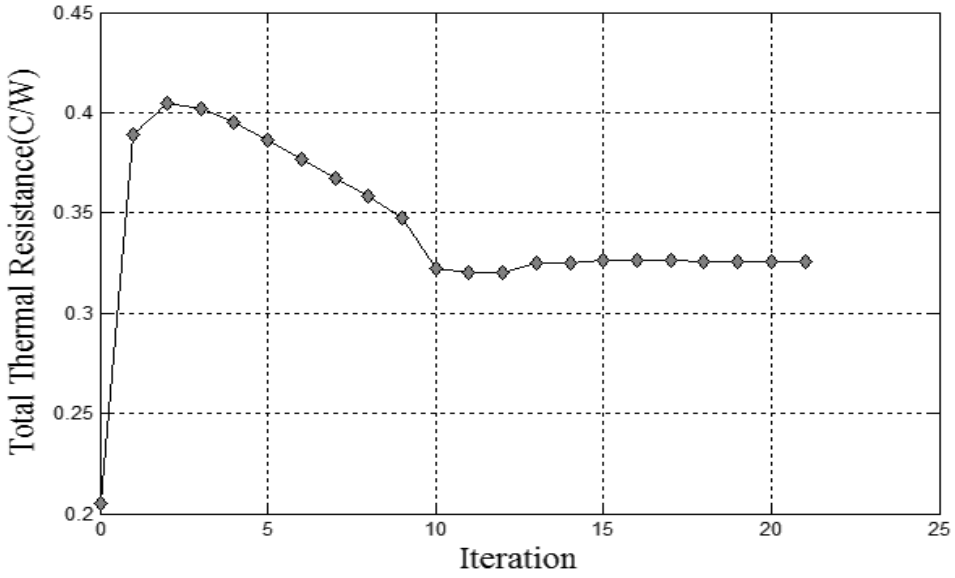

Figure 7.5 Variation of total thermal resistance

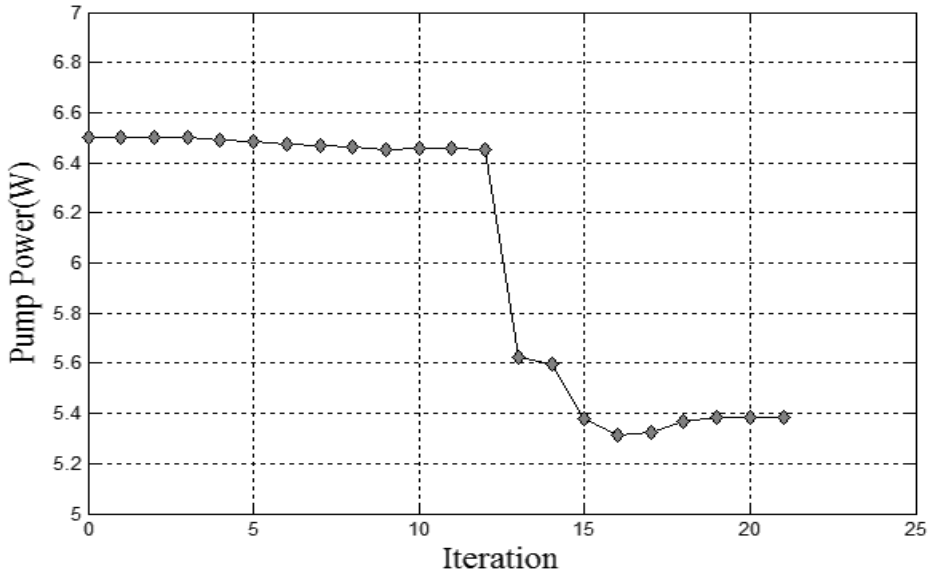

Figure 7.6 Variation of pumping power with number of iterations

The convergence of the optimization algorithm is shown in Figure 7.4, Figure 7.5 and Figure 7.6. The variation of the objective function value (combined heat transfer and pumping power) with number of iterations is shown in Figure 7.4. It is to be noted that

the objective function value is negative because the heat dissipated is to be maximized and the pumping power is to be minimized. The total number of iterations required for convergence to the optimum solution is 21. The variation of total thermal resistance and the pumping power during the optimization is shown in Figure 7.5 and Figure 7.6 .The pump power varied from an initial value of 6.5 W to an optimum value of 5.38 W. This value is in agreement with the range of the pump chosen in this study and also with the current microelectronics standards. The total thermal resistance value at the optimum point is found to be $0.325℃/W$. Thus, this optimum design gives a very low thermal resistance.

In this chapter, optimization procedure is applied to cooling in micro-electronics. A novel optimization model is created for thermal management in an LTCC heat exchanger. Hybrid optimization model developed for chiller plant optimization is used in this application also. Results obtained prove that more heat can be transferred from the micro-electronics without compromising their performance.

CHAPTER 8 - CONCLUSIONS AND FUTURE WORK

Present research work aims at investigating into two non-traditional optimization techniques necessary for solving complex engineering problems. A Multi-level optimization method is developed to solve uncertainty based engineering systems. Two types of uncertainties considered are the probabilistic and the interval uncertainty. Modified Ant Colony Optimization and Multi-Level Ant Colony Optimization procedures are developed for multi-objective problems. The developed methods are illustrated using structural and mechanical engineering problems. Results obtained indicate the validity of the methods.

Practical applications demonstrate the credibility of any original contributions in research. Hence, in present research, novel optimization models have been developed for application in HVAC and micro-heat exchangers for electronics cooling. Case studies are performed and the results indicate the validity of the developed methods.

In future, the developed ACO and ML methods can be applied to large complex engineering problems like the chiller plant model. Uncertainty based models for practical examples solved in present research would be a new topic for research. Developing hybrid algorithms with a combination of ACO and ML optimization for engineering systems, under uncertainty, would be useful for designers to make various choices.

With knowledge and experience gained from the present research, optimization techniques could be extended to broad areas in engineering such as bio-engineering, micro-electromechanical systems and renewable energy systems, which have scope for optimization.

REFERENCE

[1] Aditya, P. A., Wang, B. P., Using Power of Ants for Optimization, AIAA-2004-1681, 45th AIAA/ASME/ASCE/AHS/ASC Structures, Structural Dynamics & Material Conference, Palm Springs, California, Apr. 2004.

[2] Adluru, H. K., Design and Analysis of Micro-Channel Heat Exchanger embedded in Low Temperature Co-fire Ceramic (LTCC), M.S. Thesis, Florida International University, Miami, FL, 2004.

[3] Afshar, A., Sharifi, F., Jalali, M. R., Non-dominated Archiving Multi-Colony Ant Algorithm for Multi-Objective Optimization: Application to Multi-Purpose Reservoir Operation, Engineering Optimization, vol. 41, no. 4, pp. 313-325, 2009.

[4] Alexandrov, N. M., Lewis, R. M., Analytical and Computational Aspects of Collaborative Optimization for Multidisciplinary Design, AIAA Journal, vol. 40, no. 2, pp. 301-309, 2002.

[5] Amey, D. I., Keating, M. Y., Smith, M. A., Horowitz, S. J., Donahue, P. C., Needes, C. R., Low Loss Tape Materials System for 10 to 40 GHz Application, Proceedings of the International Symposium on Microelectronics, IMAPS, Boston, MA, USA, pp. 654-658, 2000.

[6] Ansari, D., Hussain, A., Kim, K. Y., Multiobjective Optimization of a Grooved Micro-Channel Heat Sink, IEEE Transactions on Components and Packaging Technologies, vol. 33, no. 4, pp. 767-776, Dec. 2010.

[7] Antonsson, E. K., Otto, K. N., Imprecision in Engineering Design, ASME Journal of Mechanical Design, vol. 17, no. 2, pp. 25-32, 1995.

[8] Aravelli, A., Rao, S. S., Energy Optimization in Chiller Plants: A Novel Formulation and Solution using a Hybrid Optimization Technique, Engineering Optimization, In-press, 2012.

[9] Aravelli, A., Rao, S. S., Adluru, H. K., Design Optimization of Micro-Channel Heat-Exchanger Embedded in LTCC, Proceedings of the 45th International Symposium on Micro-Electronics, IMAPS, San Diego, Sep. 2012.

[10] Aravelli, A., Rao, S. S., Adluru, H. K., Multi-Objective Design Optimization of Micro-Channel Cooling System using High Performance Thermal Vias in LTCC Substrates, Journal of Micro-Electronics and Electronic Packaging, vol. 10, pp. 40-47, 2013.

[11] Athan, T. W., Papalambros, P. Y., A Note on Weighted Criteria Methods for Compromise Solutions in Multi-Objective Optimization, Engineering Optimization, no. 27, pp.155-176, 1996.

[12] Austin, S. B., Optimum Chiller Loading, ASHRAE Journal, vol. 33, no. 7, pp.40-43, 1991.

[13] Austin, S. B., Chilled Water System Optimization, ASHRAE Journal, vol. 35, no. 7, pp. 50-56, 1993.

[14] Avery, G., Improving the Efficiency of Chilled Water Plants, ASHRAE Journal, vol. 43, no. 5, pp. 14-18, 2001.

[15] Baran, B., Schaerer, M., A Multiobjective Ant Colony System for Vehicle Routing Problem with Time Windows, Proceedings of the 21st IASTED International Conference on Applied Informatics, pp. 97-102, 2003.

[16] Barthelemy, M. J., Riley, M. F., Improved Multilevel Optimization Approach for the Design of Complex Engineering Systems, AIAA Journal, vol. 26, no. 3, pp. 353-360, 1988.

[17] Bau, H. H., Optimization of Conduit's Shape in Micro-Heat Exchangers, International Journal of Heat and Mass Transfer, vol. 41, pp. 2717-2723, 1998.

[18] Beckmann, M., Kunzi, H. P., Test Examples for Non-Linear Programming Codes, Lecture Notes in Economics and Math Systems, Springer-Verlag, 1980.

[19] Beghi, A., Cecchinato, L., Rampazzo, M., A Multi-Phase Genetic Algorithm for the Efficient Management of Multi-Chiller System, Energy Conversion and Management, vol. 52, pp. 1650-1661, 2011.

[20] Belhardj, S., Mimouni, S., Saidane, A., Benzohra, M., Using Micro-Channels to Cool Micro-Processors: A Transmission-line-matrix Study, Microelectronics Journal, vol. 34, pp. 247-253, 2003.

[21] Bellenger, L. G., Becker, J. D., Selecting High-Efficiency Centrifugal Chillers: A System Approach, HPAC Heating/Piping/Air Conditioning Journal, vol. 68, no. 7, pp. 41-49, 1996.

[22] Berrichi, A., Yalaoui, F., Amodeo, L., Mezghiche, M., Bi-Objective Ant Colony Optimization Approach to Optimize Production and Maintenance Scheduling, Computers and Operations Research, vol. 37, pp. 1584-1596, 2010.

[23] Biswal, L., Chakraborty, S., Som, S. K., Design Optimization of Single-Phase Liquid Cooled Microchannel Heat Sink, IEEE Transactions on Components and Packaging Technologies, vol. 32, no. 4, pp. 876-886, Dec. 2009.

[24] Brandt, M. A. (editor), Criteria and Methods of Structural Optimization, Developments in Civil and Foundation Engineering, Martinus Nijhoff Publishers, Boston, pp. 273-286, 1986.

[25] Braun, J. E., Klein, S. A., Mitchell, J. W., Beckman, W. A., Application of Optimal Control to Chilled Water System without Storage, ASHRAE Transactions, vol. 95, no. 1, pp. 663-675, 1989.

[26] Braun, J. E., Doderrich, G. T., Near-Optimal Control of Cooling Towers for Chilled Water Systems, ASHRAE Transactions, vol. 96, no. 2, pp. 806-813, 1990.

[27] Braun, R. D., Powell, R. W., Lepsch R. A., Comparison of Two Multidisciplinary Optimization Strategies for Launch Vehicle Design, Journal of Spacecraft Rockets, vol. 32, no. 3, pp. 404-410, 1995.

[28] Browne, M. W., Bansal, P. K., Steady-State Model of Centrifugal Liquid Chillers, International Journal of Refrigeration, vol. 21, no. 5, pp. 343-358, 1998.

[29] Cai, J., Ma, X., Li, Q., Li, L., Peng, H., A Multi-Objective Chaotic Ant Swarm Optimization for Environmental/Economic Dispatch, Electrical power and energy systems, vol. 32, pp. 337-344, 2010.

[30] Capriles, P. V. S. C., Fonseca, L. G., Barbosa, H. J. C., Lemonge, A. C. C., Rank-Based Ant Colony Algorithms for Truss Weight Minimization with Discrete Variables, Communications in Numerical Methods in Engineering, vol. 23, no. 6, pp. 553-575, 2007.

[31] Chaharsooghi, S. K., Amir, H., Kermani M., An Effective Ant Colony Optimization Algorithm (ACO) for Multi-Objective Resource Allocation Problem (MORAP), Applied Mathematics and Computation, vol. 200, pp. 167-77, 2008.

[32] Chang, Y. C., Application of Genetic Algorithm to the Optimal Chilled Water Supply Temperature Calculation of Air Conditioning Systems for Saving Energy, Energy Research, vol. 31, no. 8, pp. 796-810, 2007.

[33] Chang, Y. C., Lin, F. A., Lin, C. H., Optimal Chiller Sequencing by Branch and Bound Method for Saving Energy, Energy Conversion and Management, vol. 46, pp. 2158-2172, 2005.

[34] Charles, V. Camp, Barron, J. Bichon, Design of Space Trusses Using Ant Colony Optimization, Journal of Structural Engineering, vol. 130, no. 5, pp. 741-751, 2004.

[35] Chica, M., Cordon, O., Damas, S., Bautista, J., Multi-Objective Constructive Heuristics for the 1/3 Variant of the Time and Space Assembly Line Balancing Problem: ACO and Random Greedy Search, Information Sciences, vol. 180, pp. 3465-3487, 2010.

[36] Chen, C. W., Lee, C. W., Chen, C. Y., To Enhance the Energy Efficiency of Chiller Plants with System Optimization Theory, Energy and Environment, vol. 21, no. 5, pp. 409-424, 2010.

[37] Das, I., Dennis, J. E., A Closer Look at Drawbacks of Minimizing Weighted Sums of Objectives for Pareto Set Generation in Multicriteria Optimization Problems, Structural Optimization, vol. 14, pp. 63-69, 1997.

[38] Ding, L., Chen, W., Tan, J., Feng, Y., Multi-Objective Disassembly Line Balancing via Modified Ant Colony Optimization Algorithm, IEEE, 5th International Conference on Bio-Inspired Computing: Theories and Applications, pp. 426-430, Changsha, China, Sep. 2010.

[39] DOE, High Performance Commercial Buildings: A Technology Roadmap, developed by the representatives of commercial building industry, State and community programs, US Department of Energy, 2003.

[40] Doerner, K., Hartl, R. F., Teimann, M., Are COMPETants More Competent for Problem Solving? – The Case of Full Truck Load Transportation, Central European Journal of Operations Research, vol. 11, no. 2, pp. 115-141, 2003.

[41] Doerner, K., Gutjahr, W. J., Hartl, R. F., Strauss, C., Stummer, C., Pareto Ant Colony Optimization: A Meta-Heuristic Approach to Multiobjective Portfolio Selection, Annals of Operation Research, vol. 131, no. 1-4, pp. 79-99, 2004.

[42] Dorigo, M., Maniezzo, V., Colorni, A., Ant System : An Autocatalytic Optimizing Process, Technical Report, Dipartmento di Electronica e Informazione, Politechnico di Milano, 1991.

[43] Dorigo, M., Gambardella, L. M., Ant Colony System: A Cooperative Learning Approach to the Travelling Salesman Problem, IEEE Transactions on Evolutionary Computation, vol. 1, no. 1, pp. 53-66, 1997.

[44] Dorigo, M., Stutzle, T., Ant Colony Optimization, MIT press, Cambridge, MA, 2004.

[45] Du, X., Chen, W., Towards a Better Understanding of Modeling Feasibility Robustness in Engineering Design, ASME Journal of Mechanical Design, vol. 122, no. 4, pp. 385-394, 2000.

[46] Eckenrode, R. T., Weighing Multiple Criteria, Management Sciences, vol. 12, no. 3, pp. 180-192, 1965.

[47] Eschenauer, H., Koski, J., Osyczka, A., Multicriteria Design Optimization Procedures and Applications, Springer-Verlag, Berlin, 1990.

[48] Flake, B. A., Parameter Estimation and Optimal Supervisory Control of Chilled Water Plants, Ph. D. Dissertation, University of Wisconsin-Madison, Madison, WI, USA, 1998.

[49] Fonseca, L. G., Capriles, P. V. S. C., Barbosa, H. J. C., Lemonge, A. C. C., A Stochastic Rank-Based Ant System for Discrete Structural Optimization, Proceedings of the IEEE 2007 Swarm Intelligence Symposium, SIS, pp. 68-75, ISBN: 1-4244-0708-7, 2007.

[50] Garcia-Martinez, C., Cordon, O., Herrera, F., A Taxonomy and Empirical Analysis of Multiple Objective Ant Colony Optimization Algorithm for the Bi-Criteria TSP, European Journal of Operations Research, vol. 180, pp. 116-148, 2007.

[51] Golinski, J., Optimal Design Synthesis Problems Solved by Means of Nonlinear Programming and Random Methods, Journal of Mechanisms, vol. 5, pp. 287-309, 1970.

[52] Gu, X., Renauld, J. E., Ashe, L. M., Decision Based Collaborative Optimization, ASME Journal of Mechanical Design, vol. 124, pp. 1-13, 2002.

[53] Harpole, G. M., Eninger J. E., Micro-Channel Heat Exchanger Optimization, Proceedings of 7th IEEE Semi Thermal Symposium, Scottsdale, AZ, pp. 59-63, Feb. 1991.

[54] Hartman, T. B., All-Variable Speed Centrifugal Chiller Plants, ASHRAE Journal, vol. 43, no. 9, pp. 43-52, 2001.

[55] Hartman, T. B., Designing Efficient Systems with the Equal Marginal Performance Principle, ASHRAE Journal, vol. 47, no. 7, pp. 64-70, 2005.

[56] Hartman, T. B., New Vistas with Relational Control, The Hartman Company Report, USA, 2006

[57] Hartman, T. B., Relational Control - 21st Century More Effective Control Get More Effective System Performances, The Hartman Company Report, USA, 2007.

[58] Hemmatiana, H., Fereidoona, A., Ali, S., Ardeshir, B., Optimization of Laminate Stacking Sequence for Minimizing Weight and Cost Using Elitist Ant System Optimization, Advances in Engineering Software, vol. 57, pp. 8-18, 2013.

[59] Hicham, C., Farouk, Y., Lionel, A., Frederic, D., Buffer Sizing in Assembly Lines Using a Lorenz Multi-Objective Ant Colony Optimization Algorithm, International Conference on Machine and Web Intelligence, pp. 283-287, Algiers, Algeria, Oct. 2010.

[60] Hobbs, B. F., A Comparison of Weighing Methods in Power Plant Sitting, Decision Sciences, no. 11, pp. 725-737, 1980.

[61] Huang, Z. H., Gu, Y. K., Du, X., An Interactive Fuzzy Multi-Objective Optimization Engineering Design, Engineering Applications of Artificial Intelligence, vol. 19, no. 5, pp. 451-460, 2006.

[62] Huang, F. L., Zhong, M. P., Gu, J. M., Liu, G. W., Robust Design in Injection Molding Processing Based on Multi-Objective Ant Colonies Algorithm with Crossover Variation, Applied Mechanics and Materials, vol. 88-89, pp. 279-284, 2011.

[63] Hwang, C.L., Yoon, K., Multiple Attribute Decision Making Methods and Applications: A State of the Art Survey, In: Beckmann, M., Kunzi, H. P. (eds), Lecture Notes in Economics and Mathematical Systems, No. 186, Berlin, Springer-Verlag, 1981.

[64] Hydeman, M., Zhou, G., Optimizing Chilled Water Plant Control, ASHRAE Journal, vol. 49, no. 6, pp. 44-54, 2007.

[65] Iredi, S., Merkle, D., Middendorf, M., Bi-Criterion Optimization with Multi Colony Ant Algorithm, Proceedings of the 1st International Conference on Evolutionary Multi-Criteria Optimization (EMO), pp. 359-372, 2001.

[66] Kandukuri, R., Thermal Conductivity of High Density Thermal Vias in Low Temperature Co-Fired Ceramics (LTCC), M. S. Thesis, Florida International University, Miami, FL, USA, 2002.

[67] Kaveh, A., Shojaee, S., Optimal Design of Skeletal Structures Using Ant Colony Optimization, International Journal for Numerical Methods in Engineering, vol. 70, no. 5, pp. 563-581, 2007.

[68] Kirsch, U., Reiss, M., Shamir, U., Optimum Design by Partitioning Into Substructures, Journal of Structural Division, ASCE, vol. 98, no. 1, pp. 249-261, 1972.

[69] Kirsch, U., Multilevel Approach to Optimum Structural Design, Journal of Structural Division, ASCE, vol. 101, no. 4, pp. 957-974, 1975.

[70] Kirsner, W., 3GPM/Ton Condenser Water Flow Rate: Does it Waste Energy?, ASHRAE Journal, vol. 38, no. 2, pp. 63-69, 1996.

[71] Kirsner, W., Designing for 420 F Chilled Water Supply Temperature - Does it save energy?, ASHRAE Journal, vol. 40, no. 1, pp. 37-42, 1998.

[72] Kleiner, M. B., Stefan, A. K., Haberger, K., High Performance Forced Air Cooling Scheme Employing Micro-channel Heat Exchangers, IEEE Transactions on Component Packaging Technology, Part A, vol. 18, no. 4, pp. 795-804, 1995.

[73] Knight, R. W., Hall, D. J., Goodling, J. S., Jaeger, R. C., Heat Sink Optimization with Applications to Micro-channels, IEEE Transactions on Components Hybrids and Manufacturing Technology, vol. 15, no. 5, pp. 832-842, 1992.

[74] Kokkolaras, M., Mourelatos, Z. P., Papalambros, P. Y., Design Optimization of Hierarchically Decomposed Multilevel Systems Under Uncertainty, ASME Journal of Mechanical Design, vol. 128, pp. 503-508, 2006.

[75] Koski, J., Defectiveness of Weighing Method in Multi-Criterion Optimization of Structures, Communications in Applied Numerical Methods, no. 1, pp. 333-337, 1985.

[76] Koski, J., Silvennoinen, R., Norm Methods and Partial Weighing in Multi-criterion Optimization of Structures, International Journal of Numerical Methods in Engineering, vol. 24, pp. 1101-1121, 1987.

[77] Kreutz, E. W., Pirch, N., Ebert, T., Wester, R., Ollier, B., Loosen, P., Poprawe, R., Simulation of Micro-Channel Heat Sinks for Optoelectronic Microsystems, Microelectronics Journal, no. 31, pp. 787-790, 2000.

[78] Kroo, I., Altus, S., Braun, R, Gage, P., Sobieski, I., Multidisciplinary Optimization Methods for Aircraft Preliminary Design, 5th AIAA/NASA/USAF/ISSMO Symposium on Multidisciplinary Analysis and Optimization, Panama City, FL, AIAA, no. 1, pp. 697-707, AIAA-94-4325, Sep. 1994.

[79] Kuhn, H. W., Tucker, A. W., Nonlinear Programming, Proceedings of the 2nd Berkley Symposium, Mathematics and Statistical Probability, pp. 481-492, 1995.

[80] Kumar, S. A., Mahendra, A. K., Goutham, G., Multi-Objective Shape Optimization Using Ant Colony Coupled Computational Fluid Dynamics Solver, Computers and Fluids, vol. 46, no. 1, pp. 298-305, 2011.

[81] Li, G., Zhou, R. G., Duan, L., Chen, W. F., Multi-Objective Multilevel Optimization for Steel Frames, Engineering Structures, vol. 21, pp. 519-521, 1999.

[82] Li, L., Wang, K., Zhou, C., An Improved Ant Colony Algorithm Combined with Particle Swarm Optimization for Multi-Objective Flexible Job Shop Scheduling, International Conference on Machine Vision and Human Machine Interface, 2010.

[83] Lu, L., Cai, W., Soh, Y. C., Xie, L., Li, S., HVAC System Optimization – Condenser Water Loop, Energy Conversion and Management, vol. 45, pp. 613-630, 2004.

[84] Lu, L., Cai, W., Soh, Y. C., Xie, L., Global Optimization for Overall HVAC systems–Part I Problem Formulation and Analysis, Energy Conversion and Management, vol. 46, pp. 999-1014, 2005.

[85] Ma, Z., Wang, S., Supervisory and Optimal Control of Central Chiller Plants using Simplified Adaptive Models and Genetic Algorithm, Applied Energy, vol. 88, pp. 198-211, 2011.

[86] Mc. Allister, C. D., Simpson, T. W., Multidisciplinary Robust Design Optimization of an Internal Combustion Engine, ASME, Journal of Mechanical Design, vol. 25, pp. 124-130, 2003.

[87] Messac, A., Physical Programming: Effective Optimization for Computational Design, AIAA Journal, vol. 34, no. 1, pp. 149-158, 1996.

[88] Morris, T., Blaine, S., Chiller Plant Optimization Tool, ASHRAE Journal, vol. 50, no. 7, pp. 54-60, 2008.

[89] Mudawar, I., Weilin, Q., Analysis of Three-dimensional Heat Transfer in Micro-channel Heat Sinks, International Journal of Heat and Mass transfer, no. 45, pp. 3973-3985, 2002.

[90] Muhanna, R. L., Mullem, R. L., Development of Interval Based Methods for Fuzziness in Continuum Mechanics, Proceedings of ISUMA-NAFLPS'95, pp. 145-150, 1995.

[91] Muhanna, R. L., Mullem, R. L., Structural Analysis With Fuzzy Based Load Uncertainty, Proceedings of 7th ASCE EMD/STD, Joint Specific Conference on Probabilistic Mechanical and Structural Reliability, Massachusetts, pp. 310-313, 1996.

[92] Muhanna, R. L., Mullem, R.L., Formulation of Fuzzy Finite Element Methods for Mechanics Problems, Computer Aided Civil and Infrastructure Engineering, vol. 14, pp. 107-117, 1999.

[93] Ndao, S., Peles, Y., Jensen, M. K., Multi-Objective Thermal Design Optimization and Comparative Analysis of Electronic Cooling Technologies, International Journal of Heat and Mass Transfer, vol. 52, no. 19-20, pp. 4317-4326, 2009.

[94] Ng, E. Y. K., Poh, S. T., Investigate Study of Manifold Micro-Channel Heat Sinks for Electronic Cooling Design, Journal of Electronic Manufacturing, vol. 9, no. 2, pp. 155-166, 1999.

[95] Oakley, D. R., Sues, R. H., Rhodes, G. S., Performance Optimization of Multidisciplinary Mechanical Systems Subject to Uncertainties, Probability in Engineering Mechanics, vol. 13, no. 1, pp. 15-26, 1998.

[96] Olson, R. T., Liebman, S., Optimization of a Chilled Water Plant Using Sequential Quadratic Programming, Engineering Optimization, vol. 15, no. 1, pp. 171-191, 1990.

[97] Ostendorp, C., Chilled Water Plant Optimization by Resetting the Condenser Water Temperature, Energy Engineering, vol. 107, no. 5, 2010.

[98] Panahi, H., Reza, T. M., Solving a Multi-Objective Open Shop Scheduling Problem by a Novel Hybrid Ant Colony Optimization, Expert Systems with Applications, vol. 38, pp. 2817-2822, 2011.

[99] Papalambros, P. Y., Wilde, D. J., Principles of Optimal Design: Modeling and Computation, Cambridge University Press, New York, USA, 2000.

[100] Philips, R. J., Micro-channel Heat Sinks, In: Advances in Thermal Modeling of Electronic Components and Systems, A. Bar-Cohen and A. D. Kraus, Eds., no. 2, pp. 109-184, 1990.

[101] Rajeev, G., Krishnamoorthy, C. S., Discrete Optimization of Structures using Genetic Algorithm, Journal of Structural Engineering, vol. 118, no. 5, pp. 1233-1250, 1992.

[102] Rao, J. R., Roy, N., Fuzzy Set Theoretic Approach of Assigning Weights to Objectives in Multicriteria Decision Making, International Journal of System Sciences, no. 20, pp. 1381-1386, 1989.

[103] Rao, S. S., Structural Optimization by Chance Constrained Programming Techniques, Computers and Structures, vol. 12, no. 6, pp, 777-781, 1980.

[104] Rao, S. S., Multi-objective Optimization of Fuzzy Structural Systems, International Journal of Numerical Methods in Engineering, vol. 24, no. 6, pp. 1157-1171, 1987.

[105] Rao, S. S., Game Theory Approach for Multi-objective Structural Optimization, Computers and Structures, vol. 25, no.1, pp. 119-127, 1987.

[106] Rao, S. S., Applied Numerical Methods for Engineers and Scientists, Prentice Hall, Upper Saddle River, N.J., Sep. 2001.

[107] Rao, S. S., Engineering Optimization: Theory and Practice, John Wiley and Sons Inc., June 2009.

[108] Rao, S. S., Hati, S. K., Game Theory Approach in Multi-criteria Optimization of Function Generating Mechanisms, Journal of Mechanical Design, vol. 101, 398-406, 1979.

[109] Rao, S. S., Freiheit, A., Modified Game Theory Approach to Multiobjective Optimization, Journal of Mechanical Design, vol. 113, pp. 286-291, 1991.

[110] Rao, S. S., Sawyer, J. P., Fuzzy Finite Element Approach for the Analysis of Imprecisely Defined Systems, AIAA Journal, vol. 33, no. 12, pp. 2364-2370, 1995.

[111] Rao, S .S., Berke, L., Analysis of Uncertain Structural Systems using Interval Analysis, AIAA Journal, vol. 35, no. 4, pp. 727-735, 1997.

[112] Rawling, M. R., Balling, R. J., Collaborative Optimization with Disciplinary Conceptual Design, 7th AIAA/USAF/NASA/ISSMO Symposium on Multidisciplinary Analysis and Optimization, St. Louis, MO, AIAA, no. 3, pp. 1580-1587, AIAA-98-4928, Sep. 1998.

[113] Ray, T., Golinski's Speed Reducer Problem Revisited, AIAA Journal, vol. 41, no. 3, pp. 556-558, 2003.

[114] Reddy, M. J., Kumar, D. N., An Efficient Multi-objective Optimization Algorithm based on swarm intelligence for engineering design, Engineering Optimization, vol. 39, no. 1, pp. 49-68, 2007.

[115] Rohl, P. J, Schrage, D. P., Multidisciplinary Wing Design of a High Speed Civil Transport Aircraft by Multilevel Decomposition Techniques, In: Proceedings of the, 4th AIAA/Air Force/NASA Symposium on Multidisciplinary Analysis and Optimization, AIAA 92-4721, Sep. 1992.

[116] Ryu, J. H., Choi, D. H., Kim, S. J., Numerical Optimization of the Thermal Performance of a Microchannel Heat Sink, International Journal of Heat and Mass Transfer, vol. 45, no. 13, pp. 2823-2827, 2002.

[117] Sakalkar, V., Hajela, P., Multilevel Decomposition Based Non-Deterministic Design Optimization, In: Proceedings of the 49th AIAA/ASME/ASCE/AHS/ASC Structures, Structural Dynamics & Material Conference, Schaumburg, IL, USA, AIAA-2008-2221, 2008.

[118] Salama, M., Garba, J., Demsetz, L., Udwadia, F., Simultaneous Optimization of Controlled Structures, Computational Mechanics, vol. 3, pp. 275-282, 1988.

[119] Samalam, V. K., Convective Heat Transfer in Microchannels, Journal of Electronic Materials, vol. 18, no. 5, pp. 611-618, 1989.

[120] Sameer, D. K., Ravendra, K., Sanyasi, R., Rao, N. D., Ant Colony Optimization Based Algorithm for Engineering Design, Proceedings of the International Conference on Computer Aided Engineering, Indian Institute of Technology Madras, Chennai, India, 2007.

[121] Sandesh, S., Shankar, K., Structural Identification Using Ant Colony Optimization Technique in the Time Domain, Proceedings of the International Conference on Computer Aided Engineering, Indian Institute of Technology Madras, Chennai, India, 2007.

[122] Schmit, L. A., Ramanathan, R. K., Multilevel Approach to Minimum Weight Design Including Buckling Constraints, AIAA Journal, vol. 16, no. 2, pp. 97-104, 1978.

[123] Seok, P. J., Sung, J. K., Kyung, W. P., Experimental Investigation of Thermal Characteristics for a Micro-channel Heat Sink Subject to an Impinging Jet using a Micro-thermal Sensor Array, Sensors and Actuators, A 105, pp. 211-224, 2003.

[124] Serra, M., Venini, P., On Some Applications of Ant Colony Optimization Metaheuristic to Structural Optimization Problems, 6th World Congress of Structural and Multi-disciplinary Optimization, Rio de Janeiro, Brazil, No. 3101, 2005.

[125] Shelton, S. V., Joyce, C. T., Cooling Tower Optimization for Centrifugal Chillers, ASHRAE Journal, vol. 33, no. 6, pp. 28-36, 1991.

[126] Shung-Wen, K., Sheng-Hong, T., Ming-Han, K., Metallic Micro Heat Pipe Heat Spreader Fabrication, Applied Thermal Engineering, vol. 24, pp. 299-309, 2003.

[127] Sobhan, C. B., Garimella, S. V., A Comparative Analysis of Studies on Heat Transfer and Fluid Flow in Micro-channels, Microscale Thermophysical Engineering, vol. 15, pp. 293-311, 2001.

[128] Sobieski, J. S., James, B. B, Dovi, A. R., Structural Optimization by Multilevel Decomposition, AIAA Journal, vol. 23, no. 11, pp. 1775-1782, 1985.

[129] Sobieski, J. S., James, B. B., Riley, M. F., Structural Sizing by Generalized Multilevel Optimization, AIAA Journal, vol. 25, no. 1, pp. 139-145, 1987.

[130] Sobieski, J., Kroo, I., Aircraft Design Using Collaborative Optimization, AIAA-96-0715, 34th Aerospace Sciences Meeting and Exhibit, Reno, Nevada, USA, Jan. 1996.

[131] Stadler, W., Caveats and Boons of Multicriteria Optimization, Micro-computing in Civil Engineering, no. 10, pp. 291-299, 1995.

[132] Steuer, R. E., Multiple Criteria Optimization: Theory, Computation and Application, Malabar, Robert E. Krieger Publishing, 1989.

[133] Stoecker, W. F., Procedures for Simulating the Performance of Components and Systems for Energy Calculations, ASHRAE, New York, 1975.

[134] Stutzle, T., Hoos, H. H., Max-Min Ant system, Future Generation Computer Systems, vol. 16, no. 8, pp. 889-914, 2000.

[135] Su, J., Renauld, J. E., Automatic Differentiation in Robust Optimization, AIAA Journal, vol. 35, no. 6, pp. 1072-79, 1997.

[136] Sues, R. H., Cesare, M. A., Pageau, S. S., Wu, Y. T., Reliability Based Optimization Considering Manufacturing and Operational Uncertainties, Journal of Aerospace Engineering, no. 14, pp. 166-174, 2001.

[137] Sun, J., Optimal Supervisory Control of a Central Chilled Water Plant with Heuristic Search Sequential Quadratic Programming, Engineering Optimization, vol. 42, no. 9, pp. 863-885, 2010.

[138] Sun, J., Reddy, T. A., Optimal Control of Building HVAC&R Systems Using Complete Simulation-Based Sequential Quadratic Programming (CSB-SQP), Building and Environment, vol. 40, pp. 657-669, 2005.

[139] Sunar, M., Kahraman, R., A Comparative Study of Multi-objective Methods in Structural Design, Turkish Journal of Engineering and Environmental Science, no. 25, pp. 69-78, 2001.

[140] Tappeta, R. V., Renauld, J. E., Multiobjective Collaborative Optimization, ASME Journal of Mechanical Design, vol. 119, no. 3, pp. 403-411, 1997.

[141] Tuckerman, D. B., Pease, R. F. W., High-Performance Heat Sinking for VLSI, IEEE Electron Device Letters, vol. 2, no. 5, pp. 126-129, 1981.

[142] Upadhye, H. R., Kandlikar, S. G., Optimization of Micro-Channel Geometry for Direct Chip Cooling Using Single Phase Heat Transfer, Proceedings of 2nd International Conference on Microchannels and Minichannels, pp. 679-685, June 2004.

[143] Walley, P., Statistical Reasoning with Imprecise Probabilities, Chapman and Hall, London, 1991.

[144] Walsh, L. J., Young, C., Pritchard, J. I., Adelman, M.H., Mantay, W., Multilevel Decomposition Approach to Integrated Aerodynamic/dynamic/structural Optimization of Helicopter Rotor Blades, In: Proceedings of AHS Aeromechanics Specialists Conference, San Francisco, California, 1994.

[145] Wang, S. W., Ma, Z. J., Supervisory and Optimal Control of Building HVAC systems: A review, HVAC and R Research, vol. 14, no. 1, pp. 3-32, 2008.

[146] Wei, X., Joshi, Y., Optimization Study of Stacked Micro-Channel Heat Sinks for Micro-Electronic Cooling, IEEE Transactions on Components and Packaging Technologies, vol. 26, no. 1, pp. 55-61, Mar. 2003.

[147] Weisburg, A., Bau, H. H., Zemel, J. N., Analysis of Microchannels for Integrated Cooling, International Journal of Heat and Mass Transfer, vol. 35, no. 10, pp. 2465-2474, 1992.

[148] Wierzbicki, A. P., A Methodological Approach to Comparing Parametric Characterizations of Efficient Solutions, In: Fadel, G., Grauer, M., Kurzhanski, A., Wierzbicki, A.P. (eds), Large-scale Modeling and Interactive Decision Analysis, Lecture notes in Economics and Mathematical Systems, no. 273, pp. 27-45, Berlin, Springer-Verlag, 1986.

[149] Wit, D. A. J., Keulen, F. V, Numerical Comparison of Multi-level Optimization Techniques, Proceedings of the 48th AIAA/ASME/ASCE/AHS/ASC Structures, Structural Dynamics & Material Conference., AIAA 2007-1895, 2007.

[150] Wright, N., Numerical Optimization, Special Series in Operations Research, 2006.

[151] Yagmahan, B., Yenisey, M. M., A Multi-objective Ant Colony System Algorithm for Flow Shop Scheduling Problem, Expert Systems with Applications, vol. 37, pp. 1361-1368, 2010.

[152] Yu, F. W., Chan, K. T., Environmental Performance and Economic Analysis of All-variable Speed Chiller Systems with Load based Speed Control, Applied Thermal Engineering, vol. 29, no. 9, pp. 1721-29, 2009.

[153] Zampino, M. A., Adluru, H., Liu, Y., Jones, W. K., LTCC Substrates with Internal Cooling Channel and Heat Exchangers, Proceedings of the 36th International Symposium on Microelectronics, IMAPS, Boston, 2003.

[154] Zeljkovic, V., Maksimovic, S., Multilevel Optimization Approach Applied to Aircraft Nose Landing Gear, Scientific Technical Review, LVI, no. 2, 2006.

[155] Zheng, J., Wang, S. W., Energy Efficient Control of Variable Speed Pumps in Complex Buildings Central Air-conditioning Systems, Energy and Buildings, vol. 41, no. 2, pp. 197-205, 2009.

[156] Zhou, H. J., Jing, C., Zhen, L., Optimal Mechanism Design of a Shearing Machine Using An Ant Colony Optimization Algorithm, Applied Mechanics and Materials, vol. 52, pp. 938-942, 2011.

[157] Zhu, D. M., An Improved Templeman's Algorithm for Optimum Design of Trusses with Discrete Member Size, Engineering Optimization, vol. 9, no. 4, pp. 303-312, 1986.

[158] Zong, X., Xiong, S., Multi-objective Ant Colony Optimization Model for Emergency Evacuation, 6th International Conference on Natural Computation (ICNC 2010), vol. 6, pp. 2774-2778, Aug. 2010.